Regulation studies of tacrolimus biosynthesis and generation of derivatives

---

Regulationsstudien der Tacrolimus-Biosynthese und Herstellung von Derivaten

Dissertation

der Mathematisch-Naturwissenschaftlichen Fakultät
der Eberhard Karls Universität Tübingen
zur Erlangung des Grades eines
Doktors der Naturwissenschaften
(Dr. rer. nat.)

vorgelegt von
Tomke Bakker
aus Filderstadt

Tübingen
2021

Gedruckt mit Genehmigung der Mathematisch-Naturwissenschaftlichen Fakultät der Eberhard Karls Universität Tübingen.

Tag der mündlichen Qualifikation:	22.02.2021
Stellvertretender Dekan:	Prof. Dr. József Fortágh
1. Berichterstatter:	Prof. Dr. Harald Groß
2. Berichterstatter:	PD Dr. Bertolt Gust

Contents

List of abbreviations VII

Summary X

Zusammenfassung XII

1 Introduction 1

1.1 Tacrolimus . . . 1
1.2 Mode of action of tacrolimus . . . 2
1.3 Biosynthesis of tacrolimus . . . 3
1.3.1 FK506 biosynthetic gene cluster . . . 3
1.3.2 Characteristic features of the PKS system . . . 5
1.4 Efforts to increase tacrolimus production . . . 6
1.5 PKS engineering to generate derivatives of natural compounds . . . 8
1.6 Aims of this study . . . 10

2 Materials and Methods 12

2.1 Materials . . . 12
2.1.1 Devices . . . 12
2.1.2 Equipment . . . 14
2.1.3 Consumables . . . 15
2.1.4 Chemicals . . . 15
2.1.5 Primers . . . 19
2.1.6 Enzymes . . . 25
2.1.7 Kits . . . 26
2.1.8 Size standards for gel electrophoresis . . . 26
2.1.9 Antibiotics and Inductors . . . 27
2.1.10 Strains . . . 27
2.1.11 Plasmids and Cosmids . . . 29
2.1.12 Media, Solutions and Buffers . . . 37
2.1.13 Software . . . 42
2.2 Methods . . . 42
2.2.1 Cultivation and strain maintenance . . . 42
2.2.1.1 Cultivation conditions . . . 42

2.2.1.2 Preparation of spore stocks . . . 43
2.2.2 Methods of molecular biology . . . 43
2.2.2.1 Isolation of genomic DNA from *Streptomyces tsukubaensis* . . . 43
2.2.2.2 Isolation of plasmid or cosmid DNA of *E. coli* – mini- and maxi-preparation . . . 43
2.2.2.3 Amplification of DNA . . . 44
2.2.2.4 Precipitation of DNA . . . 45
2.2.2.5 Purification/extraction of DNA with phenol/chloroform/isoamyl alcohol . . . 45
2.2.2.6 Purification of DNA using the Cycle Pure Kit . . . 45
2.2.2.7 DNA restriction . . . 46
2.2.2.8 Ligation of DNA . . . 46
2.2.2.9 Transformation of DNA . . . 46
2.2.2.10 Agarose gel electrophoresis . . . 47
2.2.2.11 Colony PCR . . . 48
2.2.2.12 Sequencing . . . 49
2.2.2.13 Gibson Assembly . . . 49
2.2.2.14 Blue-White-Screening . . . 50
2.2.2.15 PCR targeting . . . 50
2.2.2.16 Intergeneric conjugation of DNA from *E. coli* to *Streptomyces* . . . 52
2.2.2.17 CRISPR-Cas9 editing . . . 53
2.2.3 DACA . . . 55
2.2.3.1 Amplification and biotinylation of promoter fragments for the DACA . . . 55
2.2.3.2 10 L fermentation of *Streptomyces tsukubaensis* NRRL18488 . . . 58
2.2.3.3 Protein extraction . . . 59
2.2.3.4 Bradford protein assay . . . 59
2.2.3.5 Preparation of the Dynabeads^{TM} M-280 Streptavidin . . . 59
2.2.3.6 DNA affinity capturing assay (DACA) . . . 59
2.2.3.7 TCA precipitation of proteins . . . 60
2.2.4 Simultaneous overexpression of several regulatory proteins . . . 60
2.2.4.1 Cloning strategy . . . 61
2.2.4.2 Cultivation of generated mutant strains . . . 62
2.2.5 PKS engineering . . . 63
2.2.5.1 Module swap . . . 64
2.2.5.2 AT domain swap . . . 68
2.2.5.3 ACP domain swap . . . 69
2.2.6 Analytics . . . 71
2.2.6.1 HPLC . . . 71
2.2.6.2 LC-MS . . . 71

2.2.6.3 HR-MS and MS^2 . . . 72
2.2.6.4 NMR . . . 72

3 Results **74**
3.1 DACA . . . 74
3.1.1 Determination of cell dry weight and tacrolimus production during the 10 L fermentation . . . 74
3.1.2 Identification and quantification of DNA-binding proteins via label free mass spectrometry . . . 75
3.1.2.1 Positive controls of the DACA . . . 76
3.1.2.2 Proteins binding unspecifically to all promoter regions of the tacrolimus biosynthetic gene cluster . . . 77
3.1.2.3 Proteins binding specifically to one promoter region of the tacrolimus biosynthetic gene cluster . . . 77
3.1.2.4 Proteins of the tacrolimus biosynthetic gene cluster . . . 82
3.2 Overexpression of putative regulatory proteins of tacrolimus biosynthesis . . . 85
3.2.1 Non-integrative overexpression of putative regulatory proteins . . . 85
3.2.2 Comparison of non-integrative and integrative overexpression of selected putative regulatory proteins . . . 87
3.2.3 Impact of cultivation scale on tacrolimus production . . . 90
3.3 Simultaneous overexpression of several regulatory proteins . . . 91
3.4 PKS engineering . . . 94
3.4.1 Module swap . . . 96
3.4.1.1 Module swap in heterologous host strains . . . 96
3.4.1.2 Module swap in the natural producer *Streptomyces tsukubaensis* NRRL18488 . . . 98
3.4.2 AT domain swap . . . 98
3.4.3 ACP domain swap . . . 99
3.4.3.1 ACP domain swap in heterologous host strains . . . 99
3.4.3.2 ACP domain swap in the natural producer *Streptomyces tsukubaensis* NRRL18488 . . . 100

4 Discussion **106**
4.1 DACA . . . 106
4.1.1 Fermentation . . . 106
4.1.2 Positive controls of the DACA . . . 106
4.1.3 Proteins of the tacrolimus biosynthetic gene cluster . . . 107
4.2 Overexpression of putative regulatory proteins of tacrolimus biosynthesis . . . 108
4.2.1 Non-integrative overexpression of putative regulatory proteins . . . 108

4.2.2 Comparison of non-integrative and integrative overexpression of selected putative regulatory proteins 112
4.3 Simultaneous overexpression of several regulatory proteins 115
4.4 PKS engineering 117

5 Bibliography **124**

6 List of Tables **135**

7 List of Figures **137**

8 Appendix **139**

Acknowledgements **145**

List of abbreviations

°C	degree Celsius
ACP	acyl carrier protein
antiSMASH	antibiotics and secondary metabolite analysis shell
Apra	apramycin
AT	acyltransferase
aTc	anhydrotetracycline
BGC	biosynthetic gene cluster
bp	base pair
BSA	bovine serum albumin
Carb	carbenicillin
Cml	chloramphenicol
CoA	coenzyme A
crRNA	CRISPR RNA
d	day
DACA	DNA affinity capturing assay
ddH_2O	double destilled water
DEBS	6-deoxyerythronolide B synthase
DH	dehydratase
DMSO	dimethyl sulfoxide
DNA	deoxyribonucleic acid
dNTP	deoxyribonucleoside 5'-triphosphate
DTT	dithiothreitol
E. coli	*Escherichia coli*
EDTA	ethylenediaminetetraacetic acid
e.g.	for example
ESI	electrospray ionization
et al.	*et alia*
FK506	tacrolimus
FKBP	FK506-binding protein
FW	forward
g	gram
h	hour
HPLC	high performance liquid chromatography
HR	high resolution
IPTG	isopropyl ß-D-1-thiogalactopyranoside

Kan	kanamycin
KirACP5	ACP domain of module 5 of the kirromycin BGC
KR	ß-ketoacyl reductase
KS	ß-ketoacyl synthase
L	liter
LB	lysogeny broth
LC	liquid chromatography
m	milli
M	Molar
min	minute
MOPS	3-(*N*-morpholino)propanesulfonic acid
MRM	multiple reaction monitoring
MRS	multiple recombineering site
MS	mass spectrometry
MTBE	methyl tert-butyl ether
MW	molecular weight
m/z	mass-to-charge ratio
n	nano
n/a	not available
Ndx	nalidixic acid
NMR	nuclear magnetic resonance
NRPS	nonribosomal peptide synthetase
OD_{600}	optical density at 600 nm
oriT	origin of transfer
PCR	polymerase chain reaction
PKS	polyketide synthase
PMSF	phenylmethylsulfonyl fluoride
PPTase	phosphopantetheinyl transferase
PSI	pound-force per square inch
RBS	ribosomal binding site
RNA	ribonucleic acid
RNase	ribonuclease
RP	reverse phase
RT	room temperature
RV	reverse
S.	*Streptomyces*
SDS	sodium dodecyl sulfate
sec	second
sgRNA	single guide RNA
SOB	super optimal broth
SOC	super optimal broth with catabolite respression
SOP	standard operating procedure
Strep	streptomycin

TE	thioesterase
TOF	time-of-flight
tracrRNA	trans-activating CRISPR RNA
triton-X-100	polyethylene glycol *p*-(1,1,3,3-tetramethylbutyl)-phenylether
TSA	tryptic soy broth agar
TSB	tryptic soy broth
TSS	transcriptional start site
UV	ultraviolet
VLC	vacuum liquid chromatography
vs.	versus
x g	g-force
X-Gal	5-bromo-4-chloro-3-indolyl-ß-*D*-galactopyranoside
YEME	yeast extract-malt extract
μ	micro

Summary

Initially discovered in 1984, the 23-membered polyketide macrolide tacrolimus (FK506) has proved to be an efficient immunosuppressive agent and is meanwhile used as major drug to prevent the rejection of organ transplants such as kidney and liver (Kino and Goto, 1993; Ng *et al.*, 2017). This natural compound is produced by *Streptomyces tsukubaensis* NRRL18488 and related strains with its biosynthesis involving a type I PKS/NRPS system (Blažič *et al.*, 2012). The biosynthetic pathway leading to the production of tacrolimus has been investigated in detail in previous studies and enabled to identify two pathway-specific regulators, FkbN and FkbR (Mo *et al.*, 2012). However, little is known about global regulators influencing the biosynthesis of this outstanding immunosuppressant.

This study aimed to investigate the regulation of tacrolimus biosynthesis. Therefore, a DNA affinity capturing assay (DACA) was performed in order to identify proteins binding specifically to promoter regions of the tacrolimus biosynthetic gene cluster. In total, 1044 proteins were detected in the DACA binding to the promoter regions Ptcs6, PfkbO, PfkbG, PallA and the negative control fragment P16S. 40 out of those proteins were chosen for further investigations due to their specific binding to one promoter region within the biosynthetic gene cluster. Following individual non-integrative overexpression of those proteins in the wild type producer strain *Streptomyces tsukubaensis* NRRL18488, 14 out of the 40 proteins significantly increased tacrolimus production. Tacrolimus production was maximized upon overexpression of a two-component sensor histidine kinase detected on the promoter region Ptcs6 (2.3-fold production increase). A subsequently conducted comprehensive study including seven of the previously identified protein candidates binding to different promoter regions aimed at identifying a putative difference between an integrative and non-integrative overexpression of the respective regulator genes in *Streptomyces tsukubaensis* NRRL18488. This study revealed a certain dose-response effect of some regulatory proteins and indicated that the overexpression of certain regulators such as FkbN is favored under integrative conditions. With the intention to further increase tacrolimus production on the regulatory level, some of the most promising regulatory proteins identified previously were simultaneously overexpressed in an integrative way. Thereby, a combined overexpression of the already mentioned sensor histidine kinase with a TetR family transcriptional regulator proved to elicit a 3.2-fold increase in tacrolimus production in *Streptomyces tsukubaensis* NRRL18488.

A further goal of this study was the biosynthetic generation of derivatives of tacrolimus. In order to produce a tacrolimus derivative containing a 9-allyl or a 9-ethyl moiety that could potentially act as FKBP-51 inhibitor, three different PKS engineering approaches were pursued. All approaches focused on a modification of module 10 within the PKS assembly line which

is responsible for introducing the functional group in position 9 of the tacrolimus molecule. To generate the desired 9-allyl derivative, a module swap approach and an AT domain swap approach were conducted, both intending to introduce the promiscuous AT domain of module 4 from the FK506 PKS assembly line into module 10. While these two approaches allowed to diminish tacrolimus production by *Streptomyces tsukubaensis* NRRL18488 and the heterologous producer strain *Streptomyces coelicolor*, the production of the intended derivative could not be detected, possibly due to a shortage of allylmalonyl-CoA precursor supply. The third PKS engineering strategy focused on an ACP domain swap, aiming at replacing the ACP domain of module 10 with the ACP5 domain of the kirromycin biosynthetic gene cluster (Musiol *et al.*, 2011). Knowing that KirACP5 is specifically loaded with ethylmalonyl-CoA by the *trans*AT KirCII, this approach should in principle allow to generate 9-ethyl tacrolimus upon the expression of the *trans*AT KirCII in ACP domain swap mutant strains. Although tacrolimus production was abolished in ACP domain swap mutant strains, the detection of the 9-ethyl derivative was not possible, neither in *Streptomyces tsukubaensis* NRRL18488 mutant strains nor in heterologous *Streptomyces coelicolor* producer strains. However, one of the generated ACP domain swap mutant strains unexpectedly produced 9-deoxo-31-*O*-demethyl FK506, a known intermediate in tacrolimus biosynthesis.

Zusammenfassung

Bereits kurz nach seiner Entdeckung im Jahre 1984 stellte sich heraus, dass das 23-gliedrige Polyketid-Makrolid Tacrolimus (FK506) ein sehr wirksames Immunsuppressivum ist. Mittlerweile ist Tacrolimus das wichtigste Medikament zur Verhinderung von Abstoßungsreaktionen nach Organtransplantationen von beispielsweise Leber und Niere (Kino and Goto, 1993; Ng *et al.*, 2017). Der Naturstoff wird von *Streptomyces tsukubaensis* NRRL18488 und verwandten Stämmen produziert, wobei die Biosynthese auf ein TypI PKS/NRPS-System zurückzuführen ist (Blažič *et al.*, 2012). Der Biosyntheseweg, der zur Produktion von Tacrolimus führt, wurde in vorausgehenden Studien detailliert untersucht und ermöglichte die Identifizierung von zwei Cluster-spezifischen Regulatoren, FkbN und FkbR (Mo *et al.*, 2012). Jedoch ist bisher wenig bekannt über globale Regulatoren, welche die Biosynthese dieses bedeutenden Immunsuppressivums beeinflussen.
In dieser Arbeit sollte die Regulation der Tacrolimus-Biosynthese untersucht werden. Hierzu wurde ein sogenannter *DNA affinity capturing assay* (DACA) durchgeführt, um Proteine zu identifizieren, die spezifisch an Promoter-Regionen des Tacrolimus Biosynthese-Genclusters binden. Insgesamt wurden 1044 Proteine im DACA nachgewiesen, die an die Promoter-Regionen Ptcs6, PfkbO, PfkbG, PallA und das Fragment der Negativkontrolle, P16S, gebunden hatten. 40 dieser Proteine wurden daraufhin für weitere Untersuchungen ausgewählt, da sie spezifisch an eine der Promoter-Regionen im Biosynthese Gencluster gebunden hatten. Nachdem diese Proteine einzeln in einem nicht-integrativen System im Wildtyp-Produzenten *Streptomyces tsukubaensis* NRRL18488 überexprimiert worden waren, zeigte sich, dass 14 dieser 40 Proteine die Tacrolimus-Produktion signifikant erhöht hatten. Eine maximale Tacrolimus-Ausbeute wurde durch Überexpression einer Zweikomponenten-Sensorhistidinkinase beobachtet, die am Promoter-Fragment Ptcs6 identifiziert worden war (2,25-fache Produktionssteigerung). Eine nachfolgend durchgeführte, umfassende Analyse unter Einbeziehung von sieben der vorab identifizierten Protein-Kandidaten, welche an verschiedene Promoter-Bereiche binden, zielte darauf ab, einen möglichen Unterschied zwischen integrativer und nicht-integrativer Überexpression der jeweiligen Regulator-Gene in *Streptomyces tsukubaensis* NRRL18488 aufzudecken. Diese Untersuchung offenbarte einen Dosis-Wirkungs-Effekt einiger Regulator-Proteine und verdeutlichte, dass die Überexpression gewisser Regulatoren, wie beispielsweise FkbN, unter integrativen Bedingungen begünstigt ist. Um die Tacrolimus-Produktion auf regulatorischem Level weiter zu erhöhen, sollten in einem weiteren Ansatz einige der zuvor identifizierten, vielversprechendsten Regulator-Proteine gemeinsam integrativ überexprimiert werden. Eine gemeinsame Überexpression der bereits erwähnten Sensorhistidinkinase mit einem Transkriptionsregulator der TetR-Familie ermöglichte eine 3,2-fache Erhöhung der Tacrolimus-Produktion in *Streptomyces tsukubaensis*

NRRL18488.

Ein weiteres Ziel dieser Arbeit bestand in der biosynthetischen Herstellung von Tacrolimus-Derivaten. Um Tacrolimus-Derivate mit einer 9-Allyl- bzw. 9-Ethyl-Gruppe herzustellen, die möglicherweise als FKBP-51-Inhibitoren fungieren könnten, wurden drei verschiedene PKS-*Engineering*-Ansätze verfolgt. Alle drei Ansätze zielten darauf ab, Modul 10 innerhalb des PKS-Systems zu modifizieren, um somit gezielt die Position 9 des Tacrolimus-Moleküls zu verändern. Um das gewünschte 9-Allyl-Derivat herzustellen, wurden ein Modul-Austausch und ein AT-Domänen-Austausch vorgenommen, jeweils in der Absicht, die promiskuitive AT-Domäne von Modul 4 des FK506 PKS-Systems in Modul 10 einzufügen. Obwohl diese Ansätze dazu führten, dass die Tacrolimus-Produktion in *Streptomyces tsukubaensis* NRRL18488 und dem heterologen Produzentenstamm *Streptomyces coelicolor* verringert wurde, konnte eine Produktion des gewünschten Derivats nicht nachgewiesen werden, möglicherweise aufgrund eines Mangels der Allylmalonyl-CoA-Vorläuferverbindung. Die dritte PKS-*Engineering*-Strategie beabsichtigte einen ACP-Domänen-Austausch. Die ACP-Domäne von Modul 10 sollte durch die ACP5-Domäne des Kirromycin-Biosynthese-Genclusters ersetzt werden (Musiol *et al.*, 2011). Basierend auf dem Wissen, dass die KirACP5 durch die *trans*AT KirCII spezifisch mit Ethylmalonyl-CoA beladen wird, sollte dieser Ansatz es prinzipiell ermöglichen, 9-Ethyl-Tacrolimus herzustellen, indem die *trans*AT KirCII in den Mutanten mit ausgetauschter ACP-Domäne exprimiert wird. Obwohl nachweislich kein Tacrolimus mehr von den hergestellten Mutanten mit KirACP5-Domäne produziert wurde, konnte eine Produktion des 9-Ethyl-Derivats weder in *Streptomyces tsukubaensis* NRRL18488-Mutanten noch in heterologen *Streptomyces coelicolor*-Mutanten nachgewiesen werden. Allerdings produzierte eine der hergestellten Mutanten mit ACP-Domänen-Austausch unerwarteterweise 9-Deoxo-31-*O*-demethyl FK506, ein bekanntes Intermediat der Tacrolimus-Biosynthese.

1 Introduction

1.1 Tacrolimus

In search of new immunosuppressive agents, tacrolimus (FK506) was initially discovered in culture broths of *Streptomyces tsukubaensis* no. 9993 in 1984 (Kino and Goto, 1993). Regarding its potency, this new 23-membered macrolide lactone soon proved to be superior to cyclosporin, which had been the immunosuppressive drug of choice up to then (Kino *et al.*, 1987). Tacrolimus shows IC_{50} values a hundred times lower compared to cyclosporin, both *in vitro* and *in vivo*. Referred to as Prograf®, tacrolimus was admitted as immunosuppressive drug in 1994 (https://www.fda.gov). Due to the outstanding efficacy of FK506 as rescue or primary immunosuppressant therapy upon liver or kidney transplants and increased patient/graft survival rates (Peters *et al.*, 1993), research on tacrolimus was expanded. In following studies the anti-inflammatory properties of tacrolimus on human basophils (de Paulis *et al.*, 1991) and its antifungal activity e.g. against *Malassezia furfur* (Nakagawa *et al.*, 1996) were discovered. After further related studies, the natural compound was additionally approved for the treatment of inflammatory diseases and eczema in 2000 (Protopic®, https://www.fda.gov). Beyond that, tacrolimus was also found to exhibit neuroprotective and neuroregenerative activities by interacting with the immunophilin FKBP-52 (Snyder *et al.*, 1998). Periyasamy *et al.* (2007) could show that FK506 is able to negatively control the proliferation of prostate cells *in vitro* which could additionally allow a potential application of this drug in cancer chemotherapy.

The wide scope of tacrolimus is based on multiple immunophilins participating in mediating its action. Immunophilins are protein receptors, so-called prolyl isomerases, that are expressed in a certain cell type and range in sizes from 12 kDa to 70 kDa (Marks, 1996). While the 12 kDa FK506-binding protein (FKBP-12) mediates the immunosuppressive property of tacrolimus in T-cells (see 1.2), there are further known immunophilins that implement additional functions of this drug. For instance, FKBP-13 and FKBP-65 are located in the endoplasmatic reticulum where they influence the folding of type III collagen (Zeng *et al.*, 1998). FK506 was coherently shown to delay the folding of the collagen triple-helix. The immunophilin FKBP-25 binds to microtubules to promote their polymerization and stabilize their network, thus offering a potential therapeutic target for microtubules-associated diseases (Dilworth *et al.*, 2018). FKBP-51 and FKBP-52 were originally identified to be associated with steroid hormone receptors (Gold *et al.*, 1999) and thus contribute to different hormone-dependent diseases such as stress-related diseases, immune and reproductive functions and metabolic diseases (Storer *et al.*, 2011). FKBP-51 was further found to be expressed in T-cells where, just as FKBP-12, it is able to inhibit calcineurin

(Baughman *et al.*, 1995). Consequently, several immunophilins may participate in executing the immunosuppressive function of tacrolimus (Gold *et al.*, 1999).

1.2 Mode of action of tacrolimus

The immunosuppressive effect of tacrolimus relies on its property to inhibit T-cell activation and proliferation (figure 1). Therefore, tacrolimus binds to FKBP-12 located in T-cells and this complex then acts on calcineurin (CaN), a calcium/calmodulin-dependent serine-threonine phosphatase (Liu *et al.*, 1991). Consequently, calcineurin can no longer dephosphorylate the nuclear factor of activated T-cells (NF-ATc). Missing dephosphorylation inhibits the cytoplasmatic form of this transcription factor to translocate to the nucleus, where it is necessary for the transcription initiation of T-cell growth factors as interleukin-2 (IL-2). Blocked T-cell growth leads to the immunosuppressive effect of tacrolimus (Marks, 1996).

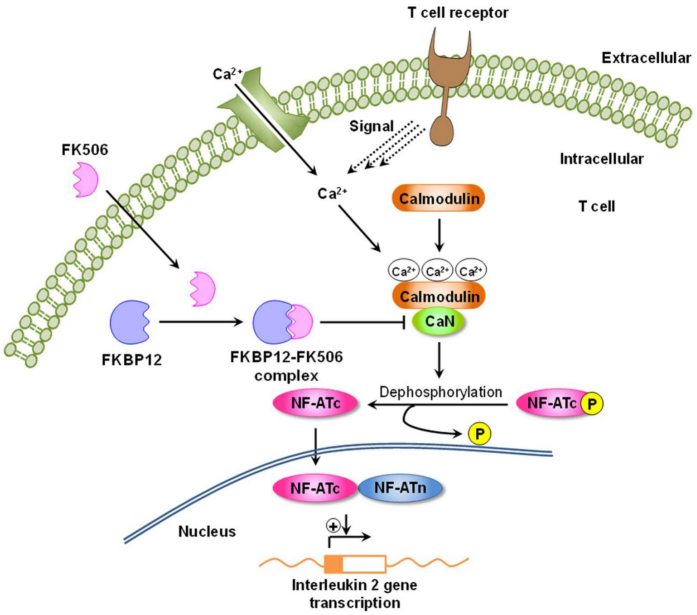

Figure 1: **Mode of action of FK506**.
FKBP12 (FK506-binding protein 12), CaN (calcineurin), NF-ATc (calcium-calmodulin-sensitive subunits of nuclear factor of activated T-cell transcription complexes), NF-ATn (nuclear subunits of NF-AT transcription complexes).
(Ban *et al.*, 2016).

According to Lee *et al.* (2018), the positions C-9 and C-31 of tacrolimus might be important sites to control the affinity of tacrolimus towards FKBP-12. Moreover, the region comprising C-13 to C-24 has been described to be the calcineurin binding region of FK506, including its methoxy oxygens which form hydrogen bonds with the tryptophan 352 of calcineurin (Griffith *et al.*, 1995).
The binding of FK506 to one of the other immunophilins mentioned above results in further effects besides immunosuppression. However, these are likewise caused by an inhibition of the

peptidyl-propyl *cis-trans* isomerase activity (PPIase) of the respective immunophilin (Gaali *et al.*, 2011).
Recently, FKBP-51, an Hsp90-associated co-chaperone that is best known for its regulatory role on steroid hormone receptors (Cioffi *et al.*, 2011), has been increasingly investigated as promising drug target. FKBP-51 has been described to be involved in stress-related disorders and depression (Schmidt *et al.*, 2012), long term pain (Maiarù *et al.*, 2016) and additionally plays a role in energy and glucose homeostasis (Balsevich *et al.*, 2017). Generating specific FKBP-51 inhibitors that do not exert immunosuppressive functions is therefore of great interest.

1.3 Biosynthesis of tacrolimus

1.3.1 FK506 biosynthetic gene cluster

Tacrolimus biosynthesis involves a hybrid type I polyketide synthase/nonribosomal peptide synthetase (PKS/NRPS) system. The biosynthetic gene cluster spans 82.9 kbp and consists of 26 genes organized as at least 9 operons (Jones *et al.*, 2013; Bauer *et al.*, 2017) (figure 2). The function of most of the cluster proteins is known owing to various overexpression and knockout studies described in literature.

Figure 2: **Tacrolimus biosynthetic gene cluster.**
The genes *fkbA*, *fkbB* and *fkbC*, depicted in blue, make up the PKS part of the cluster. FkbP (orange) represents the NRPS part. Further information on the individual genes is given in the text.

(4*R*,5*R*)-4,5-dihydroxycyclohex-1-enecarboxylic acid (DHCHC), the starter unit for tacrolimus biosynthesis, is generated from chorismate by hydrolysis. The reaction is catalyzed by a chorismatase encoded by *fkbO* (Barreiro and Martínez-Castro, 2014). The genes *fkbA*, *fkbB* and *fkbC* encode the polyketide synthase comprising 10 modules with 54 domains in total (figure 3). During polyketide chain elongation, different extender units are incorporated: two malonyl-CoA, two methoxymalonyl-CoA, five methylmalonyl-CoA and one allylmalonyl-CoA molecule (Mo *et al.*, 2011). Allylmalonyl-CoA is a quite unusual building block in PKS systems and results in the particular allyl group located in position 9 of the tacrolimus molecule. The biosynthetic pathway for the generation of this rare extender unit is located in the FK506 biosynthetic gene cluster and includes the genes *allD-allA* (Goranovič *et al.*, 2010). The genes *fkbL-fkbG* are in turn responsible for methoxymalonyl-ACP biosynthesis.
Several proteins are involved in post-PKS processing reactions. FkbL, a lysine cyclodeaminase, catalyzes the α-deamination of lysine followed by its cyclization. The NRPS enzyme FkbP

afterwards activates and attaches the resulting *L*-pipecolate to the polyketide chain which is detached from the PKS by the thioesterase FkbQ. Two post-PKS genes, *fkbM* and *fkbD*, encoding a 31-*O*-methyltransferase and a cytochrome P450 C-9-hydroxylase, finally lead to the generation of tacrolimus (Motamedi and Shafiee, 1998).

FkbN and FkbR have been described as pathway-specific regulatory proteins. While FkbN is a known positive regulator of tacrolimus biosynthesis, the role of FkbR is controversial. In the strain *Streptomyces tsukubaensis* NRRL18488, FkbR has been described as positive regulator, increasing tacrolimus production by 30 % upon its overexpression (Goranovič *et al.*, 2012). However, in *Streptomyces* sp. strain KCTC11604BP, production was slightly decreased upon overexpression of FkbR and a deletion of the gene caused a 1.9-fold increase in production (Mo *et al.*, 2012). Regarding the production of ascomycin, a natural derivative of FK506, FkbR has been proven to be a positive regulator (Song *et al.*, 2017). *tcs6*, a quite small gene located upstream of *fkbN*, encodes a putative lipoprotein whose function in tacrolimus biosynthesis is still uncertain. Likewise, the role of the genes *allM-allS* is unknown (Barreiro and Martínez-Castro, 2014) as they do not seem to be involved in tacrolimus biosynthesis (Mo *et al.*, 2011). Regarding the genes *allM-allS*, two types of a tacrolimus biosynthetic gene cluster can be distinguished. A first group, including the strains *Streptomyces tsukubaensis* NRRL18488 and *Streptomyces* sp. KCTC11604BP, contains these genes whereas the second group depicts a shorter version of the cluster missing these genes (e.g. *Streptomyces tacrolimicus* and *Streptomyces kanamyceticus* KCTC9225) (Barreiro and Martínez-Castro, 2014).

In order to enable the heterologous expression of the tacrolimus biosynthetic gene cluster, Jones *et al.* (2013) designed pAC20N, a BAC vector carrying the entire FK506 biosynthetic gene cluster with additional flanking regions of around 8.5 kb and 17.5 kb, respectively. This vector proved to be suitable for heterologous tacrolimus production in different strains of *Streptomyces coelicolor*. However, compared to the wild type producer strain *Streptomyces tsukubaensis* NRRL18488, which produces between 60 mg/L and 80 mg/L, the yields obtained with heterologous producer strains were extremely low (e.g. *Streptomyces coelicolor* M1146: 1.2 mg/L). Nevertheless, an overexpression of FkbN in the heterologous host strains could raise production to 5.5 mg/L.

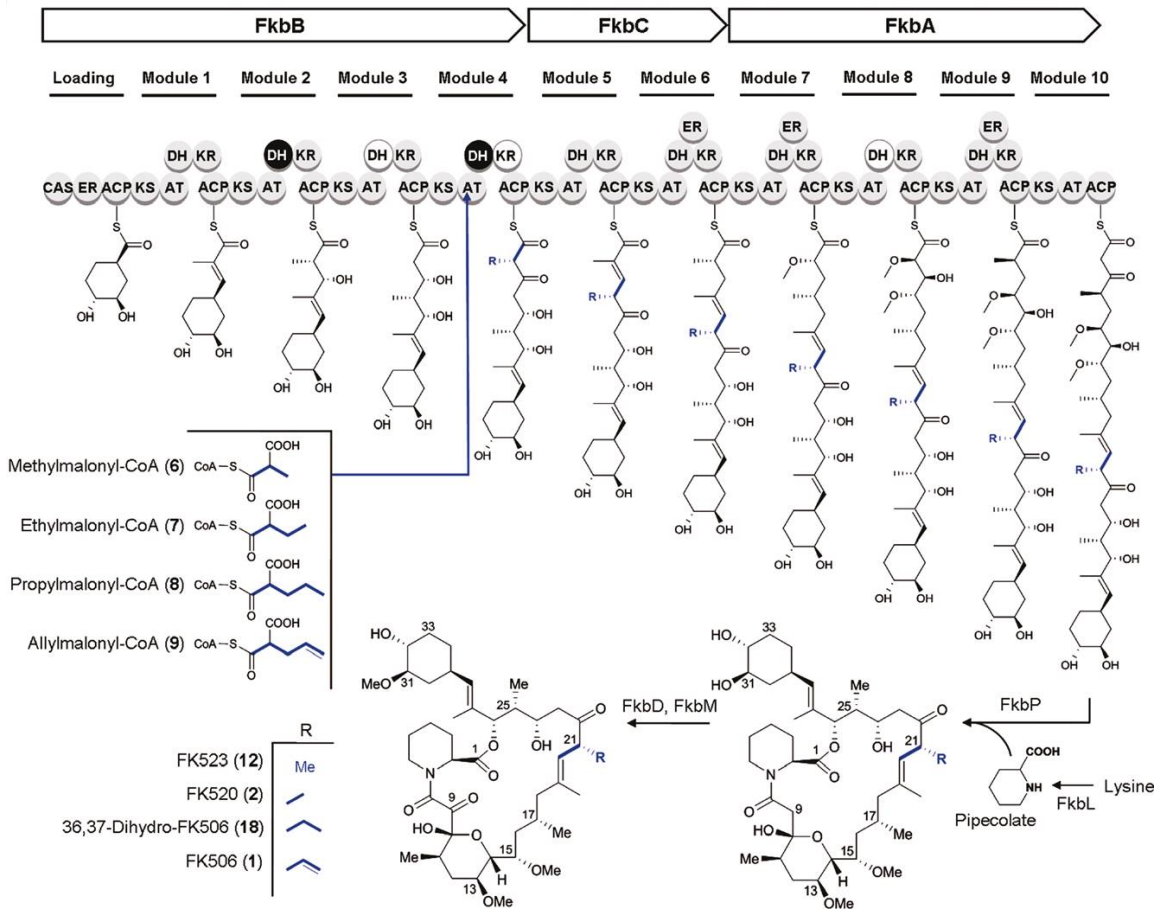

Figure 3: **Schematic representation of tacrolimus biosynthesis**.
Circles represent domains within each module. Black circles signify that domains are not predicted to be active from the final structure and white circles state that domains are nonfunctional due to deletions in the active sites, respectively.
(Mo *et al.*, 2011).

1.3.2 Characteristic features of the PKS system

An outstanding characteristic of the PKS system of tacrolimus producer strains is the property to naturally produce derivatives of FK506. This fact is ascribed to the promiscuous AT domain of module 4 which is able to not only introduce the unique allylmalonyl-CoA precursor, but also to accept methylmalonyl-CoA, ethylmalonyl-CoA and propylmalonyl-CoA as extender units. This flexibility results in the incorporation of different side chains at position 21 of the molecule and consequently the production of 35-desmethyl-FK520 (FK523), ascomycin (FK520) and 36,37-dihydro-FK506, respectively (Mo *et al.*, 2011). A further interesting feature about the PKS system of tacrolimus is the fact that the gene *fkbQ*, encoding a type II thioesterase, is not located just downstream of the last module of the PKS. In contrast, it is located on the opposite strand within another operon.

1.4 Efforts to increase tacrolimus production

As tacrolimus is a commercially available drug with outstanding immunosuppressive properties, there are ongoing efforts to increase production yields of the producer strains. Chemical synthesis of complex natural products such as FK506 is unprofitable due to low efficiency and high costs and is thus not considered to be an alternative for large-scale production (Turło *et al.*, 2012). Several approaches have been pursued to achieve tacrolimus yield optimizations, often combining different strategies. Besides classical approaches including random mutagenesis, media optimization and precursor feeding, modern strategies focusing on synthetic biology and metabolic engineering are pursued and studies of regulatory pathways are included (Fu *et al.*, 2016).
Screening for appropriate production media to achieve high tacrolimus yields has been performed extensively. Turło *et al.* (2012) supplemented their production medium with piperidine (pipecolic acid)- and pyridine-derivatives (picolinic acid, nicotinic acid, nicotinamide) which resulted in a 3- to 7-fold enhancement of the productivity of tacrolimus in *Streptomyces tsukubaensis* FERM BP-927. Further, Martínez-Castro *et al.* (2013) investigated the effect of different factors, such as starch, phosphate concentration, cross-regulation of phosphate and lysine, stressing factors, glucose supplementation and MOPS buffering, starch and nitrogen sources and the pH value on tacrolimus production in *Streptomyces tsukubaensis* NRRL18488. Thereby, they e.g. figured out that the addition of lysine positively influences tacrolimus production while increased nitrogen concentrations suppress its production. Du *et al.* (2014) developed a high producer strain based on genome shuffling and a dynamic fed-batch strategy with supplementation of the precursors disodium malonate and disodium methylmalonate. Additionally, propionic acid, propylene glycol and propanol as biosynthesis precursors have been proven to increase tacrolimus production up to 5.5-fold in *Streptomyces tsukubaensis* FERM BP-927 (Gajzlerska *et al.*, 2015). Just as substances and precursors improving tacrolimus production upon addition to the production medium, tacrolimus repressing carbon sources such as glucose and glycerol have been identified (Ordóñez-Robles *et al.*, 2017).
Further approaches include combinations of exogenous feeding strategies and metabolic engineering of biosynthetic pathways. For instance, Mo *et al.* (2009) noticed an increased tacrolimus production upon feeding of methyl oleate and concluded that this compound might be important for providing methylmalonyl-CoA for tacrolimus biosynthesis. They consequently overexpressed three metabolic pathways for methylmalonyl-CoA supply. The methylmalonyl-CoA mutase (MCM) pathway was identified as dominant way for methylmalonyl-CoA production in the FK506 producer *Streptomyces clavuligerus* CKD1119 and resulted in a 1.5-fold increased tacrolimus production following its overexpression. Likewise, pathways for allylmalonyl-CoA and methoxymalonyl-CoA precursor biosynthesis have been overexpressed individually, resulting in tacrolimus yields increased by 100 % and 30 %, respectively (Chen *et al.*, 2012). A combined overexpression of both pathways even increased production by 125 %. In another study, Huang, Xia, Li, Wen and Jia (2013) fed different nutrients such as soybean oil, lactate and succinate to the production medium and coincidentally overexpressed the genes *fkbO*, *fkbL*, *fkbP*, *fkbM*

and *fkbD*. These genes encode proteins involved in providing the starter unit for chain assembly (DHCHC) and post-PKS processing reactions. Feeding in combination with overexpression resulted in a 3.2-fold increase in tacrolimus production in *Streptomyces tsukubaensis* D852. A further strategy, described by Wang, Liu, Liu, Liang and Wen (2017), used metabolomics and network analysis to identify the pentose phosphate way (PPP), the shikimate pathway and the aspartate pathway as limiting factors for tacrolimus biosynthesis in *Streptomyces tsukubaensis* D852. After feeding exogenous precursors and observing the effects on metabolomic profiles they overexpressed the chorismate synthase gene *aroC* and the dihydrodipicolinate synthase gene *dapA*, leading to 1.4- and 1.2-fold increased tacrolimus production rates, respectively. The same group published an additional approach which used genome-scale dynamic flux balance to identify bottlenecks of tacrolimus biosynthesis. The identified target genes, *gcdh*, *tktB*, *msdh* and *ask*, respectively, were subsequently deleted or overexpressed, resulting in 129.8 % increased tacrolimus production compared to the wild type (Wang, Liu, Liu, Wang and Wen, 2017).

Increasing tacrolimus production yields based on optimizations of regulatory pathways involved in the biosynthesis of the natural compound is a further promising and frequently performed strategy. As mentioned earlier, Mo *et al.* (2012) were the first to identify the cluster encoded protein FkbN as a positive regulator of tacrolimus biosynthesis, resulting in 2-fold increased tacrolimus production upon its overexpression. Additionally, they figured out that the cluster protein FkbR is a negative regulator of tacrolimus biosynthesis in *Streptomyces* sp. KCTC11604BP. The positive regulatory effect of FkbN on tacrolimus production was confirmed by Goranovič *et al.* (2012), however, they identified FkbR as positive regulator in *Streptomyces tsukubaensis* NRRL18488.

Apart from cluster-specific regulators, global regulators might influence tacrolimus production. Considerable research was applied to proteins located in the so called *bul* region, which contains genes involved in the biosynthesis of γ-butyrolactone autoregulator molecules. The γ-butyrolactone family contains the best known autoregulators of *Streptomyces* which control several cellular functions as well as antibiotic production. In a first study, the two γ-butyrolactone receptor homologues *bulR1* and *bulR2* were investigated and *bulR1* was found to be a positive regulator of tacrolimus (Salehi-Najafabadi *et al.*, 2014). A subsequent study focused on two *Streptomyces* antibiotic regulatory proteins (SARP), namely BulY and BulZ. Overexpression of these proteins resulted in an increased transcription of the γ-butyrolactone receptor *tsuR1* and raised tacrolimus production levels compared to the control (1.6-fold for *bulZ*) (Chen *et al.*, 2015). Further studies on BulZ were conducted by Ma *et al.* (2018), indicating that the protein additionally positively influences spore differentiation and that it activates the transcription of the genes *bulZ* and *bulS2*. In turn, BulS2, a putative γ-butyrolactone synthetase, also positively influences tacrolimus biosynthesis. A combined overexpression of *bulZ* and *bulS2* increased tacrolimus production by 36 %.

1.5 PKS engineering to generate derivatives of natural compounds

As tacrolimus targets various immunophilins, which are expressed in different cell types, there is an interest in designing derivatives of tacrolimus, so called tacrologues, that selectively inhibit a certain immunophilin and therefore evoke a specific effect. Several efforts have already been made to prepare derivatives of tacrolimus in order to achieve compounds with increased specificity or altered activity following their binding to different immunophilins.
In an early approach, tacrolimus was chemically modified at the C-21 side chain which led to 24 new molecules with various functional groups at this position (Organ *et al.*, 1993). However, the complex structure of tacrolimus hampers chemical modifications and recent approaches have mainly focused on manipulations of the polyketide synthase assembly line (Ban *et al.*, 2016).
For instance, Moss *et al.* (2013) replaced the polyketide synthase loading module with the equivalent from the avermectin polyketide synthase that is known to incorporate branched acyclic and cyclic carboxylic acids. This led to the production of several analogues which could be used to generate new calcineurin inhibitors.
Currently, there are many attempts to obtain derivatives of natural products through PKS engineering approaches. These include module swaps within a PKS system (Weissman, 2016) or engineering or swapping of acyltransferases, the domains required for the specific incorporation of a certain acyl-CoA extender unit (Musiol-Kroll and Wohlleben, 2018).
The 6-deoxyerythronolide B-producing polyketide synthase (DEBS), composed of the subunits DEBS1, DEBS2 and DEBS3, has been used as scaffold for several PKS engineering approaches. The PKS is encoded by the genes *eryAI*, *eryAII* and *eryAIII*, each of which harbors two modules. In an early attempt, Gokhale *et al.* (1999) combined module 1 of DEBS with other modules of the same PKS or with a module of the rifamycin PKS and thereby successfully produced new triketides. In another study, bimodular and trimodular PKS were constructed based on DEBS1-TE, a derivative of the above mentioned PKS which only contains modules 1 and 2 and a thioesterase (TE) (Ranganathan *et al.*, 1999). Multiple domains have been substituted by appropriate counterparts of the rapamycin PKS, resulting in the production of the predicted target lactones. Subsequently, Rowe *et al.* (2001) also constructed a synthetic PKS based on the 6-deoxyerythronolide B-producing polyketide synthase. They introduced an extension module from the rapamycin-producing PKS between module 1 and module 2 of DEBS1. Co-expression of the new DEBS multienzyme with the multienzymes DEBS2 and DEBS3 resulted in the production of the expected macrolactones.
An alternative to swapping whole modules, which causes ultimate modifications within a PKS, is to exchange single domains. For instance, Oliynyk *et al.* (1996) replaced the acyltransferase (AT) domain from module 1 of DEBS1-TE with the AT domain from module 2 of the rapamycin PKS and thereby produced novel triketide lactones. Likewise, Ruan *et al.* (1997) replaced the methylmalonyl-CoA-specific AT domains of module 1 and module 2 of DEBS1 with three heterologous, malonyl-CoA specific AT domains and thereby successfully produced novel derivatives of erythromycin. However, domain swapping experiments not only included the AT domains

responsible for introducing a certain extender unit, but also ketoreductase (KR) (Annaval *et al.*, 2015) and dehydratase (DH) (Yong and Byeon, 2005) domains. Fisch *et al.* (2011) conducted rational domain swaps between two fungal polyketide synthases, encoding the biosynthesis of tenellin (TENS) and desmethylbassianin (DMBS), and were able to produce specific compounds such as bassianin. Nevertheless, examples of successful domain swapping are, overall, quite rare (Drufva *et al.*, 2020).

An even less drastic intervention in the natural architecture of a PKS compared to domain swaps is the exchange of single amino acids within the AT domains of modules in order to change their specificity. Lau *et al.* (1999) exchanged different sets of amino acids between malonyl and methylmalonyl transferases within the DEBS and thus identified a short C-terminal segment of 23-35 amino acids that is present in all AT domains and determines their substrate specificity. Meanwhile, several conserved amino acid motifs which are required for specificity or stereoselectivity of the different domains within PKS modules have been described (Drufva *et al.*, 2020). This knowledge allows to use site directed mutagenesis approaches for rational engineering of PKS.

The biosynthesis of tacrolimus including a modular type I polyketide synthase should also offer the opportunity to biosynthetically produce derivatives of tacrolimus by PKS engineering approaches. Regarding ascomycin, the natural derivative of tacrolimus produced by a similar PKS, Revill *et al.* (2002) published an approach to generate 13- and 15-desmethoxy analogs of ascomycin by replacing the respective acyltransferases of module 7 and 8. Shen *et al.* (2018) used site-directed mutagenesis to specifically mutate five residues in the AT domain of module 4 within the tacrolimus PKS. This study allowed to identify the residues responsible for the incorporation of the rare extender unit allylmalonyl-CoA in position 21 of the tacrolimus molecule.

Initial investigations of the TacroDrugs project partner Prof. Dr. Felix Hausch (University of Darmstadt, Germany) indicated that a derivative of tacrolimus harboring an additional allyl moiety in position 9 could potentially act as FKBP-51 inhibitor. As mentioned earlier, this immunophilin is known to be involved in various cellular processes responsible for depression, chronic pain and obesity (Schmidt *et al.*, 2012). Therefore, there is a special interest in generating a tacrologue with an allyl group in position 9 of the molecule. PKS engineering is a promising approach for this aim as module 4 of the PKS system is naturally capable to introduce the rare extender unit allylmalonyl-CoA. Thus, using genetic engineering to replace module 10 of the FK506 PKS with module 4 of the same PKS could result in a derivative with the desired allyl group in position 9. Alternatively, exchanging the AT domain of module 10 with the AT domain of module 4 should serve the same purpose.

1.6 Aims of this study

This study comprised two main aims: The first aim was to study the regulation of tacrolimus biosynthesis in order to improve the production yields of this natural product. The second aim focused on the generation of derivatives of tacrolimus, so called tacrologues, using PKS engineering approaches.

With regard to the first aim, it could be shown in previous studies that there is a tight control of transcription mediated by regulators directly binding to promoter regions within a biosynthetic gene cluster (Bekiesch *et al.*, 2016). Therefore, the first objective was to identify putative regulatory proteins of tacrolimus biosynthesis. This included the following tasks:

- Implementation of a DNA affinity capturing assay (DACA) followed by identification and quantification of DNA-binding proteins via label free mass spectrometry.
- Overexpression of 40 selected putative regulatory proteins of tacrolimus biosynthesis in the wild type producer strain *Streptomyces tsukubaensis* NRRL18488.
- Comparison of integrative and non-integrative overexpression of the most promising positive regulators of tacrolimus biosynthesis in the wild type producer strain *Streptomyces tsukubaensis* NRRL18488.

The second objective regarding the regulation studies of tacrolimus biosynthesis was a combined overexpression of several positive regulators of tacrolimus biosynthesis in the wild type producer strain *Streptomyces tsukubaensis* NRRL18488.

Regarding the second aim of generating tacrologues, the intention was to introduce an allyl group at position 9 of the tacrolimus molecule in order to produce a compound that should specifically inhibit FKBP-51, a protein known to be involved in depression, chronic pain and obesity (Schmidt *et al.*, 2012).
The first objective was to prepare this derivative by replacing the original module 10 (located within *fkbA*) of the PKS assembly line with module 4 (located within *fkbB*) of the same PKS system due to the natural capability of module 4 to introduce an allyl side chain. This approach was pursued in the wild type producer strain *Streptomyces tsukubaensis* NRRL18488 as well as in heterologous producer strains *Streptomyces coelicolor* M512, M1146, M1152 and M1154 and *Streptomyces albus* J1074. To this end, the following tasks were accomplished:

- Identification of the cluster boundaries of module 4 and module 10.
- Knockout of the original module 10 within *fkbA* using both the CRISPR-Cas9 strategy (native host) and PCR-targeting (pAC20N).
- Integration of module 4 at the position of module 10 using the CRISPR-Cas9 technology (native host) and homologous recombination (pAC20N).

- Cultivation of the generated mutant strains and analysis of extracts by HPLC and LC-MS for the production of 9-allyl tacrolimus.

The second objective consisted in preparing the 9-allyl derivative of tacrolimus by replacing the malonyl-CoA-specific AT domain of module 10 (located within *fkbA*) with the allylmalonyl-CoA-specific AT domain of module 4 (located in within *fkbB*). After identification of appropriate linker sequences between the different domains of the respective PKS modules, this AT domain swap was performed in the wild type producer strain *Streptomyces tsukubaensis* NRRL18488 using the CRISPR-Cas9 technology.
As a third objective, a 9-ethyl derivative of tacrolimus was to be prepared making use of the *trans*AT KirCII of the kirromycin biosynthetic gene cluster which specifically loads ethylmalonyl-CoA onto the KirACP5 domain (Musiol *et al.*, 2011). The following tasks were carried out to generate mutant strains for the production of 9-ethyl tacrolimus in *Streptomyces tsukubaensis* NRRL18488 and heterologous host strains *Streptomyces coelicolor* M512, M1146, M1152 and M1154:

- Identification of the boundaries of the ACP domain of module 10 in the FK506 biosynthetic gene cluster.
- Knockout of the natural ACP domain of module 10 using both the CRISPR-Cas9 strategy (native host) and PCR-targeting (pAC20N).
- Integration of KirACP5 at the position of the original ACP domain of module 10 using the CRISPR-Cas9 technology (native host) and homologous recombination (pAC20N).
- Conjugation of resulting mutant strains with the plasmid pEM11CII encoding the *trans*AT KirCII.
- Cultivation of the generated mutant strains and analysis of extracts by HPLC and LC-MS for the production of 9-ethyl tacrolimus.
- NMR analysis of the compound produced by one of the ACP domain swap mutant strains.

2 Materials and Methods

2.1 Materials

2.1.1 Devices

Table 1: **Devices used in this study.**

Device	Specification	Manufacturer
Autoclaves	Systec VX-100 Systec DE-23	Systec GmbH, Linden, Germany
Centrifuges	• Sorvall RC6 Plus (rotor SLA-1500)	• Thermo Fisher Scientific, Waltham, Massachusetts, USA
	• VWR Micro Star AR Ch500057 PP75003424	• Thermo Fisher Scientific, Waltham, Massachusetts, USA
	• Centrifuge 5415R (rotor F 45-24-11)	• Eppendorf, Hamburg, Germany
	• Centrifuge 5810R (rotor A-4-62)	• Eppendorf, Hamburg, Germany
	• Multifuge 1 S-R 75002005 G Sorvall Heraeus	• Thermo Fisher Scientific, Waltham, Massachusetts, USA
Cleanbench	Heraeus	Thermo Fisher Scientific, Waltham, Massachusetts, USA
Electroporator	MicroPulser^{TM} Electroporator	Bio-Rad Laboratories, Inc., Hercules, California, USA
Freeze Dryer	Christ	Martin Christ Gefriertrocknungsanlagen GmbH, Osterode am Harz, Germany
French Press	SLM Aminco French Press	

Device	**Specification**	**Manufacturer**
HPLC	**Columns**:	
	Reprospher 100 C18 (150 mm x 4.6 mm, 3 μm)	Dr. Maisch HPLC GmbH, Ammerbuch, Germany
	Poroshell 120 EC-C18 (150 mm x 4.6 mm, 2.7 μm)	Agilent Technologies, Santa Clara, California, USA
	Kinetex®PFP 100 *Å* (250 mm x 4.6 mm, 5 μm)	Phenomenex Inc., Torrance, California, USA
	System:	
	• Agilent 1260 Infinity II • Agilent 1100 Series	Agilent Technologies, Santa Clara, California, USA
Incubators	• Innova® 44 Incubator Shaker Series	• Eppendorf, Hamburg, Germany
	• Certomat HK	• Sartorius AG, Göttingen, Germany
	• Heraeus Instruments Function Line	• Thermo Fisher Scientific, Waltham, Massachusetts, USA
Laboratory Shaker	TS 100 Thermo Shaker	PEGLAB Biotechnologie GmbH, Erlangen, Germany
Magnetic stirrer	Heidolph MR Hei-Standard	Heidolph Instruments GmbH & Co. KG, Schwabach, Germany
Microwave	Sharp Inverter	SHARP, Sakai, Japan
(Micro) scales	• Sartorius MC210 P ISO9001	• Sartorius AG, Göttingen, Germany
	• Kern 572	• KERN & SOHN GmbH, Balingen, Germany
NanoDrop	NanoDrop 1000	Thermo Fisher Scientific, Waltham, Massachusetts, USA
NMR spectrometer	BRUKER Avance III HD 400 MHz Nano Bay	Bruker, Rheinstetten, Germany; Fällanden, Switzerland
Photographic documentation of agarose gels	VILBER	PEQLAB Biotechnologie GmbH, Erlangen, Germany
pH meter	HANNA Instruments pH 211 Microprocessor pH-Meter	Sigma-Aldrich®, St. Louis, Missouri, USA

Device	Specification	Manufacturer
Rotary evaporator	• Rotavapor R-210 • Vacuum Controller V-855 • Vacuum Pump V-700 • Recirculating Chiller F-108 • Heating Bath B-491	Büchi Deutschland, Essen, Germany
SpeedVac Vacuum Concentrator	Concentrator plus	Eppendorf, Hamburg, Germany
Thermocyclers	• iCycler BioRad • peqSTAR	• Bio-Rad Laboratories, Inc., Hercules, California, USA • PEQLAB Biotechnologie GmbH, Erlangen, Germany
Vortex mixer	VF2	IKAR-Werke GmbH& Co.KG, Staufen, Germany
24-square deepwell plates	CR1424, CR1224	Enzyscreen B. V., Al Leiden, Netherlands

2.1.2 Equipment

Table 2: **Equipment used in this study.**

Equipment	Specification	Manufacturer
Beakers	polypropylene and glass, various volumes	VITLAB GmbH, Grossostheim, Germany
Erlenmeyer flaks	various volumes	Kimble™ KIMA™, Kimble Chase Life Science and Research Products, Vineland, USA
Pipettes	10000 μL, 1000 μL, 200 μL, 20 μL, 2 μL	Eppendorf, Hamburg, Germany
Round-bottom flasks	1000 mL, 250 mL, 50 mL	DURAN Group GmbH, Wertheim/Main, Germany
Schott flasks	1000 mL, 500 mL, 100 mL	DURAN Group GmbH, Wertheim/Main, Germany

2.1.3 Consumables

Table 3: **Consumables used in this study.**

Consumable	Specification	Manufacturer
Centrifuge tubes	50 mL, 15 mL	greiner bio-one, Frickenhausen, Germany
Cover slides	18 mm x 18 mm	
Culture dishes	9.2 mm x 1.3 mm	greiner bio-one, Frickenhausen, Germany
DNA Gel Loading Dye	6 x concentrated; 0.5 μg	Thermo Fisher Scientific, Waltham, Massachusetts, USA
Electroporation cuvettes	Peqlab brand, 0.2 cm gap	PEQLAB Biotechnologie GmbH, Erlangen, Germany
Eppendorf® Safe-Lock microcentrifuge tubes	2 mL, 1.5 mL	Eppendorf, Hamburg, Germany
HPLC vials & caps		
Microscope slides	76 mm x 26 mm, 1 mm thickness	Carl Roth GmbH + Co. KG, Karlsruhe, Germany
Parafilm		Bemis®, Neenah, WI, USA
Pasteur pipettes	Hirschmann®	Hirschmann GmbH & Co. KG, Eberstadt, Germany
Pipette tips	10000 μL, 1000 μL, 200 μL, 2 μL	Eppendorf, Hamburg, Germany
Single tubes for PCR		
Sterile filters	0.2 μm	Sartorius AG, Göttingen, Germany
Syringes	10 mL, 20 mL	MEDI-KS Berlin GmbH, Berlin, Germany
96-well plates for PCR		

2.1.4 Chemicals

Table 4: **Chemicals used in this study.**

Chemical	Chemical formula	Manufacturer
Acetic acid	$C_2H_4O_2$	Sigma-Aldrich®, St. Louis, Missouri, USA
Acetone	C_3H_6O	
Acetonitrile	C_2H_3N	J.T.Baker®Chemicals, Center Valley, Pennsylvania, USA
Agarose	LE 9012-30-6	Genaxxon bioscience GmbH, Ulm, Germany

Chemical	Chemical formula	Manufacturer
Ammonium molybdate tetrahydrate	$(NH_4)_6Mo_7O_{24}{\cdot}4H_2O$	Santa Cruz Biotechnology, Dallas, Texas, USA
Antifoam		Sigma-Aldrich®, St. Louis, Missouri, USA
Benzamidine	$C_7H_8N_2$	Sigma-Aldrich®, St. Louis, Missouri, USA
Boric acid	H_3BO_3	Merck Chemicals GmbH, Darmstadt, Germany
BSA		Merck Chemicals GmbH, Darmstadt, Germany
Calcium chloride	$CaCl_2$	Merck Chemicals GmbH, Darmstadt, Germany
Copper sulfate	$CuSO_4{\cdot}5H_2O$	Merck Chemicals GmbH, Darmstadt, Germany
Deuterated chloroform	$CDCl_3$	Sigma-Aldrich®, St. Louis, Missouri, USA
Dichlormethane	CH_2Cl_2	
Dithiothreitol	$C_4H_{10}O_2S_2$	Carl Roth GmbH & Co. KG, Karlsruhe, Germany
Dipotassium hydrogen phosphate	K_2HPO_4	Carl Roth GmbH & Co. KG, Karlsruhe, Germany
DMSO	C_2H_6OS	Sigma-Aldrich®, St. Louis, Missouri, USA
dNTPs		Genaxxon bioscience GmbH, Ulm, Germany
Dynabeads™M-280 Streptavidin		Thermo Fisher Scientific, Waltham, Massachusetts, USA
EDTA	$C_{10}H_{16}N_2O_8$	Carl Roth GmbH & Co. KG, Karlsruhe, Germany
Ethanol	C_2H_6O	
Ethidium bromide	$C_{21}H_{20}BrN_3$	Carl Roth GmbH & Co. KG, Karlsruhe, Germany
Ethylacetate	$C_4H_8O_2$	Carl Roth GmbH & Co. KG, Karlsruhe, Germany
Ferrous sulfate	$FeSO_4{\cdot}7H_2O$	Merck Chemicals GmbH, Darmstadt, Germany
Glucose	$C_6H_{12}O_6$	Carl Roth GmbH & Co. KG, Karlsruhe, Germany
Glycerol (99 % +)	$C_3H_8O_3$	Thermo Fisher Scientific, Waltham, Massachusetts, USA
Isopropanol	C_3H_8O	Carl Roth GmbH & Co. KG, Karlsruhe, Germany

Chemical	Chemical formula	Manufacturer
ISP4	International Streptomyces project medium 4	Difco Becton Dickinson, Franklin Lakes, New Jersey, USA
IPTG	$C_9H_{18}O_5S$	Carl Roth GmbH & Co. KG, Karlsruhe, Germany
L-arabinose		Sigma-Aldrich®, St. Louis, Missouri, USA
L-glutamic acid monosodium salt hydrate	$C_5H_8NNaO_4 \cdot H_2O$	Sigma-Aldrich®, St. Louis, Missouri, USA
Magnesium sulfate	$MgSO_4 \cdot 7H_2O$	Merck Chemicals GmbH, Darmstadt, Germany
Magnesium chloride	$MgCl_2 \cdot 6H_2O$	Carl Roth GmbH & Co. KG, Karlsruhe, Germany
Manganese sulfate	$MnSO_4 \cdot H_2O$	Merck Chemicals GmbH, Darmstadt, Germany
Mannitol	$C_6H_{14}O_6$	Carl Roth GmbH & Co. KG, Karlsruhe, Germany
Methanol	CH_4O	Honeywell, Thermo Fisher Scientific, Waltham, Massachusetts, USA
MOPS	$C_7H_{15}NO_4S$	Carl Roth GmbH & Co. KG, Karlsruhe, Germany
MTBE	$C_5H_{12}O$	Carl Roth GmbH & Co. KG, Karlsruhe, Germany
Pepstatin A	$C_{34}H_{63}N_5O_9$	Carl Roth GmbH & Co. KG, Karlsruhe, Germany
peqGREEN		PEQLAB Biotechnologie GmbH, Erlangen, Germany
Phenol/Chloroform/ Isoamyl alcohol	25:24:1 (v/v)	Carl Roth GmbH & Co. KG, Karlsruhe, Germany
Phosphoric acid	H_3PO_4	Sigma-Aldrich®, St. Louis, Missouri, USA
PMSF	$C_7H_7FO_2S$	Sigma-Aldrich®, St. Louis, Missouri, USA
Polygoprep	60-50 C_{18}	Macherey-Nagel, Düren, Germany
Potassium acetate	$C_2H_3KO_2$	Carl Roth GmbH & Co. KG, Karlsruhe, Germany
Potassium chloride	KCl	Carl Roth GmbH & Co. KG, Karlsruhe, Germany
Potassium dihydrogen orthophosphate	KH_2PO_4	Carl Roth GmbH & Co. KG, Karlsruhe, Germany
Rubidium chloride	RbCl	Carl Roth GmbH & Co. KG, Karlsruhe, Germany

Chemical	**Chemical formula**	**Manufacturer**
Salmon sperm DNA		Thermo Fisher Scientific, Waltham, Massachusetts, USA
SDS	$NaC_{12}H_{25}SO_4$	Carl Roth GmbH & Co. KG, Karlsruhe, Germany
Sodium chloride	NaCl	Carl Roth GmbH & Co. KG, Karlsruhe, Germany
Sodium hydroxide	NaOH	Sigma-Aldrich®, St. Louis, Missouri, USA
Soluble starch		Difco Becton Dickinson, Franklin Lakes, New Jersey, USA
Soy flour		SOBO Naturkost, Köln, Germany
Theophylline	$C_7H_8N_4O_2$	Carl Roth GmbH & Co. KG, Karlsruhe, Germany
Tacrolimus	$C_{44}H_{69}NO_{12}$	Tacrolimus INRESA Médical, Bartenheim, France
Trichloroacetic acid	$C_2HCl_3O_2$	Carl Roth GmbH & Co. KG, Karlsruhe, Germany
Trifluoroacetic acid	$C_2HF_3O_2$	Sigma-Aldrich®, St. Louis, Missouri, USA
Triton-X-100	$C_{14}H_{22}O(C_2H_4O)_n$ (n=9-10)	Fluka, Thermo Fisher Scientific, Waltham, Massachusetts, USA
Trizma base	$NH_2C(CH_2OH)_3$	Sigma-Aldrich®, St. Louis, Missouri, USA
Tryptone		Difco Becton Dickinson, Franklin Lakes, New Jersey, USA
TSB		Difco Becton Dickinson, Franklin Lakes, New Jersey, USA
X-Gal		Carl Roth GmbH & Co. KG, Karlsruhe, Germany
Yeast extract		Difco Becton Dickinson, Franklin Lakes, New Jersey, USA
Zinc sulfate	$ZnSO_4 \cdot 7\ H_2O$	Merck Chemicals GmbH, Darmstadt, Germany

2.1.5 Primers

Table 5: **Primers used for the DACA.**

	Primer	Sequence	Description
1	Ptcs6a_F	GAGGAGTCGTCGATGTGGAGACCACCCAATTCAGCTGCCGGCC	507 bp promoter fragment upstream of *tcs6* (Ptcs6) + 23 bp DAC Biotin = 530 bp
	Ptcs6a_R	CCCTGGTGAAGGACCGTTCCTCG	
2	Ptcs6b_F	GGTTCATGGCGCACATCCGG	594 bp promoter fragment upstream of *tcs6* (Ptcs6) + 23 bp DAC Biotin = 617 bp
	Ptcs6b_R	GAGGAGTCGTCGATGTGGAGACCGATGCGCCCGTCGACAGCCG	
3	PfkbO_F	GAGGAGTCGTCGATGTGGAGACCCATGACCGGTGCCGTGCTCG	439 bp promoter fragment upstream of *fkbO* (PfkbO) + 23 bp DAC Biotin = 462 bp
	PfkbO_R	AGCTGCGCGTACGTCACGGC	
4	PfkbG_F	CCTGTCGTCCCGCAGTGACACC	296 bp promoter fragment upstream of *fkbG* (PfkbG) + 23 bp DAC Biotin = 319 bp
	PfkbG_R	GAGGAGTCGTCGATGTGGAGACCGATACGTCACCGGCGCCACC	
5	PallA_F	CCGGTACGTACGACCCTTGG	546 bp promoter fragment upstream of *allA* (PallA) + 23 bp DAC Biotin = 569 bp
	PallA_R	GAGGAGTCGTCGATGTGGAGACCAGCCTCCTGGACGACTGACC	
6	P16S_F2	GCGGCGTGCTTAACACATGC	473 bp fragment of the 16S rRNA gene (P16S) + 23 bp DAC Biotin = 496 bp
	P16S_R2	GAGGAGTCGTCGATGTGGAGACCCGTATTACCGCGGCTGCTGG	

Table 6: **Primers used for overexpression studies.**
Forward amplification primers include a *Hind*III restriction site and reverse amplification primers a *Spe*I restriction site, respectively.

	Primer	Sequence	Description
1	IFCAGPOI_05107_FW	AAAAAAAAGCTTATGGCAGAGACCGAGACCACGAC	IFCAGPOI_05107
	IFCAGPOI_05107_RV	AAAAAAACTAGTTCACCCGCGCGGGCGCAG	(627 bp)
2	IFCAGPOI_04345_FW	AAAAAAAAGCTTATGAATCTCAAGGAACTGAACTGAAC	IFCAGPOI_04345
	IFCAGPOI_04345_RV	AAAAAAACTAGTTCACGGGATGCCCTTTCGTAC	(837 bp)
3	IFCAGPOI_03331_FW	AAAAAAAAGCTTGTGAGCTTCCGCCTCCGCGC	IFCAGPOI_03331
	IFCAGPOI_03331_RV	AAAAAAACTAGTTCACAGGCGGTCCAGGACGAC	(1623 bp)
4	IFCAGPOI_00860_FW	AAAAAAAAGCTTATGGACGAAACCGCGCGCGCC	IFCAGPOI_00860
	IFCAGPOI_00860_RV	AAAAAAACTAGTTCAGCCCGCAGATGTCCGCGTG	(1536 bp)
5	IFCAGPOI_01458_FW	AAAAAAAAGCTTATGGCAGAGAACAGGACAAC	IFCAGPOI_01458
	IFCAGPOI_01458_RV	AAAAAAACTAGTTCATAGCTCTCCCATCAACTC	(870 bp)
6	IFCAGPOI_02551_FW	AAAAAAAAGCTTATGACACCGCAGCAGGCAGGG	IFCAGPOI_02551
	IFCAGPOI_02551_RV	AAAAAAACTAGTTCAGATCAGCCGGCGTGCCG	(720 bp)
7	IFCAGPOI_03512_FW	AAAAAAAAGCTTATGGCAGGCGAGACCGTCATC	IFCAGPOI_03512
	IFCAGPOI_03512_RV	AAAAAAACTAGTCTAGAAGGGGGGCTCGTCCG	(606 bp)
8	IFCAGPOI_04383_FW	AAAAAAAAGCTTGTGGGACGCGGGGCGCAGTCG	IFCAGPOI_04383
	IFCAGPOI_04383_RV	AAAAAAACTAGTTCAGCGGCGCTTCGGCGCGGC	(582 bp)
9	IFCAGPOI_04468_FW	AAAAAAAAGCTTATGACGCGTGTACTGCTCGC	IFCAGPOI_04468
	IFCAGPOI_04468_RV	AAAAAAACTAGTCTAGTTCTTCTCGAAGCGGAAG	(678 bp)
10	IFCAGPOI_05876_FW	AAAAAAAAGCTTATGTCCGGCCACTCTAAATGG	IFCAGPOI_05876
	IFCAGPOI_05876_RV	AAAAAAACTAGTTCAGATGTCGACCTTCGCC	(752 bp)

	Primer	Sequence	Description
11	IFCAGPOI_05926_FW	AAAAAAAAGCTTGTGTCTGCTAGGTCGGCAGG	IFCAGPOI_05926
	IFCAGPOI_05926_RV	AAAAAAACTAGTTCACCAGACCGGACCGGAG	(921 bp)
12	IFCAGPOI_05966_FW	AAAAAAAAGCTTATGCGCATGGAGGACCTGG	IFCAGPOI_05966
	IFCAGPOI_05966_RV	AAAAAAACTAGTTCAGATGCTCGGCGGACG	(447 bp)
13	IFCAGPOI_05976_FW	AAAAAAAAGCTTGTGGGCGCGGCCCAGTTGG	IFCAGPOI_05976
	IFCAGPOI_05976_RV	AAAAAAACTAGTTCAGGCGACGAAGGTACGCGG	(1479 bp)
14	IFCAGPOI_06286_FW	AAAAAAAAGCTTATGACCGACCCCGGGGACGG	IFCAGPOI_06286
	IFCAGPOI_06286_RV	AAAAAAACTAGTTCAGCGCTTGAACCCCACGCAG	(804 bp)
15	IFCAGPOI_00339_FW	AAAAAAAAGCTTATGCGGTGCATGACGAACGCG	IFCAGPOI_00339
	IFCAGPOI_00339_RV	AAAAAAACTAGTTCACAGCCATCCGCTGCGC	(993 bp)
16	IFCAGPOI_01482_FW	AAAAAAAAGCTTGTGGTATTGGTGGAACGTTCGC	IFCAGPOI_01482
	IFCAGPOI_01482_RV	AAAAAAACTAGTTCAGCAGGCCGAGCCGTTG	(2763 bp)
17	IFCAGPOI_03805_FW	AAAAAAAAGCTTATGTGTGGAGCGAAGGCCGG	IFCAGPOI_03805
	IFCAGPOI_03805_RV	AAAAAAACTAGTTCAGACCGCGATCGCGACC	(288 bp)
18	IFCAGPOI_06136_FW	AAAAAAAAGCTTGTGTACTCTCGGTCCCATGAAC	IFCAGPOI_06136
	IFCAGPOI_06136_RV	AAAAAAACTAGTTCAGTGCGCATGCGGGTCC	(615 bp)
19	IFCAGPOI_05711_FW	AAAAAAAAGCTTATGATGCGGCTCGGCATCAATCTC	IFCAGPOI_05711
	IFCAGPOI_05711_RV	AAAAAAACTAGTTCAGGCCAGTCCGGCGTGC	(1050 bp)
20	IFCAGPOI_01705_FW	AAAAAAAAGCTTGTGCCCGATACTGGGTGGG	IFCAGPOI_01705
	IFCAGPOI_01705_RV	AAAAAAACTAGTTCAGTCGCCGATGAGGGCG	(1242 bp)
21	IFCAGPOI_02717_FW	AAAAAAAAGCTTATGGCCGACTCCAGTTTCG	IFCAGPOI_02717
	IFCAGPOI_02717_RV	AAAAAAACTAGTTCAGCGGTAGTTGACGAACTG	(489 bp)
22	IFCAGPOI_03574_FW	AAAAAAAAGCTTATGACCTCGCTTCCGACCGGC	IFCAGPOI_03574
	IFCAGPOI_03574_RV	AAAAAAACTAGTTCAGGTCGCCGGAAGCTGGTAG	(789 bp)
23	IFCAGPOI_04736_FW	AAAAAAAAGCTTATGACGGTCACTCTGGCGGATGTCGC	IFCAGPOI_04736
	IFCAGPOI_04736_RV	AAAAAAACTAGTTCAGCCGCGGGGCGGCGCC	(1062 bp)
24	IFCAGPOI_05697_FW	AAAAAAAAGCTTATGACCACAGCGGGCCATGGCC	IFCAGPOI_05697
	IFCAGPOI_05697_RV	AAAAAAACTAGTTCAGACGCCCGGCAGGGTGG	(741 bp)
25	IFCAGPOI_06331_FW	AAAAAAAAGCTTATGCCGACACGCCGTCAGTCC	IFCAGPOI_06331
	IFCAGPOI_06331_RV	AAAAAAACTAGTTCAGCCGTCCGCACCGCCG	(1986 bp)
26	IFCAGPOI_00009_FW	AAAAAAAAGCTTGTGAGCGGCGCATCCGACC	IFCAGPOI_00009
	IFCAGPOI_00009_RV	AAAAAAACTAGTTCAGGCTCCGATTCCGATGGC	(585 bp)
27	IFCAGPOI_00306_FW	AAAAAAAAGCTTATGAACGGAACGGCGGAGGCAGGAC	IFCAGPOI_00306
	IFCAGPOI_00306_RV	AAAAAAACTAGTTCAGCCGGGTCTCTTGGCCGCC	(522 bp)
28	IFCAGPOI_05548_FW	AAAAAAAAGCTTGTGACCACCCGGCGCACCCG	IFCAGPOI_05548
	IFCAGPOI_05548_RV	AAAAAAACTAGTTCAGGCGCCGCCGGTGTGGAC	(1329 bp)
29	IFCAGPOI_06487_FW	AAAAAAAAGCTTATGCCGGAACCGAGGACACTC	IFCAGPOI_06487
	IFCAGPOI_06487_RV	AAAAAAACTAGTTCAGTCGGCCCTGGCCAGG	(2913 bp)
30	IFCAGPOI_06489_FW	AAAAAAACTAGTTCACGGGGCGATGCCCCC	IFCAGPOI_06489
	IFCAGPOI_06489_RV	AAAAAAAAGCTTATGAAGGGACGAGTCCTAGTCG	(645 bp)
31	IFCAGPOI_04513_FW	AAAAAAAAGCTTATGAAGGGACGAGTCCTAGTCG	IFCAGPOI_04513
	IFCAGPOI_04513_RV	AAAAAAACTAGTTCAGCTCGGTCCCGCCTTG	(678 bp)
32	IFCAGPOI_05727_FW	AAAAAAAAGCTTGTGGCAATCCGCGTTCTGCTGGTC	IFCAGPOI_05727
	IFCAGPOI_05727_RV	AAAAAAACTAGTCTACTGCGCGCCCGGGCGC	(672 bp)
33	IFCAGPOI_00682_FW	AAAAAAAAGCTTATGACCGTGGACACCAGCCCG	IFCAGPOI_00682
	IFCAGPOI_00682_RV	AAAAAAACTAGTTCAGCTTCCGGTACGGGCGATC	(1416 bp)
34	IFCAGPOI_01589_FW	AAAAAAAAGCTTATGGTGCAGAAGGCCAAGATC	IFCAGPOI_01589
	IFCAGPOI_01589_RV	AAAAAAACTAGTTCAGTTCTGCGAGGGCACC	(684 bp)
35	IFCAGPOI_02857_FW	AAAAAAAAGCTTGTGGGCGTCATGTGCGGAAGG	IFCAGPOI_02857
	IFCAGPOI_02857_RV	AAAAAAACTAGTCTAAGCGGATTCGACCCCCACG	(249 bp)

	Primer	Sequence	Description
36	IFCAGPOI_03410_FW	AAAAAAAAGCTTATGTGTGAGACTGCAAGCGTGC	IFCAGPOI_03410
	IFCAGPOI_03410_RV	AAAAAAACTAGTCTAGTACGTCCCGGACGGG	(699 bp)
37	IFCAGPOI_03597_FW	AAAAAAAAGCTTGTGAGCAGCAGGCCATCCCG	IFCAGPOI_03597
	IFCAGPOI_03597_RV	AAAAAAACTAGTTCAGTTGGTGCCGATCTTGGCG	(4014 bp)
38	IFCAGPOI_04924_FW	AAAAAAAAGCTTATGAGCGTGCGTACCCAGCC	IFCAGPOI_04924
	IFCAGPOI_04924_RV	AAAAAAACTAGTTCAGAAGCCGAGCTTGCGGAG	(945 bp)
39	IFCAGPOI_05636_FW	AAAAAAAAGCTTATGAACGACCAGCACGACCAC	IFCAGPOI_05636
	IFCAGPOI_05636_RV	AAAAAAACTAGTCTACTTCTTGCGGCCGCGC	(1449 bp)
40	IFCAGPOI_06421_FW	AAAAAAAAGCTTATGACCAGTGGGGTGGCGTTCC	IFCAGPOI_06421
	IFCAGPOI_06421_RV	AAAAAAACTAGTTCACCGCCGCCCGGAAACGG	(1296 bp)
41	IFCAGPOI_01486_FW	AAAAAAAAGCTTGTGGAGGACGATCGGCCGGGC	IFCAGPOI_01486
	IFCAGPOI_01486_RV	AAAAAAACTAGTTCAGGCTCCGGTTCGGTGCCCG	(720 bp)
42	IFCAGPOI_06084_FW	AAAAAAAAGCTTGTGGGGACCACGCATCTGGAGAC	IFCAGPOI_06084
	IFCAGPOI_06084_RV	AAAAAAACTAGTTCAGGAGGCCCTGCGCTCCTC	(765 bp)
43	IFCAGPOI_06386_FW	AAAAAAAAGCTTGTGCGAGCAGCCCCTTATGAACTGATC	IFCAGPOI_06386
	IFCAGPOI_06386_RV	AAAAAAACTAGTCTACCCGCACCGGTCGCCCC	(2760 bp)
44	pUWL_test_FW	ACGCCTGGTCGATGTCGGAC	Testprimer 1 for pUWL-apra-oriT vector (empty vector: 381 bp)
	pUWL_test_RV	GAGCGAGGAAGCGGAAGAGC	
45	pUWL_test_FW_new	CACTTCGTGCAGGCGGTACC	Testprimer 2 for pUWL-apra-oriT vector (empty vector: 444 bp)
	pUWL_test_RV	GAGCGAGGAAGCGGAAGAGC	
46	pUWL_test_FW_new	CACTTCGTGCAGGCGGTACC	Testprimer 3 for pUWL-apra-oriT vector (empty vector: 426 bp)
	pUWL_test_RV_new	GCGCCCAATACGCAAACCGC	

Table 7: **Primers used for simultaneous overexpression of regulators (AGOS system).** Forward amplification primers include a *Spe*I restriction site and reverse amplification primers a *Xba*I restriction site, respectively.

	Primer	Sequence	Description
1	AGOS_1_05107_FW	AAAAAA ACTAGT ATGGCAGAGACCGAGACCACGACCG	IFCAGPOI_05107 (627 bp)
	AGOS_1_05107_RV	AAAAAA TCTAGA TCACCCGCGCGGGCGCAGCC	
2	AGOS_3_03331_FW	AAAAAA ACTAGT GTGAGCTTCCGCCTCCGCG	IFCAGPOI_03331 (1623 bp)
	AGOS_3_03331_RV	AAAAAA TCTAGA TCACAGGCGGTCCAGGACGAC	
3	AGOS_16_01482_FW	AAAAAA ACTAGT GTGGTATTGGTGGAACGTTCGCG	IFCAGPOI_01482 (2763 bp)
	AGOS_16_01482_RV	AAAAAA TCTAGA TCAGCAGGCCGAGCCGTTGC	
4	AGOS_23_04736_FW	AAAAAAACTAGTATGACGGTCACTCTGGCGGATGTCGCCG	IFCAGPOI_04736 (1062 bp)
	AGOS_23_04736_RV	AAAAAA TCTAGA TCAGCCGCGGGGCGGCGCCG	
5	AGOS_30_06489_FW	AAAAAA ACTAGT ATGCCCAGAAGTGCCGATCCCCACC	IFCAGPOI_06489 (645 bp)
	AGOS_30_06489_RV	AAAAAA TCTAGA TCACGGGGCGATGCCCCCCG	
6	AGOS_40_06421_FW	AAAAAA ACTAGT ATGACCAGTGGGGTGGCGTTCCTC	IFCAGPOI_06421 (1296 bp)
	AGOS_40_06421_RV	AAAAAA TCTAGA TCACCGCCGCCCGGAAACGG	

	Primer	Sequence	Description
7	AGOS_fkbN_06386_FW	AAAAAA ACTAGT GTGCGAGCAGCCCCTTATGAACTGATC	IFCAGPOI_06386 (2760 bp)
	AGOS_fkbN_06386_RV	AAAAAA TCTAGA CTACCCGCACCGGTCGCCCC	
8	fkbN_test_FW	GTACTCGTCCAGCGGATGAC	Testprimers for IFCAGPOI_06386 (1179 bp)
	fkbN_test_RV	AGAGCAGATGCAGCCCGAAG	
9	pLW_test_FW	CAGCGTGACATCATTCTGTG	Testprimers for pLW entry plasmids (empty vector: 252 bp)
	pLW_test_RV	CAAGCTTCCCACTTAGAATTC	
10	mrsMR02_FW_test	CCACCTGACGTCTAAGAAAC	Testprimers for mrsMR02 destination vector (empty vector: 1603 bp)
	mrsMR02_RV_test	CCTCTGTCGTTTCCTTTCTC	

Table 8: **Primers used for the module swap approach.**
Numbers in brackets indicate the expected fragment size.

	Primer	Sequence	Description
1	knockout_M10_FW	GAGCACGGTGGGCGGGTCGTCGTCCGCGCCGTCGCCGAG ATTCCGGGGATCCGTCGACC	Long PCR primers to amplify the apra_MRS cassette for a knockout of module 10 (1291 bp)
	knockout_M10_RV	CGGGACCGGGACCGGGACCGGGACCGGGACCGGGACGAG TGTAGGCTGGAGCTGCTTC	
2	knockout_M10_test_FW	GTCGAGGAGATCGGCGATGG	Testprimers for the knockout of module 10 (1454 bp)
	knockout_M10_test_RV	CGGGCATCTGCTGGAACTGC	
3	500_up_F	AAAAAA GAATTC CGCGTACCCCGGAGCCGGTG	Amplification of 500 bp upstream homology arm including *Eco*RI and *Xba*I restriction sites (574 bp)
	500_down_R	CCGCCGGATAGTCGA TCTAGA GCGACCCCGCCCG-GCAGCCGGCAGGCCATGCCCACGATCGCCAGCGGTTC GTCCCGGTCCCGGTCCCGGTC	
4	500_down_F	GCCGGGCGGGGTCGC TCTAGA TCGACTATCCGGCG-GCCGGGACACTCACCCGCCACCTGCTCACGCTCCTG GGCGACGGCGCGGACGACGAC	Amplification of 500 bp downstream homology arm including *Eco*RI and *Xba*I restriction sites (574 bp)
	500_down_R	AAAAAA GAATTC ACAGGCGTCGGCCGCCTCGAC	
5	M4_FW	GAACCGCTGGCGATCGTGGG	Amplification primers for module 4 (4598 bp)
	M4_RV	CAGGAGCGTGAGCAGGTGGC	
6	GKMS_1_FW	TCCATCTCCGTCAGGAGTTC	Testprimers (1) for module 4 flanked by 500 bp (520 bp)
	GKMS_1_RV	TAGAAGTACGAGAGACGGCC	
7	GKMS_2_FW	TCGGCGTCAGCGGCACCAAC	Testprimers (2) for module 4 flanked by 500 bp (688 bp)
	GKMS_2_RV	GCGAGTTCGCGCTGGAGCAG	
8	GKMS_3_FW	CAGTACTCGGGCTGGTTCGC	Testprimers (3) for module 4 flanked by 500 bp (547 bp)
	GKMS_3_RV	AACAGCGGCGCGTGATGCAG	
9	M4N_R_F	TGCGCTCCGTGAGGAACAGC	Testprimers (1) for the module swap (1440 bp)
	M4N_R_R	GGCATCTGCTGGAACTGCTCGG	
10	M4N_L_F	CTCGATCCCGTCCAGACAGGCG	Testprimers (2) for the module swap (929 bp)
	M4N_L_R	CGGCAGACCGAACTGCTCGACG	

	Primer	Sequence	Description
11	SC1TR01_Seq_f	GCCACCTGACGTCTAAGAAAC	Testprimers for SuperCosI (empty vector: 217 bp)
	SC1TR01_Seq_r	CCGTGGAATGAACAATGGAAG	
12	M4_test1_FW	CACCGGTGTGTTCATCGGCG	Primers for sequencing of module 4 (934 bp)
	M4_test2_RV	GGACGGTGAATCCGGAGCCG	
13	M4_test3_FW	GGACACGGCGCGATGGGTTC	Primers for sequencing of module 4 (1009 bp)
	M4_test4_RV	CGCGGCGTCCGCCGTCGTCG	
14	M4_test5_FW	GGCGCTGCCCGCGACCGGCG	Primers for sequencing of module 4 (1490 bp)
	M4_test6_RV	GGCAGGGTGCCGCCGCTTGC	
15	M4_test7_FW	CCGACGGTCTGTGGCGGCTG	Primers for sequencing of module 4 (492 bp)
	M4_test8_RV	CGCAGCGACTGACCGGCCTG	
16	M4_test9_FW	CCTCGGGGACCCCATCGAAG	Primers for sequencing of module 4 (541 bp)
	M4_test10_RV	CGGTGCGGGTGGAGAACAGC	
17	M4_test11_FW	GGGTACGTCCGGACGCCGTC	Primers for sequencing of module 4 (961 bp)
	M4_test12_RV	CGTGGCTCGCCGGGCACTCC	
18	M4_test13_FW	CGTGGCTCGCCGGGCACTCC	Primers for sequencing of module 4 (641 bp)
	M4_test14_RV	CGCCGTCGGCGGCGGTGAAG	
19	M4_test15_FW	GTACGGGTCCATTCGAGCGG	Primers for sequencing of module 4 (406 bp)
	M4_test16_RV	GACGGCACCGGCAGTGGTTC	
20	Deletion_up_FW	GACCACACCGCCGCCCTGGC	Testprimers for the deletion (upstream) (924 bp)
	Deletion_up_RV	GGCCGAGCCGCGGTACGTGG	
21	Deletion_down_FW	GCCTCCTCCCAGGTGAGATG	Testprimers for the deletion (downstream) (939 bp)
	Deletion_down_RV	CCGAGTTCGCCCGCTTCATG	

Table 9: **Primers used for the AT domain swap approach.**

	Primer	Sequence	Description
1	pCRISPR-TT_ATM4_FW1	CATG CCATGG GACGGGCGCTGCAAATCGTT GTTTTA-GAGCTAGAAATAGC	Amplification of spacer 1 (123 bp) flanked by *Nco*I and *Sna*BI restriction sites
	pCRISPR_TT_RV	ACGCC TACGTA AAAAAAGCACCGACTCGGTGCC	
2	pCRISPR-TT_ATM4_FW2	CATG CCATGG GTCCTCGAATCCATCCC GTTGTTTTA-GAGCTAGAAATAGC	Amplification of spacer 2 (123 bp) flanked by *Nco*I and *Sna*BI restriction sites
	pCRISPR_TT_RV	ACGCC TACGTA AAAAAAGCACCGACTCGGTGCC	
3	1000bp_up_ATS_F	GTCGACGGTATCGATAAGCTT GATATC CATGGACC-CGCAGCAGCGCC	Amplification of 1000 bp upstream homology arm (1036 bp)
	1000bp_up_ATS_R	CGAGGATGACGTGGGCGTTGGTGCCG CTGAGCCC-GAACGCGGAGAC	

	Primer	Sequence	Description
4	1000bp_down_ATS_F	GAGCGCTACTGGATC GCATCCGGCCCGGGCAGGAG	Amplification of 1000 bp downstream homology arm (1036 bp)
	1000bp_down_ATS_R	CCCCCGGGCTGCAGGAATTC GATATC TGGACGAA-GAAGTCGTCCGTC	
5	ATM4-FW	GCGTTCGGGCTCAGC GGCACCAACGCCCACGTCATC	Amplification of the AT domain of module 4 (1383 bp)
	ATM4-RV	GCCCGGGCCGGATGC GATCCAGTAGCGCTCGTGGTG	
6	ATswap_test_1_FW	GTCAGCGGTGGAGGCGAGGC	Testprimers for the AT domain swap (1750 bp)
	M4_test3_FW	GGACACGGCGCGATGGGTTC	
7	M4_test10_RV	CGGTGCGGGTGGAGAACAGC	Testprimers for the AT domain swap (1603 bp)
	knockout_M10_test_R	CGGGCATCTGCTGGAACTGC	
8	ATswap_test_3_FW	CTTCGAGGATGACGTGGGCG	Testprimers for the AT domain swap (1393 bp)
	knockout_M10_test_R	CGGGCATCTGCTGGAACTGC	
9	M4N_L_F	CTCGATCCCGTCCAGACAGGCG	Testprimers for the AT domain of module 10 (1078 bp)
	AT-M10_test1_RV	CTCGCGGACCGCGGTGTGAAC	
10	AT-M10_test2_FW	CGCCCCATGCCCGTGCGCTG	Testprimers for the AT domain of module 10 (1045 bp)
	AT-M10_test3_RV	GCACTCGCGGGCGGCGTCTC	

Table 10: **Primers used for the ACP domain swap approach.**

	Primer	Sequence	Description
1	KO_ACP_M10_FW	TTCGAGCACGGTGGGCGGGTCGTCGTCCGCGCCGTCGCC ATTCCGGGGATCCGTCGACC	Long PCR primers to amplify the apra_MRS cassette for a knockout of the ACP domain of module 10 (1291 bp)
	KO_ACP_M10_RV	TGGGGCGAGGAGCCCGAAGCGGGGGACCTCGGCATC GCCTGTAGGCTGGAGCTGCTTC	
2	knockout_M10_test_FW	GTCGAGGAGATCGGCGATGG	Testprimers for the ACP domain swap (721 bp)
	ACPswap_test_RV	CTACCACTCGGTGCTGCGTG	
3	pEX-A258_FW	AAAACCTCTGACACATGCAG	Primers to amplify KirACP5 flanked by 500 bp homology arms from vector pEX-A258-KirACP5 (Eurofins) (1668 bp)
	pEX-A258_RV	CGCAACGCAATTAATGTGAG	
4	pEM11CII_test_FW	GCGCCATTCGCCATTCAGGC	Testprimers for plasmid pEM11CII (1666 bp)
	pEM11CII_test_RV	CCGGTTGGTAGGATCGACGG	
5	pCRISPR-TT_ACPM10_FW1	CATG CCATGG CGGTGCAGCGCCTGCGCAAC GTTTTA-GAGCTAGAAATAGC	Amplification of spacer 1 (123 bp) for CRISPR-Cas9 based approach
	pCRISPR_TT_RV	ACGCC TACGTA AAAAAAGCACCGACTCGGTGCC	
6	pCRISPR-TT_ACPM10_FW2	CATG CCATGG GACTCGACGTTCTTCGCACT GTTTTA-GAGCTAGAAATAGC	Amplification of spacer 2 (123 bp) for CRISPR-Cas9 based approach
	pCRISPR_TT_RV	ACGCC TACGTA AAAAAAGCACCGACTCGGTGCC	

2.1.6 Enzymes

Table 11: **Enzymes used in this study.**
Unless stated otherwise, all enzymes were purchased from New England BioLabs®$_{Inc.}$, Ipswich, Massachusetts, USA.

Enzyme	Specification
Alkaline Phosphatase	Calf Intestinal Phosphatase (CIP)
*Bae*I	CutSmart® Buffer, 37 °C, 20 μM *S*-adenosylmethionine (SAM)
Blunt/TA Ligase Master Mix	4 °C
*Eco*RI	CutSmart® Buffer, 37 °C
*Eco*RV	CutSmart® Buffer, 37 °C
Gibson Assembly® Master Mix	1 h, 50 °C
*Hind*III	CutSmart® Buffer, 37 °C
I-*Sce*I	CutSmart® Buffer, 37 °C
Lysozyme	from chicken egg white
*Nco*I	CutSmart® Buffer, 37 °C
NEBuilder® HiFi DNA Assembly Master Mix	15 min, 50 °C
*Pac*I	CutSmart® Buffer, 37 °C
*Pci*I	CutSmart® Buffer, 37 °C
Phusion® High-Fidelity DNA polymerase	see 2.2.3.1
*Pme*I	CutSmart® Buffer, 37 °C
Proteinase K	Carl Roth GmbH & Co. KG, Karlsruhe, Germany
Q5® High-Fidelity DNA polymerase	see 2.2.2.11
RNase	stock solution: 100 mg/mL working concentration 0.1 mg/mL
*Sna*BI	CutSmart® Buffer, 37 °C
*Spe*I	CutSmart® Buffer, 37 °C
*Stu*I	CutSmart® Buffer, 37 °C
*Swa*I	1x NEBuffer™ 3.1, 25 °C
Taq:Pfu polymerase (9:1)	prepared in-house (Department of Pharmaceutical Biology); see 2.2.2.3
T4 DNA Ligase	T4 DNA ligase buffer, 4 °C
*Xba*I	CutSmart® Buffer, 37 °C

2.1.7 Kits

Table 12: **Kits used in this study.**

Kit	Specification	Manufacturer
Cycle Pure Kit	purification of PCR products	PEQLAB Biotechnologie GmbH, Erlangen, Germany
pGEM®-T Easy Vector cloning kit	kit for TA cloning approaches	Promega, Madison, Wisconsin, USA
QIAquick PCR Purification Kit	purification of PCR products	QIAGEN, Hilden, Germany
QIAquick Gel Extraction Kit	purification of DNA from agarose gels	QIAGEN, Hilden, Germany
Quick Blunting™ Kit	generation of blunt-ended DNA	New England BioLabs®Inc., Ipswich, Massachusetts, USA
Quick Ligation™ Kit	execution of efficient blunt end ligations	New England BioLabs®Inc., Ipswich, Massachusetts, USA

2.1.8 Size standards for gel electrophoresis

Table 13: **Size standards used in this study.**

Size standard	Specification	Manufacturer
GeneRuler 1 kb DNA Ladder	250-10000 bp	Thermo Fisher Scientific, Waltham, Massachusetts, USA
GeneRuler High Range DNA Ladder	10171-48502 bp	Thermo Fisher Scientific, Waltham, Massachusetts, USA

2.1.9 Antibiotics and Inductors

Table 14: **Antibiotics and inductors used in this study.**

Antibiotic	Concentration of stock solution [mg/mL]	Concentration in media [μg/mL]	Solvent
Anhydrotetracycline (aTc)	5	1	100 % ethanol
Apramycin (Apra)	50	50	ddH_2O
Carbenicillin (Carb)	50	50	ddH_2O
Chloramphenicol (Cml)	25	25	100 % ethanol
Kanamycin (Kan)	50	50	ddH_2O
Nalidixic acid (Ndx)	25	25	0.3 M NaOH
Theophylline (Theo)	28.83 (160 mM)	1801.64 (10 mM)	0.1 M NaOH
Thiostrepton (Thio)	50	60	DMSO

2.1.10 Strains

Table 15: **Strains used in this study.**

Organism	Strain	Genotype	Reference	Application
E. coli	BW25113	*Δ(araD-araB)567, Δ(rhaD-rhaB)568, ΔlacZ4787(::rrnB-3), hsdR514, rph-1*	Datsenko and Wanner (2000)	used for λ-RED recombination (PCR targeting)
E. coli	DH5α	*huA2, lacΔU169, phoA, glnV44, Φ 80', lacZΔM15, gyrA96, recA1, relA1, endA1, thi-1, hsdR17*		cloning strain
E. coli	DH10β	*F'mcrAΔ-(mrr hsdRMS-mcrBC), φ80dlacZΔM15, ΔlacX74, deoR, recA1, araD139, Δ(ara,leu)7697, galUgalKλ⁻rpsL, end, A1, nupG*		cloning strain for large vectors/BACs

Organism	Strain	Genotype	Reference	Application
E. coli	ET12567	*dam-13::Tn9, dcm-6, hsdM, hsdR, recF143 zjj201::Tn10 galK2, gal T22, ara14, lacY1, xyl5, leuB6, thi1, tonA31, rpsL136, hisG4, tsx78, mtli, glnV44*	MacNeil *et al.* (1992)	used for inter-generic conjugation
E. coli	XL1-Blue	*recA1, endA1, gyrA96 (nal^r), thi-1, hsdR17($r_k^-m_k^+$), supE44, relA1, lac [F´, proAB$^+$, lacI^{q}ZΔM15, Tn10,(Tet^r)]*	Stratagene Inc., La Jolla, California, USA	cloning strain
Streptomyces tsukubaensis	NRRL18488	WT	Barreiro *et al.* (2012)	wild type producer strain
Streptomyces tsukubaensis	NRRL18488-MS	WT strain with modified PKS: module 10 replaced by module 4	this study	module swap strain; 6 individual exconjugants
Streptomyces tsukubaensis	NRRL18488-AT	WT strain with modified PKS: AT domain of module 10 replaced by AT domain of module 4	this study	AT domain swap strain; 7 individual exconjugants
Streptomyces tsukubaensis	NRRL18488-ACP	WT strain with modified PKS: ACP domain of module 10 replaced by ACP5 domain of the kirromycin biosynthetic gene cluster (KirACP5)	this study	ACP domain swap strain; 4 individual exconjugants
Streptomyces coelicolor	M512	Δ*redD*, Δ*actII-ORF4*	Floriano and Bibb (1996)	heterologous host strain
	M1146	Δ*act*, Δ*red*, Δ*cpk*, Δ*cda*	Gomez-Escribano and Bibb (2011)	heterologous host strain
	M1152	Δ*act*, Δ*red*, Δ*cpk*, Δ*cda*, *rpoB*(C1298T)	Gomez-Escribano and Bibb (2011)	heterologous host strain
	M1154	Δ*act*, Δ*red*, Δ*cpk*, Δ*cda*, *rpoB*(C1298T), rpsL(A262G)	Gomez-Escribano and Bibb (2011)	heterologous host strain
Streptomyces albus	J1074	WT		heterologous host strain

2.1.11 Plasmids and Cosmids

Table 16: **Plasmids used in this study.**

Plasmid	Characteristics	Reference
pAC20N	Kan^R, $Thio^R$ tacrolimus biosynthetic gene cluster cloned into *Bam*HI restriction sites 129429 bp	Jones *et al.* (2013)
pBluescript II SK(-)	$Carb^R$ 2958 bp cloning vector	Stratagene Inc., La Jolla, California, USA
pCRISPR-TT	$Apra^R$ CRISPR-Cas9 system; temperature sensitive origin of replication 9862 bp	Albuquerque & Mendes, IBMC, University of Porto, Portugal
pEM11CII (pRM4_KirCII)	$Apra^R$ expression of KirCII under control of the *ermE** promoter 7441 bp	Musiol *et al.* (2011)
pEX-A258-KirACP5	$Carb^R$ vector harboring KirACP5 flanked by 500 bp homology arms to up- and downstream regions of ACP(M10) 2446 bp	Eurofins Genomics, Ebersberg, Germany
pGEM-T	$Carb^R$ linearized vector for TA cloning; *lacZ*α, f1-ori	Promega, Madison, Wisconsin, USA
pIJ790	Cml^R λ-RED recombination plasmid; temperature sensitive origin of replication 6084 bp	Gust *et al.* (2003)
pLW54-60	$Apra^R$ pBS II SK(+) modified with recombineering sites A-G; entry plasmids for the AGOS system	Basitta *et al.* (2017)
pR9406	$Carb^R$ helper plasmid for triparental *E. coli* conjugation	David Figurski
pTB01	$Apra^R$, $Carb^R$ pUWL-apra-oriT vector + IFCAGPOI_05107 8007 bp	this study
pTB02	$Apra^R$, $Carb^R$ pUWL-apra-oriT vector + IFCAGPOI_04345 8217 bp	this study
pTB03	$Apra^R$, $Carb^R$ pUWL-apra-oriT vector + IFCAGPOI_03331 9003 bp	this study

Plasmid	Characteristics	Reference
pTB04	Apra^R, Carb^R pUWL-apra-oriT vector + IFCAGPOI_00860 8916 bp	this study
pTB05	Apra^R, Carb^R pUWL-apra-oriT vector + IFCAGPOI_01458 8250 bp	this study
pTB06	Apra^R, Carb^R pUWL-apra-oriT vector + IFCAGPOI_02551 8100 bp	this study
pTB07	Apra^R, Carb^R pUWL-apra-oriT vector + IFCAGPOI_03512 7986 bp	this study
pTB08	Apra^R, Carb^R pUWL-apra-oriT vector + IFCAGPOI_04383 7962 bp	this study
pTB09	Apra^R, Carb^R pUWL-apra-oriT vector + IFCAGPOI_04468 8058 bp	this study
pTB10	Apra^R, Carb^R pUWL-apra-oriT vector + IFCAGPOI_05876 8133 bp	this study
pTB11	Apra^R, Carb^R pUWL-apra-oriT vector + IFCAGPOI_05926 8301 bp	this study
pTB12	Apra^R, Carb^R pUWL-apra-oriT vector + IFCAGPOI_05966 7827 bp	this study
pTB13	Apra^R, Carb^R pUWL-apra-oriT vector + IFCAGPOI_05976 8859 bp	this study
pTB14	Apra^R, Carb^R pUWL-apra-oriT vector + IFCAGPOI_06286 8184 bp	this study
pTB15	Apra^R, Carb^R pUWL-apra-oriT vector + IFCAGPOI_00339 8373 bp	this study
pTB16	Apra^R, Carb^R pUWL-apra-oriT vector + IFCAGPOI_01482 10143 bp	this study
pTB17	Apra^R, Carb^R pUWL-apra-oriT vector + IFCAGPOI_03805 7686 bp	this study

Plasmid	Characteristics	Reference
pTB18	Apra^R, Carb^R pUWL-apra-oriT vector + IFCAGPOI_06136 7995 bp	this study
pTB19	Apra^R, Carb^R pUWL-apra-oriT vector + IFCAGPOI_05711 8430 bp	this study
pTB20	Apra^R, Carb^R pUWL-apra-oriT vector + IFCAGPOI_01705 8622 bp	this study
pTB21	Apra^R, Carb^R pUWL-apra-oriT vector + IFCAGPOI_02717 7869 bp	this study
pTB22	Apra^R, Carb^R pUWL-apra-oriT vector + IFCAGPOI_03574 8169 bp	this study
pTB23	Apra^R, Carb^R pUWL-apra-oriT vector + IFCAGPOI_04736 8442 bp	this study
pTB24	Apra^R, Carb^R pUWL-apra-oriT vector + IFCAGPOI_05697 8121 bp	this study
pTB25	Apra^R, Carb^R pUWL-apra-oriT vector + IFCAGPOI_06331 9366 bp	this study
pTB26	Apra^R, Carb^R pUWL-apra-oriT vector + IFCAGPOI_00009 7965 bp	this study
pTB27	Apra^R, Carb^R pUWL-apra-oriT vector + IFCAGPOI_00306 7902 bp	this study
pTB28	Apra^R, Carb^R pUWL-apra-oriT vector + IFCAGPOI_05548 8709 bp	this study
pTB30	Apra^R, Carb^R pUWL-apra-oriT vector + IFCAGPOI_06489 8025 bp	this study
pTB31	Apra^R, Carb^R pUWL-apra-oriT vector + IFCAGPOI_04513 8058 bp	this study
pTB32	Apra^R, Carb^R pUWL-apra-oriT vector + IFCAGPOI_05727 8052 bp	this study

Plasmid	Characteristics	Reference
pTB33	Apra^R, Carb^R pUWL-apra-oriT vector + IFCAGPOI_00682 8796 bp	this study
pTB34	Apra^R, Carb^R pUWL-apra-oriT vector + IFCAGPOI_01589 8064 bp	this study
pTB35	Apra^R, Carb^R pUWL-apra-oriT vector + IFCAGPOI_02857 7626 bp	this study
pTB36	Apra^R, Carb^R pUWL-apra-oriT vector + IFCAGPOI_03410 8079 bp	this study
pTB38	Apra^R, Carb^R pUWL-apra-oriT vector + IFCAGPOI_04924 8325 bp	this study
pTB40	Apra^R, Carb^R pUWL-apra-oriT vector + IFCAGPOI_06421 8676 bp	this study
pTB41	Apra^R, Carb^R pUWL-apra-oriT vector + IFCAGPOI_01486 8100 bp	this study
pTB42	Apra^R, Carb^R pUWL-apra-oriT vector + IFCAGPOI_06084 8145 bp	this study
pTB43	Apra^R, Carb^R pUWL-apra-oriT vector + IFCAGPOI_06386 10140 bp	this study
pTB64	Carb^R SuperCosI derivative with 1112 bp insert consisting of 500 bp homology arms to the up- and downstream regions of module 10 and 50 bp capture arms for module 4, split by a *Xba*I restriction site 7913 bp	this study
pTB65	Carb^R SuperCosI derivative harboring module 4 flanked by 500 bp homology arms to the up- and downstream regions of module 10 12405 bp	this study
pTB66	Kan^R, Tsr^R pAC20N with knockout of module 10 (apra_MRS resistance cassette including *I-Sce*I site) 127729 bp	this study

Plasmid	Characteristics	Reference
pTB67	Kan^R, Tsr^R pAC20N with module 10 replaced by module 4 131114 bp	this study
pTB68	$Apra^R$ pCRISPR-TT with spacer 1 for the AT domain swap cloned into *Nco*I/*Sna*BI site 9882 bp	this study
pTB69	$Apra^R$ pCRISPR-TT with spacer 2 for the AT domain swap cloned into *Nco*I/*Sna*BI site 9882 bp	this study
pTB70	$Carb^R$ pBlueScript SK(-) with homology domain for the AT domain swap 6317 bp	this study
pTB71	$Apra^R$ pCRISPR-TT with spacer 1 for the AT domain swap and homology domain cloned into the *Stu*I site 13261 bp	this study
pTB72	$Apra^R$ pCRISPR-TT with spacer 2 for the AT domain swap and homology domain cloned into the *Stu*I site 13261 bp	this study
pTB73	Kan^R, Tsr^R pAC20N with knockout of ACP domain of module 10 (apra_MRS resistance cassette including *I-Sce*I site) 130432 bp	this study
pTB74	Kan^R, Tsr^R pAC20N with ACP domain of module 10 replaced by KirACP5 129555 bp	this study
pTB75	$Apra^R$ pCRISPR-TT with spacer 1 for the AT domain swap and homology domain (module 4 flanked by 500 bp homology arms) cloned into the *Stu*I site 15480 bp	this study
pTB76	$Apra^R$ pCRISPR-TT with spacer 2 for the AT domain swap and homology domain (module 4 flanked by 500 bp homology arms) cloned into the *Stu*I site 15480 bp	this study

Plasmid	Characteristics	Reference
pTB77	Apra^R pCRISPR-TT with spacer 1 for the ACP domain swap cloned into the *Nco*I/*Sna*BI site 9882 bp	this study
pTB78	Apra^R pCRISPR-TT with spacer 2 for the ACP domain swap cloned into the *Nco*I/*Sna*BI site 9882 bp	this study
pTB79	Apra^R pCRISPR-TT with spacer 1 for the ACP domain swap and homology domain (KirACP5 flanked by 500 bp homology arms) cloned into the *Stu*I site 11230 bp	this study
pTB80	Apra^R pCRISPR-TT with spacer 2 for the ACP domain swap and homology domain (KirACP5 flanked by 500 bp homology arms) cloned into the *Stu*I site 11230 bp	this study
pTB88	Apra^R pLW54 with IFCAGPOI_06386 cloned into the *Spe*I/*Xba*I restriction sites	Alexander Hoffreiter
pTB89	Apra^R pLW55 with IFCAGPOI_05107 cloned into the *Spe*I/*Xba*I restriction sites	Alexander Hoffreiter
pTB90	Apra^R pLW56 with IFCAGPOI_03331 cloned into the *Spe*I/*Xba*I restriction sites	Alexander Hoffreiter
pTB91	Apra^R pLW57 with IFCAGPOI_01482 cloned into the *Spe*I/*Xba*I restriction sites	Alexander Hoffreiter
pTB92	Apra^R pLW58 with IFCAGPOI_04736 cloned into the *Spe*I/*Xba*I restriction sites	Alexander Hoffreiter
pTB93	Apra^R pLW59 with IFCAGPOI_06489 cloned into the *Spe*I/*Xba*I restriction sites	Alexander Hoffreiter
pTB94	Apra^R pLW60 with IFCAGPOI_06421 cloned into the *Spe*I/*Xba*I restriction sites	Alexander Hoffreiter
pUB307	Kan^R conjugative plasmid used as helper element to mobilize vectors in triparental conjugations	Bennett *et al.* (1977)

Plasmid	**Characteristics**	**Reference**
pUWL-apra-oriT	Apra^R, Carb^R *ermE** promoter; *Hind*III & *Spe*I sites used for cloning 7410 bp	Erb *et al.* (2009)
pUZ8002	Kan^R conjugative plasmid used in biparental conjugations	Kieser *et al.* (2000)

Table 17: **Cosmids used in this study.**

Cosmid	**Characteristics**	**Reference**
mrsMR02	Kan^R, Tet^R integrative cosmid SuperCosI containing the multiple recombineering site (MRS), the integrase gene (*int*) and the attachment site (*attP*) of phage ϕC31; destination vector for the AGOS system	Basitta *et al.* (2017)
mrsHK01	Kan^R, Tet^R integrative cosmid SuperCosI containing IFCAGPOI_06386 from entry plasmid pTB88 (via *Pac*I site), the integrase gene (*int*) and the attachment site (*attP*) of phage ϕC31	Panagiota-Channa Koutsandrea
mrsAH02	Kan^R, Tet^R integrative cosmid SuperCosI containing the multiple recombineering site (MRS), IFCAGPOI_05107 from entry plasmid pTB89, the integrase gene (*int*) and the attachment site (*attP*) of phage ϕC31	Alexander Hoffreiter
mrsAH03	Kan^R, Tet^R integrative cosmid SuperCosI containing the multiple recombineering site (MRS), IFCAGPOI_03331 from entry plasmid pTB90, the integrase gene (*int*) and the attachment site (*attP*) of phage ϕC31	Alexander Hoffreiter
mrsAH04	Kan^R, Tet^R integrative cosmid SuperCosI containing the multiple recombineering site (MRS), IFCAGPOI_01482 from entry plasmid pTB91, the integrase gene (*int*) and the attachment site (*attP*) of phage ϕC31	Alexander Hoffreiter
mrsAH05	Kan^R, Tet^R integrative cosmid SuperCosI containing the multiple recombineering site (MRS), IFCAGPOI_04736 from entry plasmid pTB92, the integrase gene (*int*) and the attachment site (*attP*) of phage ϕC31	Alexander Hoffreiter
mrsAH01	Kan^R, Tet^R integrative cosmid SuperCosI containing the multiple recombineering site (MRS), IFCAGPOI_06489 from entry plasmid pTB93, the integrase gene (*int*) and the attachment site (*attP*) of phage ϕC31	Alexander Hoffreiter

Cosmid	**Characteristics**	**Reference**
mrsHK02	Kan^R, Tet^R integrative cosmid SuperCosI containing IFCAGPOI_06421 from entry plasmid pTB94 (via *Pac*I site), the integrase gene (*int*) and the attachment site (*attP*) of phage ϕC31	Panagiota-Channa Koutsandrea
mrsHK03	Kan^R, Tet^R integrative cosmid SuperCosI containing the multiple recombineering site (MRS), IFCAGPOI_03331 from entry plasmid pTB90 and IFCAGPOI_06489 from entry plasmid pTB93, the integrase gene (*int*) and the attachment site (*attP*) of phage ϕC31	Panagiota-Channa Koutsandrea
mrsHK04	Kan^R, Tet^R integrative cosmid SuperCosI containing the multiple recombineering site (MRS), IFCAGPOI_03331 from entry plasmid pTB90, IFCAGPOI_06489 from entry plasmid pTB93 and IFCAGPOI_05107 from entry plasmid pTB89, the integrase gene (*int*) and the attachment site (*attP*) of phage ϕC31	Panagiota-Channa Koutsandrea
mrsHK05	Kan^R, Tet^R integrative cosmid SuperCosI containing the multiple recombineering site (MRS), IFCAGPOI_03331 from entry plasmid pTB90, IFCAGPOI_06489 from entry plasmid pTB93, IFCAGPOI_05107 from entry plasmid pTB89 and IFCAGPOI_04736 from entry plasmid pTB92, the integrase gene (*int*) and the attachment site (*attP*) of phage ϕC31	Panagiota-Channa Koutsandrea
mrsHK06	Kan^R, Tet^R integrative cosmid SuperCosI containing the multiple recombineering site (MRS), IFCAGPOI_03331 from entry plasmid pTB90, IFCAGPOI_06489 from entry plasmid pTB93, IFCAGPOI_05107 from entry plasmid pTB89, IFCAGPOI_04736 from entry plasmid pTB92 and IFCAGPOI_01482 from entry plasmid pTB91, the integrase gene (*int*) and the attachment site (*attP*) of phage ϕC31	Panagiota-Channa Koutsandrea
mrsHK07	Kan^R, Tet^R integrative cosmid SuperCosI containing the multiple recombineering site (MRS), IFCAGPOI_03331 from entry plasmid pTB90, IFCAGPOI_06489 from entry plasmid pTB93, IFCAGPOI_05107 from entry plasmid pTB89, IFCAGPOI_04736 from entry plasmid pTB92, IFCAGPOI_01482 from entry plasmid pTB91 and IFCAGPOI_06386 from entry plasmid pTB88, the integrase gene (*int*) and the attachment site (*attP*) of phage ϕC31	Panagiota-Channa Koutsandrea
SuperCosI	Kan^R, $Carb^R$ cosmid vector	Stratagene Inc., La Jolla, California, USA

2.1.12 Media, Solutions and Buffers

Unless otherwise stated, all media, solutions and buffers were prepared using the required volume of ddH_2O to fully dissolve the components. Afterwards, they were sterilized for at least 20 minutes at 121 °C and a pressure of 2 bar. Temperature-sensitive solutions were sterile-filtered (0.2 μm pore size). For the preparation of solid media, 20 g/L agar was added to the media before autoclaving. Provided that an antibiotic was necessary for selection, it was added after sterilization and cooling of the media to around 50 °C. Liquid cultures were supplemented with the appropriate antibiotic prior to inoculation.

Table 18: **MGm-2.5 medium** (Martínez-Castro *et al.*, 2013).

Component	**Concentration**	**Amount**
L-glutamic acid monosodium salt hydrate	60 mM	8.83 g/L
$MgSO_4 \cdot 7H_2O$	0.8 mM	0.2 g/L
$CaCl_2$	9 μm	1 mL of a 9 mM stock solution/L
NaCl	17 μM	1 mL of a 17 mM stock solution/L
MOPS	100 mM	21 g/L
Soluble starch	5 % *w/v*	50 g/L
Trace element solution	1x	4.5 mL 1x solution (see table 19)
adjust pH to 6.5 with NaOH and autoclave		
$FeSO_4 \cdot 7H_2O$	32 μM	1 mL of a fresh 32 mM stock solution/L
potassium phosphate buffer (pH 6.5)	2.5 mM	2.5 mL of a 1 M stock solution/L

Table 19: **Trace element solution for MGm-2.5 medium (100x, 10 mL).**

Component	**Amount**
$CuSO_4 \cdot 5H_2O$	39 mg
H_3BO_3	5.7 mg
$(NH_4)_6Mo_7O_{24} \cdot 4H_2O$	3.7 mg
$MnSO_4 \cdot H_2O$	6.1 mg
$ZnSO_4 \cdot 7H_2O$	880 mg
sterilize by filtration and keep at 4 °C	

Table 20: **R2 medium** (Kieser *et al.*, 2000).

Component	**Amount**
Sucrose	103 g
K_2SO_4	0.25 g
$MgCl_2 \cdot 6H_2O$	10.12 g
Glucose	10 g

Component	**Amount**
Difco Casaminoacids	0.1 g
dissolve in 800 mL ddH_2O, autoclave and supplement:	
KH_2PO_4 (0.5%)	10 mL
$CaCl_2 \cdot 2H_2O$ (5M)	80 mL
L-proline (20 %)	15 mL
TES buffer (5.73 %, adjusted to pH 7.2)	100 mL
Trace element solution	2 mL (see table 21)
NaOH (1 N)	5 mL/L

Table 21: **Trace element solution for R2 medium.**

Component	**Amount**
$ZnCl_2$	40 mg/L
$FeCl_3 \cdot 6H_2O$	200 mg/L
$CuCl_2 \cdot 2H_2O$	10 mg/L
$MnCl_2 \cdot 4H_2O$	10 mg/L
$Na_2B_4O_7 \cdot 10H_2O$	10 mg/L
$(NH_4)_6Mo_7O_{24} \cdot 4H_2O$	10 mg/L
sterilize by filtration and keep at 4 °C	

Table 22: **TSB (Tryptone Soya Broth) medium** (Kieser *et al.*, 2000).

Component	**Amount**
TSB	30 g/L
add 20 g/L agar for TSA dissolve in 1 L ddH_2O and autoclave	

Table 23: **ISP4 (International Streptomyces Project) medium.**

Component	**Amount**
ISP4	37 g/L
dissolve in ddH_2O and autoclave add 10 mL of 1 M $MgCl_2$ solution (final concentration 10 mM)	

Table 24: **LB (Lysogeny Broth) medium.**

Component	**Amount**
Tryptone	10 g/L
Yeast extract	5 g/L
NaCl	5 g/L
dissolve all components in ddH_2O, fill up to 1 L and autoclave	

Table 25: **YEME (Yeast Extract Malt Extract) medium** (Kieser *et al.*, 2000).

Component	**Amount**
Yeast Extract	3 g/L
Peptone	5 g/L
Malt extract	3 g/L
Glucose	10 g/L
Sucrose	340 g/L
dissolve all components in ddH_2O, fill up to 1 L and autoclave	
add 10 mL of 1 M $MgCl_2$ solution (final concentration 10 mM)	

Table 26: **2xYT (Yeast Extract Tryptone) medium** (Kieser *et al.*, 2000).

Component	**Amount**
Difco bacto tryptone	16 g/L
Difco bacto yeast extract	10 g/L
NaCl	5 g/L
dissolve all components in ddH_2O, fill up to 1 L and autoclave	

Table 27: **MS (Mannitol Soya Flour) agar** (Kieser *et al.*, 2000).

Component	**Amount**
Mannitol	20 g/L
Soy flour	20 g/L
Agar	20 g/L
dissolve mannitol in 1 L tap water and pour 100 mL into 300 mL flasks	
add 2 g agar and 2 g soy flour per 300 mL flask	
autoclave twice (115 °C) with gentle interim shaking	

Table 28: **SOB (Super Optimal Broth) medium.**

Component	**Amount**
Tryptone	20 g/L
Yeast extract	5 g/L
NaCl	10 mM
Potassium chloride	2.5 mM
autoclave and add 20 mM $MgSO_4$	
for the preparation of SOC medium additionally add 20 mM glucose	

Table 29: **Solutions for the isolation of plasmids and cosmids.**

Component	**Concentration**
Solvent I	
Glucose	50 mM
EDTA (pH 8)	10 mM
Tris-HCl (pH 8)	25 mM
autoclave; add 1 μL/mL RNase	
Solvent II	
NaOH	0.2 M
SDS	1 %
do not autoclave; prepare fresh before use	
Solvent III	
Potassium acetate (pH 5.2)	3 M
autoclave; store on ice before use	

Table 30: **Solutions for protein isolation and processing.**

Component	**Concentration**	**Preparation**
DTT	100 mM	dissolve 0.1542 g DTT in 10 mL ddH_2O; store at -20 °C; use 10 μL/mL buffer (1 mM)
PMSF	100 mM	dissolve 0.1742 g PMSF in 10 mL methanol; store at -20 °C; use 10 μL/mL buffer (1 mM)
Pepstatin A	100 μg/mL	dissolve 1 mg Pepstatin A in 9 parts methanol and 1 part acetic acid; use 10 μL/mL buffer (1 μg/mL)

Table 31: **Bradford solution**.

Component	**Concentration**	**Amount**
Coomassie Brilliant Blue	100 mg/L	50 mg
Ethanol 95 % (*w*/*v*)	50 mL/L	25 mL
H_3PO_4 85 % (*w*/*v*)	100 mL/L	50 mL
ddH_2O		500 mL
filtrate with a paper filter until solution looks brown		
store at 4 °C		

Table 32: **Buffers used in this study.**

Component	**Concentration**	**Amount**
B+W buffer (pH 7.5)		
Tris-HCl	10 mM	0.012 g/10 mL
NaCl	2 M	1.169 g/10 mL
Potassium phosphate buffer (1 M, pH 7.8)		
KH_2PO_4	1 M	13.609 g/100 mL
K_2HPO_4	1 M	8.709 g/50 mL
mix 68 mL of KH_2PO_4 and 32 mL of K_2HPO_4.		
TAE buffer (50x, pH 7.8)		
Tris-HCl	2 M	242 g/L
Disodium EDTA	0.05 M	18.61 g/L
Acetic acid	1 M	57.1 mL
TE buffer (pH 6.8)		
Tris-HCl	50 mM	0.6 g/100 mL
EDTA	10 mM	0.4 g/100 mL
TGED buffer (pH 7.5)		
Tris-HCl	20 mM	0.242 g/100 mL
EDTA	1 mM	0.037 g/100 mL
NaCl	100 mM	0.584 g/100 mL
	(2 M)	(11.688 g/100 mL)
Triton-X-100	0.01 %	10 μL/100 mL
Glycerol	10 %	10 mL/100 mL
DTT	1 mM	10 μL/mL; add just before use
TFB1 (pH 5.8)		
Rubidium chloride	100 mM	0.6046 g/ 50 mL
Manganese chloride	50 mM	0.4047 g/ 50 mL
Potassium acetate	30 mM	0.1472 g/ 50 mL
Calcium chloride	10 mM	0.0735 g/ 50 mL
Glycerol	15 % *v*/*v*	7.5 mL
filter to sterilize and store at 4 °C.		
TFB2 (pH 8.0)		

Component	Concentration	Amount
MOPS	10 mM	0.0419 g/ 20 mL
Rubidium chloride	10 mM	0.0242 g/ 20 mL
Calcium chloride	75 mM	0.2205 g/ 50 mL
Glycerol	15 % *v/v*	3 mL
filter to sterilize and store at 4 °C.		

2.1.13 Software

Table 33: **Software used in this study.**

Name	Specification	Manufacturer
Artemis	16.0.0	Wellcome Trust Sanger Institute, Hinxton, UK
ChemBio Draw	Ultra, Version 14.0.0.117	PerkinElmer, Waltham, Massachusetts, USA
DataAnalysis	6300 Series Ion Trap LC/MS Software 6.1	BRUKER DALTONIK GmbH Life Sciences, Bremen, Germany
ImageJ	1.46r, Java 1.8.0.112 (32-bit)	Wayne Rasband, NIH, Bethesda, Maryland, USA
OpenLAB CDS	C.01.10	Agilent Technologies, Santa Clara, California, USA
SeqMan Pro	Lasergene 7	DNASTAR, Madison, Wisconsin, USA

2.2 Methods

2.2.1 Cultivation and strain maintenance

2.2.1.1 Cultivation conditions

Standard cultures of *Streptomyces tsukubaensis* NRRL18488 were set up in 100 mL MGm-2.5 medium in unbaffled 500 mL Erlenmeyer flasks at 220 rpm, 28 °C as incubation conditions. The production medium was directly inoculated using spores with a final titer of around 10^7 spores/mL. For strain maintenance, *Streptomyces tsukubaensis* NRRL18488 was cultured on solid ISP4 agar containing 10 mM $MgCl_2$ to enhance sporulation. Plates were incubated at 30 °C and stored at 4°C for long term. For conservation, spore stocks were prepared according to the beneath mentioned method (2.2.1.2).

Standard cultures of *Streptomyces coelicolor* and *Streptomyces albus* were set up in 50 mL MGm-2.5 medium in baffled 300 mL Erlenmeyer flasks at 200 rpm, 30 °C as incubation conditions. The production medium was either directly inoculated using spores or with 1 mL of a pre-culture grown for 2-3 days in TSB:YEME (1:1) medium. For strain maintenance, *Streptomyces coelicolor*

and *Streptomyces albus* were cultivated on solid MS agar containing 10 mM $MgCl_2$ to enhance sporulation.
E. coli strains were cultured in 100 mL LB medium in 300 mL unbaffled flasks or in 4 mL LB medium in test tubes at 200 rpm, 37°C unless stated otherwise. Strains harboring plasmids were cultivated under selective conditions using an appropriate antibiotic. For strain maintenance, *E. coli* was spread on LB agar plates, if necessary with an appropriate antibiotic. Plates were incubated at 37 °C and stored at 4 °C. Glycerol stocks were prepared by mixing 1 mL of *E. coli* culture with 0.5 mL of 80 % *(v/v)* glycerol followed by storage at -80 °C.

2.2.1.2 Preparation of spore stocks

For the preparation of spore stocks of *Streptomyces* strains, spores were harvested from strains grown on ISP4 agar plates (*Streptomyces tsukubaensis* NRRL18488) or MS agar plates (*Streptomyces ceolicolor* and *Streptomyces albus*) containing 10 mM $MgCl_2$. To this end, 5 mL sterile ddH_2O was added to the plates and spores were scraped off with a sterile cotton stick. The resulting suspensions were filtered through cotton placed within a sterile syringe and afterwards centrifuged (4000 x g, 10 min, 4 °C). Pellets were resuspended in 0.5 mL ice-cold 20 % glycerol. Spore suspensions were stored at -80 °C.

2.2.2 Methods of molecular biology

2.2.2.1 Isolation of genomic DNA from *Streptomyces tsukubaensis* NRRL18488

Genomic DNA was isolated from a 50 mL culture of *Streptomyces tsukubaensis* NRRL18488. The culture broth was centrifuged (6000 x g, 15 min, 4 °C) and the pellet was frozen at -80 °C for several days. After defreezing the pellet, 20 mL TE buffer (pH 6.8) was added to resuspend the pellet. 200 mg of lysozyme was added and the mixture was incubated at 37 °C for 1 hour. Afterwards, 125 μL of 0.1 M EDTA, 1 mL of 10 % SDS, 125 μL of 5 M NaCl and 100 μL Proteinase K (20 mg/mL solution) was added to 10 mL of the bacterial suspension followed by an incubation step of two hours at 37 °C. 5 mL Phenol/Chloroform was added and the tube was thoroughly mixed. After centrifugation (5000 x g, 10 min, 4 °C), the upper phase was removed, placed into a new vessel and the extraction was repeated three more times. Afterwards, the upper phase was precipitated as described below (2.2.2.4). The resulting pellet was resuspended in 800 μL Tris-HCl (10 mM, pH 8), 200 μL TE buffer (pH 6.8) and 1 μL RNase. The mixture was incubated at 37 °C for 2 hours (200 rpm) and the genomic DNA was stored at -20 °C until further use.

2.2.2.2 Isolation of plasmid or cosmid DNA of *E. coli* – mini- and maxipreparation

Alkaline lysis was used to isolate plasmids or cosmids out of *E. coli*. Depending on the required amount of DNA, mini- or maxipreparations were performed. For minipreparations, 1.5 mL of an overnight culture of the strain containing the respective plasmid was spun down (16100 x g, 1 min,

4 °C). For maxipreparations (e.g. the isolation of pAC20N from *E. coli* DH10ß), 100 mL of an overnight culture was spun down (6000 x g, 5 min, 4 °C). The resulting pellet was resuspended in 100 μL (5 mL) solvent I (table 29) containing 1 μL/mL RNase and incubated for 5 minutes (10 minutes) at room temperature. After incubation, 200 μL (10 mL) solvent II was added and the contents were thoroughly mixed by gently inverting the vessel several times. Following an incubation on ice for 5 minutes (10 minutes), 150 μL (7.5 mL) ice-cold solvent III was added and the contents were thoroughly mixed by inverting the vessel. Vessels were subsequently stored on ice for another 5 minutes (10 minutes). Afterwards, the supernatant containing plasmids was obtained by centrifugation (5 minutes (10 minutes), 16100 x g (6000 x g), 4 °C) and transferred into a new vessel. Subsequently, the DNA was purified (2.2.2.5) or precipitated (2.2.2.4). The resulting DNA pellet was dissolved in 50 μL (400 μL) ddH_2O and the DNA was stored at -20 °C until further use.

2.2.2.3 Amplification of DNA

Standard amplification of DNA by PCR was performed using a Taq:Pfu (9:1) polymerase mixture that had been prepared in-house. The corresponding standard pipetting scheme is depicted in table 34.

Table 34: **Pipetting scheme for standard PCR reactions.**

Component	**Amount**
Taq Buffer (10x)	5 μL
Template DNA	1 μL
Primer FW (100 pmol/μL)	1 μL
Primer RV (100 pmol/μL)	1 μL
dNTPs (2.5 mM each)	4 μL
Taq:Pfu polymerase (9:1)	1 μL
DMSO	2.5 μL
ddH_2O	34.5 μL

PCR reactions were assembled on ice and tubes were placed into a thermocycler to run the temperature program depicted in table 35. In order to determine the appropriate annealing temperature for a specific primer pair, a gradient from 50-70 °C annealing temperature was performed.

Table 35: **Temperature program for standard PCR reactions.**

	Temperature [°C]	Length [s]	Cycles
Hotstart	94 °C	300	1
Denaturation	94 °C	45	
Annealing	50-70 °C (primer dependent)	45	25
Elongation	72 °C	90	
Terminal elongation	72 °C	600	1
Cooling	4 °C	∞	

Alternatively, the Q5®High-Fidelity DNA polymerase was used for DNA amplifications that were not possible using the Taq:Pfu polymerase, probably due to a high GC content of the DNA or complex secondary structures (see 2.2.2.11).

2.2.2.4 Precipitation of DNA

For the precipitation of DNA with alcohol, the DNA solution was thoroughly mixed with one-tenth volume of sodium acetate and one volume of isopropanol. After incubation on ice for 10 minutes, the mixture was centrifuged for 30 minutes at 4 °C (16100 x g). The supernatant was removed and the pellet was washed with 500 μL 70 % ethanol. After a second centrifugation step (16100 x g, 10 min, 4 °C), the supernatant was discarded and the pellet was dried at room temperature. Afterwards, the pellet could be dissolved in an appropriate volume of ddH_2O. The DNA solution was stored at -20 °C.
For high-efficiency precipitations of DNA, the sodium acetate solution was replaced with lithium chloride solution. Moreover, 2.5 volumes of 100 % ethanol were used instead of isopropanol. Mixtures were incubated at -80 °C for 20 minutes prior to the centrifugation step.

2.2.2.5 Purification/extraction of DNA with phenol/chloroform/isoamyl alcohol

For purification, the DNA solution was transferred into a 2 mL safety lock tube and mixed with an equal volume of phenol/chloroform/isoamyl alcohol by vortexing for 1 minute. After centrifugation of the mixture (16100 x g, 15 min, 4 °C), the upper aqueous phase containing the DNA was removed and transferred into a new vessel. The DNA was subsequently precipitated as described in 2.2.2.4.

2.2.2.6 Purification of DNA using the Cycle Pure Kit

Purification of DNA using the Cycle Pure Kit was performed according to the manufacturers instructions. Briefly, the DNA solution was thoroughly mixed with the same volume of CP binding buffer and afterwards applied to the column (max. 750 μL). After centrifugation (10000 x g, 1 min), the flow-through was discarded and the column was washed twice with GC wash buffer.

Prior to the elution step, the empty column was again centrifuged (10000 x g, 2 min) to remove remaining wash buffer. DNA was eluted by adding 50 μL ddH_2O and centrifugation (5000 x g, 1 min).

2.2.2.7 DNA restriction

Enzymatic digestion of DNA with restriction endonucleases was performed for various purposes, e.g. for the cloning of inserts into a vector or conducting control digests of DNA isolated out of clones. In order to set up a restriction digest, it was necessary to know the approximate concentration of the DNA to be digested. Knowing that 1 U of enzyme cuts 1 μg of DNA in 1 hour, the required amount of enzyme could be estimated. Typically, the volume of a reaction mixture for an analytical digestion was chosen to be 20 μL, consisting of 0.5-1 μL restriction enzyme, 2 μL of the appropriate 10 x reaction buffer, 5-10 μL of DNA and ddH_2O. This mixture was incubated for at least 1 hour at the temperature specified for the enzyme. For preparative DNA restriction, several 20 μL restriction digest mixtures were prepared, incubated for at least 4 hours and afterwards pooled. Enzymes were heat-inactivated at their specified temperature, removed by precipitation (2.2.2.4) or purification via column (2.2.2.6).

2.2.2.8 Ligation of DNA

Ligation reactions were performed using the T4 DNA Ligase, the related buffer, insert DNA and vector DNA. Normally, ligation mixtures had a total volume of 10 μL, composed of 1 μL buffer and 1 μL ligase together with vector and insert DNA at a ratio of 1:3, respectively. Vector and insert were cut with the same enzymes prior to ligation and the amount of DNA used for the reaction was adjusted according to the respective concentrations of vector and insert DNA. Ligation was implemented at 4 °C over night or for at least 4 hours. Remaining enzyme and buffer were afterwards removed by precipitation of the DNA. If necessary, vector DNA was dephosphorylated prior to the ligation in order to prevent recircularization of the vector. For this purpose, the digested vector was incubated with alkaline phosphatase for 1 h at 37 °C.

2.2.2.9 Transformation of DNA

Preparation of electrocompetent cells

For the preparation of fresh electrocompetent *E. coli* cells, 100 mL LB medium (with antibiotics if necessary) was inoculated with a 50 μL aliquot of electrocompetent cells. Alternatively, 500 μL of an overnight culture was used for inoculation. Cells were incubated at 200 rpm, 37 °C until they had achieved a final OD_{600} between 0.4 and 0.6. Having reached this density, cells were transferred into pre-cooled vessels (2x 50 mL) and stored in an ice-water bath for 15 minutes. Cells were harvested by centrifugation (4000 x g, 10 min, 4 °C) and washed twice with 25 mL ice-cold 10 % glycerol. Following the last centrifugation step, the supernatant was discarded and

cells were resuspended in the residual 10 % glycerol. 50 μL aliquots of this bacterial solution were prepared and stored at -80 °C.

Electroporation

For the transformation of DNA, electrocompetent *E. coli* cells were thawed on ice and mixed with 2-6 μL of DNA to be transformed. The DNA-*E. coli*-mixture was transferred into a pre-cooled electroporation cuvette (0.2 cm gap) and the mixture was pulsed at 200 Ω, 25 μF and 2.5 kV. Immediately afterwards, 500 μL of pre-cooled LB medium was added to the cuvette and cells were transferred into a 1.5 mL tube. Regeneration of the cells was performed for at least one hour at 37 °C and 300 rpm. Cells were subsequently plated onto LB agar plates containing an appropriate antibiotic for selection. Plates were incubated at 37 °C overnight if not stated otherwise.

Preparation of chemically competent cells

In order to prepare chemically competent cells, 100 mL LB medium (with antibiotics if necessary) was inoculated with 500 μL of an overnight culture of the respective *E. coli* cells and incubated at 37 °C, 200 rpm until an OD_{600} between 0.4 and 0.6 was reached. Cells were cooled down on ice for ten minutes and afterwards harvested by centrifugation (4000 x g, 5 min, 4 °C). The supernatant was discarded and cells were resuspended in 30 mL of ice-cold TFB1 (table 32). The solution was incubated on ice for 90 minutes, centrifuged (4000 x g, 5 min, 4 °C) and the supernatant discarded. Subsequently, cells were resuspended in 4 mL of ice-cold TFB2 (table 32). After further incubation on ice for 10 minutes, aliquots of 100 μL were prepared and frozen at -80 °C or directly used for the heat shock.

Heat shock

100 μL chemically competent cells were thawed on ice and mixed with around 10 μL of DNA to be transformed. This mixture was incubated on ice for 30 minutes. Heat shock was carried out at 45 °C for 90 seconds. Subsequently, cells were placed on ice for another 2 minutes and afterwards 500 μL of pre-warmed LB medium was added. Regeneration of the cells was carried out at 37 °C, 300 rpm for at least one hour. Cells were plated on warm LB agar plates with appropriate antibiotics and incubated at 37 °C overnight.

2.2.2.10 Agarose gel electrophoresis

For a separation of DNA fragments according to their size, agarose gel electrophoresis was performed. To this end, agarose in the desired concentration (mostly 1 % *w/v*) was boiled up in 1xTAE buffer. After cooling the solution to room temperature, peqGREEN was added in a final concentration of 1 μL/mL. The agarose solution was poured into the tray of a gel chamber equipped with a comb and was left to cool down for polymerization. The comb was removed from the solid gel and the gel pockets were loaded with the DNA solution that had been mixed with 6x loading dye in a 6:1 ratio. By default, 6 μL (0.5 μg) of the GeneRuler 1 kb DNA ladder

was used as DNA size standard and loaded into the outer wells next to the DNA samples. Gels were run at constant voltage (10 V/cm) in 1xTAE buffer for 1-2 hours. DNA was visualized using gel documentation systems ($UV_{213\ nm}$). Using the software ImageJ and the known DNA concentration of the GeneRuler size standard, the amount of DNA in the samples could be quantified.
In case a preparative agarose gel electrophoresis was required for the isolation of a specific DNA fragment, several teeth of the gel comb were fused using an adhesive tape. This enabled the loading of large volumes of DNA samples. After careful separation of the DNA fragments at low voltage, the desired DNA fragment was excised from the gel with a scalpel under UV light with reduced intensity (70 %). DNA was extracted from the gel using a gel extraction kit according to the manual.

2.2.2.11 Colony PCR

In order to test generated mutant strains for harboring the respective plasmids or genetic modifications, colony PCR was performed. Colony PCR is an easy and PCR-based approach which allows to quickly verify the presence of a desired construct within mutant strains by using specifically designed primers.
Colony PCR with *E. coli* cells included the preparation of standard PCR mixtures (see 2.2.2.3) containing ddH_2O instead of template DNA. Single colonies of the *E. coli* clones were picked with a sterile toothpick and resuspended in the respective PCR tube. Initial denaturation in the PCR cycler was set for 10 minutes to ensure cell lysis.
In order to verify the generated *Streptomyces* mutant strains, a modified protocol was used for the colony PCR. As the Taq:Pfu polymerase prepared in-house did mostly not result in amplifications, the Q5®High-Fidelity DNA polymerase was used instead. Liquid cultures of the generated mutant strains were used as template for the colony PCR. For this purpose, 4 mL of LB medium was inoculated with 20 μL of the respective spore suspension and incubated for three days at 28 °C, 200 rpm. 1.5 mL of the medium with grown mycelium was spun down (16100 x g, 5 min) and the pellet was resuspended in 20 μL DMSO. This mixture was cooked for 10 minutes at 95 °C, cooled down and 2 μL was added to the PCR mixture which was composed as stated in table 36.

Table 36: **Pipetting scheme for the Q5®High-Fidelity DNA polymerase.**

Component	Amount
Q5 reaction buffer (5x)	10 μL
dNTPs (2.5 mM each)	4 μL
Primer FW (100 pmol/μL)	1 μL
Primer RV (100 pmol/μL)	1 μL
Template-DNA	2 μL
Q5®High-Fidelity DNA polymerase	0.5 μL
Q5 high GC enhancer (5x)	10 μL
ddH_2O	21.5 μL

The temperature program for the amplification was set up according to the manual of the Q5®High-Fidelity DNA polymerase (table 37).

Table 37: **Temperature program for the Q5®High-Fidelity DNA polymerase.**

	Temperature [°C]	Length [s]	Cycles
Hotstart	98 °C	30	1
Denaturation	98 °C	10	
Annealing	60 °C	30	30
Elongation	72 °C	90	
Terminal elongation	72 °C	120	1
Cooling	4 °C	∞	

2.2.2.12 Sequencing

Sequencing was performed at Eurofins Genomics (Ebersberg, Germany). For sequencing, DNA samples were diluted with ddH_2O to the required DNA concentration of 100 ng/μL (plasmids), 1000 ng/μL (cosmids) or 5 ng/μL (purified PCR products in the range of 300-1000 bp) in a final volume of 15 μL and, if necessary, were supplemented with 2 μL of a specifically designed sequencing primer. The obtained sequences were analyzed using the SeqMan software.

2.2.2.13 Gibson Assembly

Gibson Assembly is generally used for the assembly of multiple DNA fragments, independent of fragment length or end compatibility (New England BioLabs®$_{\text{Inc.}}$, Ipswich, Massachusetts, USA). Multiple overlapping DNA fragments can be joined in a single-tube isothermal reaction. Three enzymes are included in the Gibson Assembly Master Mix: an exonuclease, a DNA polymerase and a DNA ligase. Together, they generate a double-stranded DNA molecule that can be used for various applications.

For genetic engineering approaches using the pCRISPR-TT plasmid (2.2.2.17), Gibson Assembly was used to assemble the homology domains. The sequences of the DNA fragments to be fused were amplified by PCR using the Q5®High-Fidelity DNA polymerase. Primers had to include sequences of at least 20 bp overlapping with the respective upstream or downstream DNA fragment. Additionally, *Eco*RV restriction sites were included at both ends of the homology domain as well as homologous sequences to pBlueScript II SK(-) which was the cloning vector used for Gibson Assembly. pBluescript II SK(-) was linearized using an *Eco*RV restriction digest and mixed in equal concentration with the DNA fragments to be assembled in a total volume of 10 μL. The DNA mixture was supplemented with 10 μL of Gibson Assembly Master Mix and the solution was incubated at 45 °C for 90 minutes in a thermocycler. Afterwards, 2 μL of the assembly mixture was transformed into electrocompetent *E. coli* XL1-Blue cells. After plating on LB agar with carbenicillin, IPTG and X-Gal, positive clones were identified using Blue-White-Screening (2.2.2.14).

2.2.2.14 Blue-White-Screening

Blue-White-Screening is a useful approach in order to facilitate the screening for correct clones. The system is based on the expression of the ß-galactosidase which cleaves lactose into glucose and galactose. Vectors used for Blue-White-Screening carry the gene for the ß-galactosidase (*lacZ*) within the multiple cloning site and this allows to use the gene as reporter gene. After insertion of a gene into the multiple cloning site, the ß-galactosidase is inactivated and can no longer cleave the yellow dye X-Gal into a blue dye (5,5'-dibromo-4,4'-dichloro-indigo) and galactose. The *lacZ* gene is under the control of an IPTG-inducible promoter. The inducer binds to the *lacZ* repressor LacI, inactivates it and thereby allows the expression of (*lacZ*). In the presence of the ß-galactosidase the blue dye is formed upon induction. However, host strains with an inactivated ß-galactosidase stay uncolored and can be identified and isolated.
Blue-White-Screening requires the application of mutant strains not expressing any further gene for the ß-galactosidase. In this work, *E. coli* XL1-Blue was used as host strain and transformed with 2-3 μL of the respective plasmid. After regeneration, cells were plated on LB agar plates containing the appropriate antibiotic, 4 mM IPTG and 80 μg/mL X-Gal (dissolved in DMSO). After incubation at 37 °C over night, white clones could be distinguished from blue clones and used for further screening.

2.2.2.15 PCR targeting

Mutagenesis of *Streptomyces* strains can be achieved by using the strategy of recombineering as described by Gust *et al.* (2003). This approach takes advantage of the λ-Red (*exo*, *bet*, *gam*) proteins that promote a greatly enhanced rate of recombination with linear DNA in the targeted strain. The idea of PCR targeting is to replace a DNA sequence by a PCR-generated selectable marker which is flanked with homology arms (39 nucleotides) to the DNA region intended to be modified. Inclusion of an origin of transfer in the resistance cassette enables conjugation of the

processed cosmid DNA into *Streptomyces* strains.
PCR targeting requires the design of long PCR primers to amplify the extended resistance cassette. At its 5' end, each primer is equipped with 39 nucleotides matching the sequence adjacent to the gene to be inactivated. The 3' end matches the right or left end of the disruption cassette, respectively (19 nucleotides or 20 nucleotides). The pipetting scheme for the amplification of the extended resistance cassette is shown in table 38 and the corresponding temperature program in table 39.

Table 38: **Pipetting scheme for the amplification of the extended resistance cassette.**

Component	**Amount**	**Specification**
Taq Buffer (10x)	5 μL	1x
Template DNA (100 ng/μL)	0.5 μL	50 ng (0.06 pmol)
Primer FW (100 pmol/μL)	0.5 μL	50 pmol
Primer RV (100 pmol/μL)	0.5 μL	50 pmol
dNTPs (2.5 mM each)	4 μL	50 μM each
Taq:Pfu polymerase (9:1)	1 μL	
DMSO (100 %)	2.5 μL	5 %
ddH_2O	36 μL	

Table 39: **Temperature program for the amplification of the extended resistance cassette.**

	Temperature [°C]	**Length [s]**	**Cycles**
Hotstart	94 °C	120	1
Denaturation	94 °C	45	
Annealing	50 °C	45	10
Elongation	72 °C	90	
Denaturation	94 °C	45	
Annealing	55 °C	45	15
Elongation	72 °C	90	
Terminal elongation	72 °C	300	1
Cooling	4 °C	∞	

PCR products were purified as described in 2.2.2.6 and finally eluted from the column with 12 μL of ddH_2O.
In order to express the λ-RED genes, the plasmid pIJ790 had to be introduced into *E. coli* BW25113 via electroporation (2.2.2.9). Due to the temperature-sensitive origin of replication of the recombination plasmid pIJ790, *E. coli* BW25113 harboring this plasmid has to be grown at 30 °C as long as the plasmid is required. By means of a second transformation, the cosmid to be modified was introduced into *E. coli* BW25113/pIJ790. Main cultures of *E. coli* BW25113/pIJ790

cells containing the cosmid were set up in 10 mL SOB medium, supplemented with the appropriate antibiotics and 10 mM *L*-arabinose to induce the *red* genes (30 °C, 200 rpm). Having reached an OD_{600} of around 0.5, cells were harvested by centrifugation and prepared for electroporation by washing twice with 10 mL of 10 % glycerol. After the final washing step, glycerol was decanted and 50 μL of the remaining cell suspension was mixed with 2-4 μL of PCR product (extended resistance cassette). After a short incubation of the DNA-cell mixture on ice, electroporation was carried out as described in 2.2.2.9. Cells were regenerated in 500 μL LB medium at 37 °C, 300 rpm for one hour and afterwards spread on LB agar containing appropriate antibiotics for selection. After overnight incubation at 37 °C, single colonies were picked and used to inoculate test cultures for minipreparations (2.2.2.2). The isolated DNA served as template for PCR reactions with testprimers specifically designed to verify the insertion of the resistance cassette. Additionally, restriction analysis was performed to confirm the correct PCR targeting.

2.2.2.16 Intergeneric conjugation of DNA from *E. coli* to *Streptomyces*

Biparental conjugation (Kieser *et al.*, 2000)

Intergeneric conjugation is a means of introducing DNA into *Streptomyces*. Biparental conjugation was used for pUWL-apra-oriT and pCRISPR-TT vector constructs. Conjugation requires a methylation-defective host strain, e.g. *E. coli* ET12567, and a recipient *Streptomyces* strain. Furthermore, a plasmid carrying the *tra*-genes necessary for the transfer of genetic material in bacteria is required, e.g. pUZ8002 . Vectors to be introduced into *Streptomyces* strains require an appropriate origin of replication and an origin of transfer.
Electrocompetent *E. coli* ET12567/pUZ8002 cells were transformed (2.2.2.9) with the respective vector intended to be introduced into the *Streptomyces* strain. Selection was performed by using chloramphenicol, kanamycin and apramycin. Growing transformants were used to inoculate overnight cultures (4 mL LB medium with antibiotics) which were incubated at 200 rpm, 37 °C. Main cultures were set up in 10 mL of LB medium containing the mentioned antibiotics and 1 % (*v*/v) of pre-culture. Pre-cultures were further used for DNA isolation (2.2.2.2) to verify that the *E. coli* ET12567 cells harbor the required plasmid. Having reached an OD_{600} of around 0.5, cells of the main cultures were harvested by centrifugation (2800 x g, 4 °C, 5 min). After washing twice with 10 mL of LB medium, cell pellets were resuspended in 1 mL of LB medium and stored on ice until further use.
Meanwhile, 20 μL spore suspension (titer around 10^9 spores/mL) of the respective recipient *Streptomyces* strain was added to 500 μL of 2xTY medium and incubated for ten minutes at 50 °C (400 rpm). This heat shock was to activate germination of the respective spores. Afterwards, spores were incubated for 2-4 hours at 28 °C/30 °C at 300 rpm.
For the conjugation, 500 μL *E. coli* cells were carefully mixed with 500 μL of heat-shocked spores by inverting the tube several times. Subsequently, the mixture was briefly centrifuged (10 seconds) at 4000 x g. 800 μL of the supernatant was discarded and the remaining 200 μL was used to resuspend the pellet. A serial dilution of this suspension was prepared in ddH_2O

and 100 μL of the dilutions 10^0, 10^{-1} and 10^{-3}, respectively, was carefully plated on MS agar containing 10 mM $MgCl_2$. Plates were incubated overnight at 30 °C.
After 16-24 hours of incubation, plates were overlayed with 1 mL of ddH_2O containing 0.625 mg nalidixic acid and 1.25 mg apramycin. Incubation was continued at 30 °C for several days or weeks until exconjugants appeared.
Three potential exconjugants were picked and used to prepare serial dilutions in ddH_2O. 100 μL of the dilutions 10^{-2} and 10^{-3} were spread on ISP4 agar containing apramycin and nalidixic acid. Plates were further incubated at 30 °C.
Finally, three individual exconjugants from the dilution plates were picked and confluently spread on ISP4 agar plates containing the above-mentioned antibiotics. After further incubation at 30 °C, spores of the respective exconjugants could be harvested (2.2.1.2), verified by colony PCR (2.2.2.11) and used for subsequent experiments.

Triparental conjugation

In case cosmids conferring a kanamycin resistance were to be conjugated to *Streptomyces* strains, it was not possible to use the non-transmissible pUZ8002 helper plasmid. Therefore, the helper plasmid pUB307 was used instead. In contrast to pUZ8002, pUB307 constitutes a self-transmissible plasmid which also carries the *tra* genes. Triparental conjugation required to inoculate two *E. coli* main cultures: *E. coli* ET12567/pUB307 and E. coli ET12567 carrying the respective cosmid. Cells were harvested as described before, likewise the preparation of the spores. For conjugation, 500 μL of spores was mixed with 250 μL of each *E. coli* strain. The further procedure was the same as described for the biparental conjugation.

2.2.2.17 CRISPR-Cas9 editing

In recent years, the CRISPR-Cas technology was developed, allowing to easily perform site-specific genetic engineering in different biological systems. There already exist a few CRISPR-Cas9 systems for *Streptomyces* species as described by Cobb *et al.* (2015) and Huang *et al.* (2015). A further plasmid-based approach using pCRISPR-Cas9 was introduced by Tong *et al.* (2015) where the nuclease Cas9 is under control of the thiostrepton inducible *tipA* promoter. The working group of the TacroDrugs project partners Dr. Pedro Albuquerque and Dr. Marta Vaz Mendes (IBMC, University of Porto, Portugal) replaced the *tipA* promoter by an *ermE** promoter and a theophylline-dependent synthetic riboswitch (according to Rudolph *et al.* (2013)), generating the plasmid pCRISPR-TT. The plasmid pCRISPR-TT was used for various aims of genetic engineering in this study.
In order to work with the pCRISPR-TT plasmid, it was firstly necessary to furnish the plasmid with the appropriate single guide RNA (sgRNA) and homology arms for the double recombination event that repairs the Cas9-induced DNA nick.
The sgRNA, composed of CRISPR RNA (crRNA) and trans-activating CRISPR RNA (tracrRNA), was generated by cloning a 20 nucleotide target sequence (spacer sequence) in front of the plasmid-

encoded tracrRNA. For each genetic engineering approach, two individual and specific spacer sequences were identified using the online tool CRISPy-web (https://crispy.secondarymetabolites.org/#/input). The chosen sgRNA was amplified by PCR and cloned into pCRISPR-TT via *Nco*I and *Sna*BI restriction sites.
Gibson Assembly (2.2.2.13) was used to assemble the homology domain, consisting of 1 kb sequences located upstream and downstream of the target region and additionally the new sequence to be inserted in between them. Following successful assembly of the homology domain in pBlueScript SK(-), the fragment was verified by sequencing, excised by *Eco*RV restriction digest and then subcloned into pCRISPR-TT via the *Stu*I restriction site. The final pCRISPR-TT construct including the spacer sequence and the homology domain was transformed into *E. coli* ET12567/pUZ8002 and used for intergeneric conjugation (2.2.2.16) into the target *Streptomyces* strain.
After dilution and confluent streaking of individual exconjugants, spore suspensions were harvested as described in 2.2.1.2. The resulting spore suspension was restreaked on TSB agar (TSA) containing 10 mM theophylline for the induction of the Cas9. After 3-4 days, growing clones were spread on ISP4-$MgCl_2$ agar and tested for the expected mutation via colony PCR (2.2.2.11). Exconjugants revealing the engineered genotype were streaked confluently on ISP4-$MgCl_2$ agar to obtain spore suspensions. Finally, the pCRISPR-TT plasmid had to be cured. Therefore, the harvested spore suspensions were diluted, spread on TSA and incubated at 37 °C for 4-5 days. Growth behavior of resulting clones was tested on ISP4 and ISP4-Apra agar plates. In order to yield the final mutant strains, only exconjugants which could no longer grow under apramycin selection were used to prepare spore suspensions. An overview of all the working steps involved in CRISPR-Cas9 engineering using the plasmid pCRISPR-TT is depicted in figure 4.

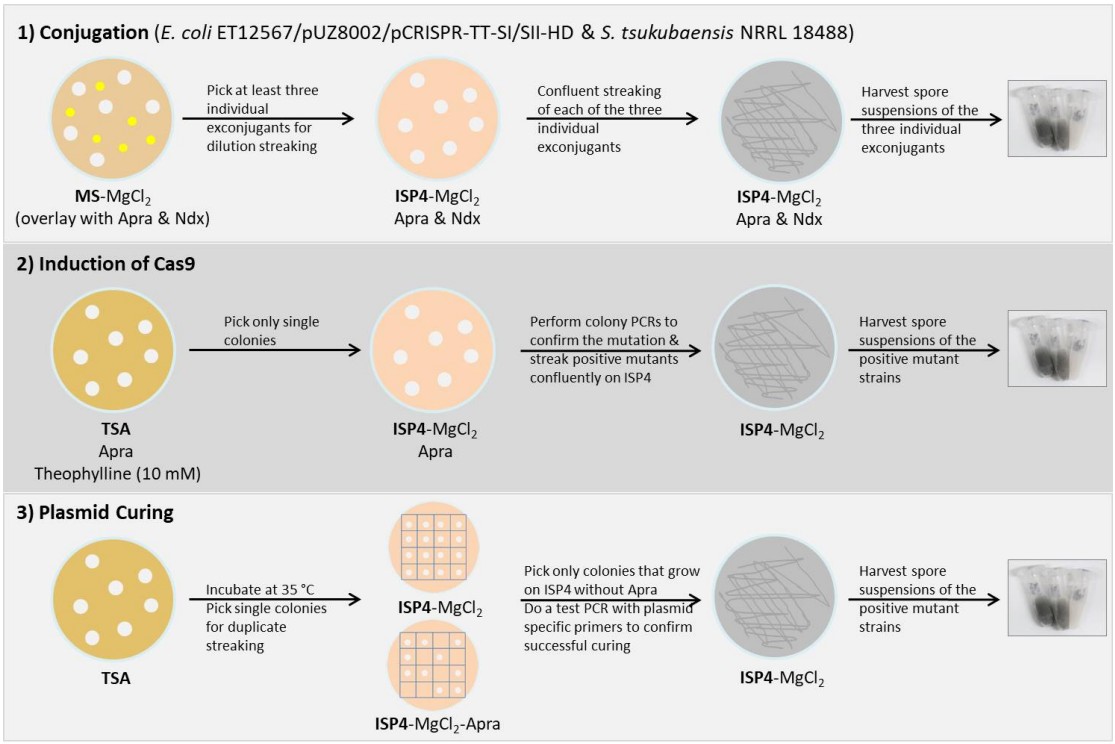

Figure 4: **CRISPR-Cas9 editing in *S. tsukubaensis* NRRL18488 using the plasmid pCRISPR-TT.**

2.2.3 DACA

2.2.3.1 Amplification and biotinylation of promoter fragments for the DACA

High expression profiles of the genes *tcs6*, *fkbO*, *fkbB*, *fkbG* and *allA* starting from the respective putative transcriptional start sites (TSS) indicated that the promoter regions upstream of these genes might be important for the binding of proteins regulating the biosynthesis of tacrolimus (Bauer *et al.*, 2017). Therefore, the following promoter regions were chosen to be analyzed in the DACA:

1) **Ptcs6** (divided into Ptcs6a: 507 bp & Ptcs6b: 594 bp)
2) **PfkbO** (439 bp)
3) **PfkbG** (296 bp)
4) **PallA** (546 bp)

Ptcs6 is a bidirectional promoter region located between the genes *fkbR* and *tcs6*. As the region is quite large, comprising 713 bp, it was split into two parts, Ptcs6a and Ptcs6b, spanning 507 bp and 594 bp, respectively. The overlap of these two regions was chosen to be 114 bp in order to fully cover all putative protein binding sites. PfkbO is also a bidirectional promoter located between *fkbO* and *fkbB*. The promoter fragment comprises 439 bp which covers the

whole intergenic region of 265 bp and additionally involves parts of the genes *fkbO* and *fkbB* (103 bp and 71 bp, respectively). PfkbG is a unidirectional promoter in front of *fkbG*. It was designed to span 296 bp in total, including the 171 bp intergenic region, 53 bp within *allS* and 72 bp within *fkbG*. The last promoter region, PallA, is also a unidirectional promoter located in front of *allA*. It spans the intergenic region of 476 bp and furthermore includes 52 bp of *allA* and 18 bp of the following coding sequence. The locations of the chosen promoter regions within the tacrolimus biosynthetic gene cluster are depicted in figure 5.

P16S, an additional promoter region spanning 473 bp of the 16S rRNA gene of *Streptomyces tsukubaensis* NRRL18488 was used as negative control to determine unspecifically binding proteins.

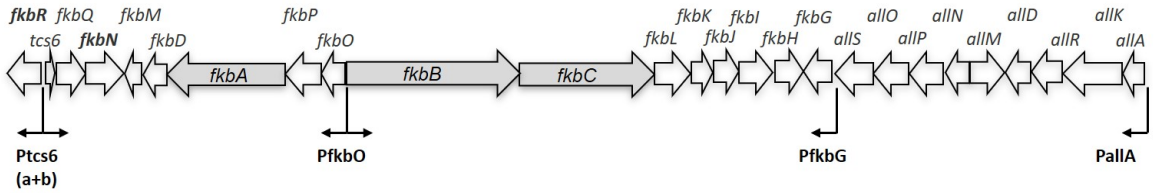

Figure 5: **Location of the selected promoter regions within the tacrolimus biosynthetic gene cluster.**

All promoter fragments were amplified using specific primer pairs (table 5) which were designed using the *Streptomyces tsukubaensis* NRRL18488 draft genome contig 908 sequence (accession number AJSZ01000908). The *Streptomyces tsukubaensis* NRRL18488 partial 16S rRNA gene sequence (GenBank accession number HE656024.1) was used to design the appropriate primers for P16S amplification.

A first PCR reaction was performed to amplify the respective promoter fragments and to add a linker sequence to one end of the promoter region. The linker sequence allowed to biotinylate the promoter fragments in a second PCR. Therefore, a DAC-biotin primer was used which bound to this linker sequence. PCR reaction mixtures for the amplification of Ptcs6a, Ptcs6b, PfkbO, PfkbG and PallA from the pAC20N cosmid corresponded to the standard PCR conditions described in 2.2.2.3. The optimal annealing temperature for each primer pair was determined using a gradient PCR with the temperature program depicted in table 40. All promoter fragments could be amplified at 67 °C.

Table 40: **Temperature program for the amplification of Ptcs6a, Ptcs6b, PfkbO, PfkbG, PallA and P16S.**

	Temperature [°C]	**Length [s]**	**Cycles**
Hotstart	94 °C	300	1
Denaturation	94 °C	30	
Annealing	Gradient: 50-70 °C	40	30
Elongation	72 °C	60	
Terminal elongation	72 °C	600	1
Cooling	4 °C	∞	

P16S was amplified using genomic DNA from spores of *Streptomyces tsukubaensis* NRRL18488 as template DNA. A spore suspension containing $6.4{\cdot}10^9$ spores/mL was therefore diluted in ddH_2O (1:10) and used as template for the PCR reaction mixture. As amplification was not possible using the Taq:Pfu polymerase, the Phusion® High-Fidelity DNA polymerase was used instead. The composition of the PCR reaction mixture is depicted in table 41 and the temperature program is shown in table 42.

Table 41: **Pipetting scheme for the amplification of P16S from genomic DNA.** During the PCR, a linker sequence was added to the fragment which allowed subsequent biotinylation.

Component	**Amount**
Buffer (5x, GC)	10 μL
Template DNA	1 μL
Primer FW (10 pmol/μL)	2.5 μL
Primer RV (10 pmol/μL)	2.5 μL
dNTPs (2.5 mM each)	4 μL
Phusion® High-Fidelity DNA polymerase	0.5 μL
DMSO	1.5 μL
ddH_2O	28 μL

Table 42: **Temperature program for the amplification of P16S from genomic DNA.**

	Temperature [°C]	Length [s]	Cycles
Hotstart	98 °C	30	1
Denaturation	98 °C	10	
Annealing	67 °C	30	25
Elongation	72 °C	30	
Terminal elongation	72 °C	600	1
Cooling	4 °C	∞	

PCR products of the first PCR reaction were purified using the Cycle Pure Kit (peqlab) (2.2.2.6) and eluted in Tris-HCl (10 mM, pH 8). The amplified promoter fragments were verified by sequencing.
A second PCR reaction was used to biotinylate the PCR products of the first PCR reactions. To this end, a biotinylated primer was used which was complementary to the linker sequence added to the promoter fragments in the first PCR. The biotinylated primer was used in combination with Ptcs6a_R, Ptcs6b_F, PfkbO_R, PfkbG_F, PallA_F and P16S_F2, respectively. The PCR program and the pipetting scheme corresponded to the first PCR. As concerns the amplification of P16S, it was possible to use the Taq:Pfu polymerase in the second PCR. After the second PCR reaction, excessive primers were removed by purification using the Cycle Pure Kit. DNA concentration was estimated using absorbance-based quantification (NanoDrop®) and image-based quantification following agarose gel electrophoresis (ImageJ).

2.2.3.2 10 L fermentation of *Streptomyces tsukubaensis* NRRL18488

The 10 L fermentation of *Streptomyces tsukubaensis* NRRL18488 was performed in cooperation with Andreas Kulik (University of Tübingen). For the pre-culture, $1 \cdot 10^{11}$ spores of *Streptomyces tsukubaensis* NRRL18488 were inoculated into 5 x 100 ml of MGm-2.5 medium in 500 mL unbaffled Erlenmeyer flasks and incubated at 28 °C and 220 rpm for 37.5 hours. Pre-cultures were pooled and 500 mL was used to inoculate 9.5 L MGm-2.5 medium in a 10 L fermenter equipped with a turbine impeller system (final spore titer: $1 \cdot 10^7$ spores/mL). After inoculation, 2 mL antifoam was added. *Streptomyces tsukubaensis* NRRL18488 was cultivated at 28 °C and 220 rpm for 240 hours. Samples were taken after 24 h and 36 h (from the pre-culture) and after 42 h, 48 h, 60 h, 66 h, 72 h, 78 h, 84 h, 90 h, 96 h, 102 h, 108 h, 114 h, 120 h, 132 h, 156 h, 168 h, 192 h, 216 h and 240 h (from the fermenter).
Cell dry weight was determined by centrifuging 1 mL of culture for 10 minutes (16100 x g) in a weighed 1.5 mL micro-reaction tube, washing the pellet with ddH_2O and drying it for at least 24 hours at 80 °C. Tacrolimus production was determined as described in 2.2.6.

2.2.3.3 Protein extraction

Cells from 200 mL-500 mL culture from the 10 L fermenter were harvested by centrifugation (4800 x g, 15 min, 4°C) after different periods of growth in order to obtain samples for protein extraction. Cell pellets were washed once with Tris-HCl (10 mM, pH 8) and stored at -80 °C until further use. The pellets from the 60 hours and 114 hours samples were subsequently resuspended in 2.5 mL/g cell wet weight TGED buffer containing 1 mM DTT, 1 mM PMSF, 1 μg/mL pepstatin A, 1 mM benzamidine and 1 mg/mL lysozyme. Cells were lyzed using a French Press with three passages at 1000 PSI on ice. Afterwards, cell debris were removed by centrifugation (38724 x g, 45 min, 4 °C) and the concentration of proteins in the supernatant was determined using the Bradford protein assay (Bradford, 1976) (2.2.3.4).

2.2.3.4 Bradford protein assay

In order to determine the protein concentration in the supernatant using the Bradford protein assay, a calibration curve was prepared using a 1 mg/mL BSA stock solution in TGED buffer. Therefore, 1 mL of Bradford reagent was mixed with 20 μL BSA-solution with concentrations of 0 mg/mL, 0.125 mg/mL, 0.250 mg/mL, 0.5 mg/mL, 0.75 mg/mL and 1 mg/mL, respectively. After incubation for 2-5 minutes, absorption at 595 nm was determined using a photometer and a calibration curve was derived. 20 μL sample was likewise mixed with the Bradford reagent and absorption was measured. The corresponding protein concentration was deduced from the calibration curve.

2.2.3.5 Preparation of the Dynabeads^{TM} M-280 Streptavidin

Due to their biotinylation, the promoter fragments could be coupled to Dynabeads^{TM} M-280 Streptavidin which were used for the DACA. Therefore, 1.25 mg of Dynabeads^{TM} M-280 Streptavidin (125 μL) were transferred into 2 mL reaction tubes. With the help of a magnet the beads were pulled to one side of the reaction tube and the supernatant was removed with a pipette. Beads were subsequently resuspended in 125 μL of B+W buffer and washed three times with this buffer. After the third wash, 125 μL of B+W buffer and 23.7 μg of the respective purified and biotinylated promoter fragment (in Tris-HCl, 10 mM, pH 8) were added in a total volume of 488.8 μL (filled up with B+W buffer if necessary). The mixtures were incubated for one hour at room temperature with gentle agitation. Thereafter, the beads were washed with B+W buffer three times and resuspended in 500 μL TGED buffer before use.

2.2.3.6 DNA affinity capturing assay (DACA)

100 μg/mL salmon sperm DNA was added to the protein extracts containing 182.28 mg (60h) and 242.25 mg (114 h) protein, respectively, and incubated for 15 minutes on ice. 500 μL of Dynabeads^{TM} M-280 Streptavidin with the respective biotinylated promoter fragment (2.2.3.5) was added and the mixture was incubated for 45 minutes at room temperature with gentle

agitation. After the incubation time, the suspension was transferred into 2 mL reaction tubes in 2 mL steps. The Dynabeads were magnetically separated from the supernatant. Thereafter, the Dynabeads were washed once with TGED buffer, once with TGED buffer containing 400 μg salmon sperm DNA and again once with 500 μL TGED buffer. The elution of the proteins was accomplished by twice adding 200 μL of TGED buffer containing 2 M NaCl. Two washing steps with TGED buffer containing 2 M NaCl and two washing steps with TGED buffer were necessary to regenerate the Dynabeads.

2.2.3.7 TCA precipitation of proteins

Eluted proteins were precipitated with 0.25 volumes (100 μL) of trichloroacetic acid (100 % *w/v* in ddH_2O). The solutions were incubated on ice for 30 minutes and centrifuged (16100 x g, 15 min, 4 °C). Afterwards, the supernatants were removed and the pellets were washed with 500 μL acetone. After centrifugation (16100 x g, 15 min, 4 °C), the supernatant was discarded and the dried pellet was stored at -80 °C until it was analyzed at the proteome center of the University of Tübingen.

2.2.4 Simultaneous overexpression of several regulatory proteins

Based on the results of the overexpression studies, six different positive regulators of tacrolimus biosynthesis were chosen to be overexpressed in parallel, hoping to generate strains producing high amounts of tacrolimus. In doing so, it was considered that these proteins bind to different promoter regions within the tacrolimus biosynthetic gene cluster. The known positive regulator of tacrolimus biosynthesis, FkbN (Goranovič *et al.*, 2012), was additionally included (table 43). Overexpression of several regulatory proteins in parallel requires a vector backbone being able to accept large inserts as well as promoter and terminator sequences for the individual genes to be cloned into the construct.
Due to these demands, the artificial gene operon assembly system (AGOS), introduced by Basitta *et al.* (2017), seemed to be a suitable method to meet these requirements. The system allows to introduce individual genes stepwise, each preceded by a *tcp830* promoter and a ribosomal binding site and followed by a terminator.
As the system had been developed in-house, the required destination vector and the individual entry plasmids were available, and as the cloning procedure is straightforward, this project was considered to be suitable for a Master thesis. The task was therefore delivered to Alexander Hoffreiter who worked on the project from April 2019 to October 2019. The work was continued by Panagiota-Channa Koutsandrea during her Master thesis from Mai 2020 to November 2020.

Table 43: **Proteins chosen for simultaneous overexpression.**
Protein annotation numbers and predicted functions are specified as well as gene sizes and the promoter fragments the proteins had bound to in the performed DACA study.

IFCAGPOI number	**Annotation**	**Size**	**Promoter** (DACA)
06386	LuxR family transcriptional regulator	2760 bp	PfkbO
05107	TetR family transcriptional regulator	627 bp	Ptcs6a
03331	two-component sensor histidine kinase	1623 bp	Ptcs6a
01482	helix-turn-helix transcriptional regulator	2763 bp	PfkbO
04736	LacI family transcriptional regulator	1062 bp	PfkbG
06489	TetR family transcriptional regulator	645 bp	PallA

2.2.4.1 Cloning strategy

The first step in the cloning procedure to generate the large overexpression vector was the amplification of the individual genes by PCR, thereby introducing *Spe*I and *Xba*I restriction sites. After amplification with the Taq:Pfu polymerase, PCR products were ligated into the pGEM®-T vector via TA ligation. Promising clones were confirmed by sequencing using T7 and SP6 standard primers. Correct inserts were excised using *Spe*I and *Xba*I restriction digest and individually cloned into the respective entry plasmid that had been digested with the same restriction enzymes (entry plasmids pLW54-60). Each entry plasmid carries an apramycin resistance cassette, a *tcp830* promoter sequence, a ribosomal binding site and a terminator sequence. Successful clones were identified using colony PCR and restriction digest. To isolate the fragments required for the subsequent targeting reactions, *Pac*I restriction digests were performed and the fragments consisting of the gene, the promoter, the ribosomal binding site and terminator sequence as well as the resistance cassette were purified using a preparative agarose gel. Subsequently, these purified fragments were used for the λ-Red/ET-mediated targeting reactions on the destination vector mrsMR02 within induced *E. coli* BW25113/pIJ790 cells (2.2.2.15). After successful integration of a gene fragment into the destination vector, the resistance cassette was excised using successive *Pme*I & *Sna*BI restriction digests. Following religation, clones having lost the resistance cassette could be identified by streaking them on LB agar plates containing apramycin and kanamycin or only kanamycin. Strains growing only on plates supplemented with kanamycin were verified by restriction digest and used for the new round of targeting with a further gene fragment (figure 6). A crucial part in this cloning procedure was a retransformation of the DNA isolated out of targeting clones as it was observed that the targeting reactions were never 100 % efficient, meaning that they always resulted in a mixture of the expected cosmid and the original, non modified cosmid.

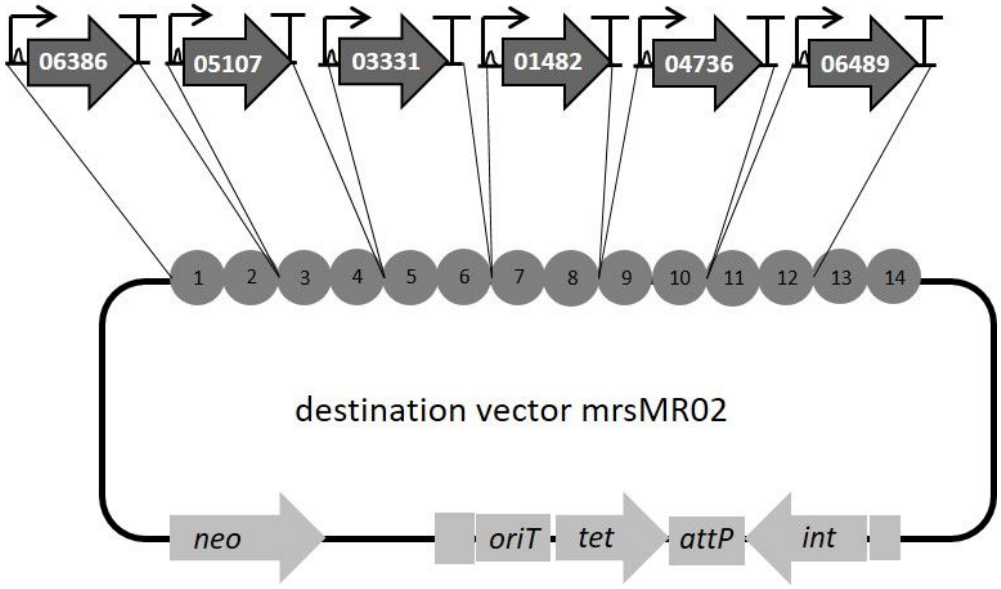

Figure 6: **Principle of AGOS used to simultaneously overexpress several regulators.** The locations of the six regulator genes within the multiple recombineering site are indicated by their respective annotation number.

2.2.4.2 Cultivation of generated mutant strains

In order to compare the effect of a non-integrative versus an integrative overexpression of regulators on tacrolimus production, *Streptomyces tsukubaensis* NRRL18488 strains individually overexpressing one of the six regulators chosen for simultaneous overexpression (table 43) and additionally the strain overexpressing IFCAGPOI_06421 were included in a comprehensive cultivation in 24-square deepwell plates. Each of the individual exconjugants overexpressing one certain regulator in a non-integrative or integrative way, respectively, was cultivated in triplicate. For mutant strains with integrative overexpression of the respective regulator, a non-induced versus an induced state was investigated by adding anhydrotetracycline (aTc) as inductor of the *tcp830* promoter.

Pre-cultures were set up in pre-weighted 50 mL reaction tubes containing 10 mL TSB medium, supplemented with apramycin (non-integrative overexpression) or kanamycin (integrative overexpression), respectively. 10 μL of the respective spore suspension was used for inoculation of the pre-culture. After incubation for two days at 28 °C, 220 rpm, the tubes were centrifuged (4000 x g, 20 min, RT) and the supernatants were discarded. The cell wet weight of all mutant strains was determined and pellets were resuspended in TSB to a final concentration of 732 mg/mL. 75 μL of these solutions was used to inoculate 3 mL MGm-2.5 medium in 24-square deepwell plates (supplemented with apramycin for non-integrative overexpression). Incubation was carried out at 28 °C, 300 rpm for 72 h, according to Bauer *et al.* (2017). Cell dry weight and tacrolimus production were determined as described in 2.2.3.2 and 2.2.6.

Regarding the cultivation of the mutant strains integratively overexpressing more than one regu-

lator, the conditions were slightly varied. The pre-cultures were adjusted to a final concentration of 2 g/mL. Once again, 75 μL thereof was used to inoculate 3 mL of MGm-2.5 medium in the 24-square deepwell plates. Cultivation time was extended to 5 and 7 days, respectively.

2.2.5 PKS engineering

Three different approaches of PKS engineering were pursued in parallel in order to biosynthetically produce the tacrologues 9-allyl tacrolimus and 9-ethyl tacrolimus. An overview of these strategies is depicted in figure 7.

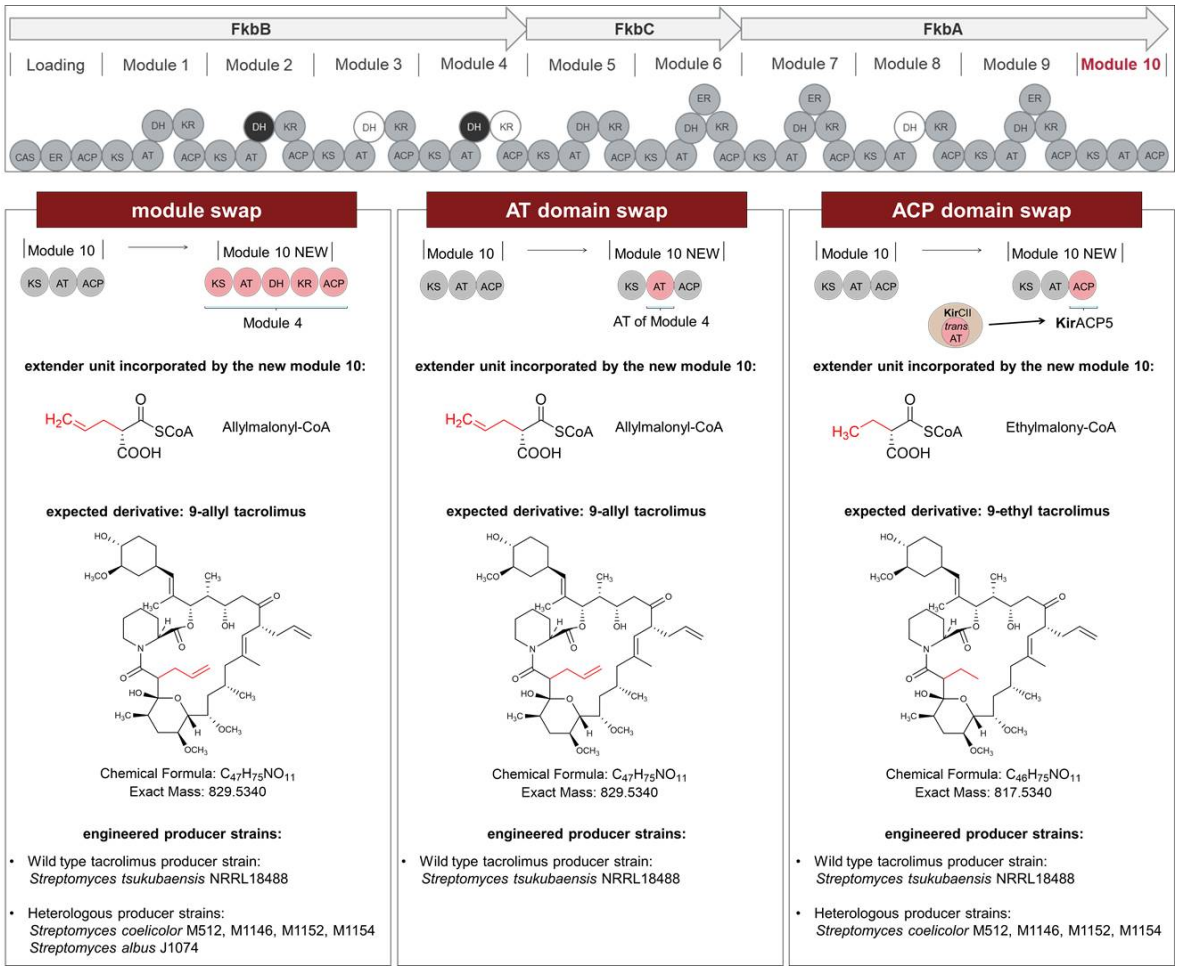

Figure 7: **Overview of the three different PKS engineering approaches pursued in this study.** Module swap and AT domain swap should result in the compound 9-allyl tacrolimus while the ACP domain swap including the *trans*AT KirCII was expected to result in the biosynthesis of 9-ethyl tacrolimus.

As module 10 of the PKS assembly line is responsible for the generation of the functional group in position 9 of tacrolimus, the PKS engineering affected module 10, either as a whole or individual domains thereof, respectively.

During tacrolimus biosynthesis, the wild type producer strain *Streptomyces tsukubaensis*

NRRL18488 introduces an allyl group in position 21 of the molecule. The incorporation of this group is accomplished by the AT domain of module 4 within the PKS assembly line due to the insertion of the rare extender unit allylmalonyl-CoA. Therefore, the idea was to use an additional module 4 at the position of module 10 for the introduction of the second allyl group in position 9.
The first approach meant to perform a module swap by knocking out module 10 followed by an introduction of module 4. On the first try, this module swap was executed on pAC20N, the BAC vector used for heterologous expression of the tacrolimus biosynthetic gene cluster, with the intention to heterologously produce the 9-allyl derivative. In a further approach, this module swap was additionally performed in the wild type producer *Streptomyces tsukubaensis* NRRL18488 using CRISPR-Cas9 editing 2.2.2.17.
Replacing a whole module within a PKS assembly line means a radical intervention into the whole system and is a quite risky intention. For this reason, a second approach was included which only focused on the AT domain of module 10. The AT domain is responsible for the selection of the respective extender unit to be incorporated into the growing polyketide chain. In contrast to the first approach, this AT domain swap was directly intended in the wild type strain *Streptomyces tsukubaensis* NRRL18488 using the CRISPR-Cas9 technology.
For the further aim of generating a 9-ethyl tacrologue, an ACP domain swap including a *trans*AT seemed to be a possible strategy. Musiol *et al.* (2011) developed a method to introduce an ethyl group into a polyketide by using the *trans*AT KirCII in combination with the KirACP5 domain, both originating from the kirromycin biosynthetic gene cluster. Regarding the preparation of a tacrologue, this meant replacing the ACP domain of module 10 with the KirACP5. In a first attempt, this ACP domain swap was performed on pAC20N for heterologous production of the derivative. The required *trans*AT KirCII for loading of KirACP5 is plasmid-encoded. The respective plasmid pEM11CII was kindly provided by Dr. Ewa Musiol-Kroll (University of Tübingen) and conjugated to the mutant strains. Furthermore, the ACP domain swap was also performed in the native producer strain *Streptomyces tsukubaensis* NRRL18488 using CRISPR-Cas9 editing.

2.2.5.1 Module swap

Sequences of module 4 and 10 were identified with the help of the antiSMASH analysis of the whole genome sequence of *Streptomyces tsukubaensis* NRRL18488. Module 4 (4598 bp) consists of 5 domains: KS (β-ketoacyl synthase), AT (acyltransferase), DH (dehydratase), KR (β-ketoacyl reductase) and ACP (acyl carrier protein). DH and KR domains are predicted to be not active and nonfunctional, respectively (Mo *et al.*, 2011). Module 10 (2919 bp) includes only 3 domains: KS, AT and ACP.
The N-terminal ends of the KS domains of module 4 and module 10 represented the upstream borders of the respective modules and could be easily identified due to the conserved EPIAIV motif (EP**L**AIV for module 4). The motifs at the C-terminal ends of the ACP domains of the

two modules are also quite conserved and were chosen as downstream borders of the exchange units (LLTLL (module 4) and LEDRL (module 10)).

Module swap in heterologous host strains

The approach for heterologous production of the 9-allyl derivative required that the module swap was executed on pAC20N. The first step comprised a knockout of module 10 using PCR targeting with a modified 773 (*aac(3)IV*) resistance cassette which contains a rare I-*Sce*I restriction site. After successful insertion of the resistance cassette, the modified pAC20N (pTB66) could therefore be linearized by I-*Sce*I restriction digest. This linearization served as selection marker for the subsequent step which involved the integration of module 4 at the position of module 10 using homologous recombination. In order to do so, module 4 had to be flanked by 500 bp homology arms to the sequences located up- and downstream of module 10. As this complex sequence could not be synthesized chemically, the respective fragment had to be assembled in a stepwise manner (see figure 8).
Due to the extremely repetitive PKS sequences revealing high GC contents, it was not possible to use Gibson Assembly for this purpose. Therefore, a SuperCosI-derived capture vector was prepared instead. Hereto, upstream and downstream homology arms were individually amplified by PCR, thereby introducing *Eco*RI restriction sites at the ends not flanking the original module 10. The ends of the homology arms intended to flank the newly inserted module 4 were extended with 50 bp sequences homologous to the outer parts of module 4 using long primers. In between these two sequences, a *Xba*I restriction site was introduced to enable a subsequent opening of the capture vector inside the homology arms.
Using an overlap PCR, the upstream and downstream fragments were fused, resulting in a DNA fragment of 1112 bp. The pipetting scheme and temperature program for this overlap PCR are depicted in table 44 and table 45.

Table 44: **Pipetting scheme for the overlap PCR.**
During the PCR, the 500 bp homology arms were joined.

Component	Amount
Taq Buffer (10x)	5 μL
Upstream homology arm	17.5 μL
Downstream homology arm	17.5 μL
dNTPs (2.5 mM each)	4 μL
Taq:Pfu polymerase (9:1)	1 μL
DMSO	5 μL

Table 45: **Temperature program for the overlap PCR.**

	Temperature [°C]	**Length [s]**	**Cycles**
Hotstart	94 °C	60	1
Denaturation	94 °C	45	
Annealing	55 °C	30	30
Elongation	72 °C	30	
Terminal elongation	72 °C	120	1
Cooling	4 °C	∞	

The product of the overlap PCR was purified using the Cycle Pure Kit (2.2.2.5). A second PCR with the forward primer of the upstream fragment and the reverse primer of the downstream fragment was performed using the Q5®High-Fidelity DNA polymerase at 68 °C annealing temperature. The fused DNA fragment was purified, digested with *Eco*RI and cloned into an *Eco*RI digested SuperCosI vector, resulting in pTB64.

As the original SuperCosI vector carries a *Xba*I restriction site which would result in an additional undesired cut of the vector besides the proposed cut between the two homology arms, it was necessary to generate a SuperCosI vector without *Xba*I restriction site. To this end, a modified SuperCosI vector harboring the caprazamycin gene cluster (clone 31C2) was digested with *Eco*RI. The fragment of 6795 bp, corresponding to the SuperCosI backbone, was purified from gel and used for ligation with the 1112 bp fragment of the fused homology arms. Sequencing was used to confirm that the homology domains contained no wrong bases.

In the next step, the SuperCosI capture vector (pTB64) was linearized using *Xba*I restriction digest. Subsequently, the vector was co-transformed with the PCR-amplified module 4 into *E. coli* BW25113/pIJ790 cells with induced λ-Red/ET genes. Vectors that had successfully captured module 4 (pTB65) were identified by colony PCR and restriction digest. The correct sequence of module 4 was subsequently verified by sequencing. Module 4 flanked by 500 bp homology arms was excised from pTB65 using an *Eco*RI restriction digest followed by purification of the 5604 bp fragment from an agarose gel.

The last step to perform the module swap on pAC20N comprised a co-transformation of the flanked module 4 and the I-*Sce*I digested pTB66 into *E. coli* BW25113/pIJ790 cells with induced λ-Red/ET genes. Screening for correct clones that had introduced module 4 at the position of module 10 (pTB67) required restriction digests, as colony PCR was complicated due to the large size of module 4 and the difficulty of designing specific primers for an amplification of the border regions of the new module 4. Three pTB67 clones were obtained which showed restriction patterns that corresponded to the expectation. One of them, pTB67-22, was analyzed by Nanopore sequencing (QBIC, University of Tübingen).

All three pTB67 clones (pTB67-1, 21 & 22) were integrated into *E. coli* ET12567 using triparental *E. coli* conjugation as described by Jones *et al.* (2013) and afterwards conjugated to *Streptomyces*

coelicolor M512, M1146, M1152 and M1154, respectively, as well as to *Streptomyces albus* J1074. Some of the generated mutant strains were further conjugated with pUWL-oriT-apra-SD-*fkbN* (Jones *et al.*, 2013) in order to increase the heterologous production of the derivatives.
Cultivation was performed in 50 mL MGm-2.5 medium in 300 mL baffled Erlenmeyer flasks at 30 °C, 200 rpm for 8-14 days. Inoculation was done using either 50 μL of the respective spore suspension or 1 mL of a pre-culture grown in 50 mL TSB:YEME (1:1) for 3-4 days under the given conditions. Screening for tacrologues was accomplished using HPLC and LC-MS measurements (see section 2.2.6).

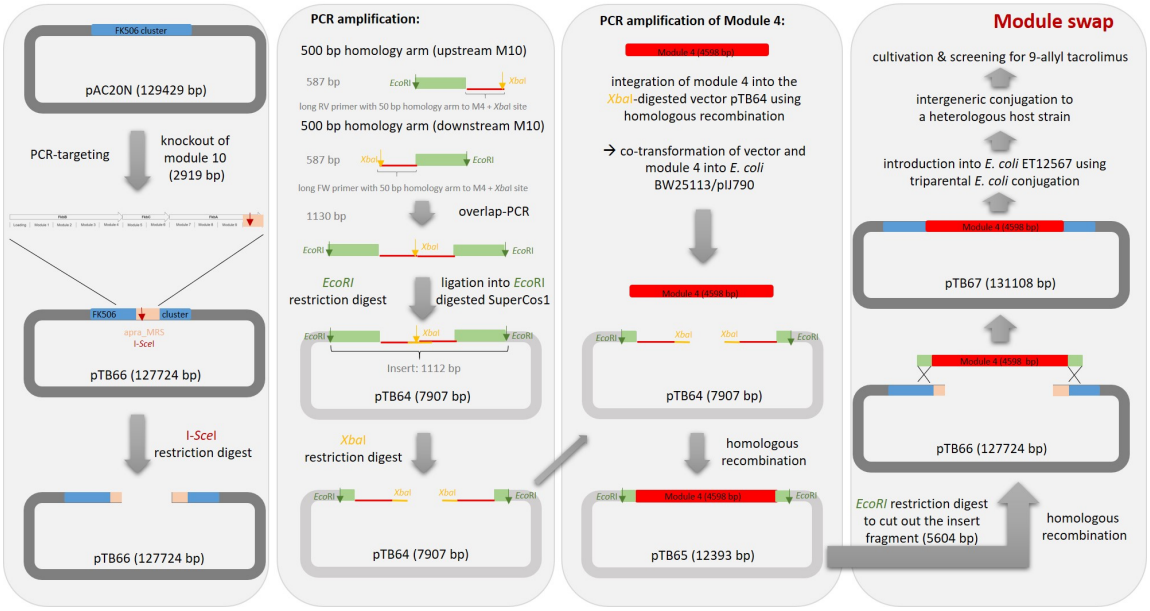

Figure 8: **Working steps to prepare the module swap on pAC20N.**
First column: preparation of pAC20N through insertion of an I-*Sce*I restriction site-containing apramycin resistance cassette at the position of module10 (pTB66). Second column: preparation of the SuperCosI capture vector (pTB64). Third column: cloning of module 4 into the capture vector (pTB65). Fourth column: final homologous recombination event to achieve the module swap on pAC20N (pTB67).

Module swap in the natural producer *Streptomyces tsukubaensis* NRRL18488

A further module swap approach was performed in the wild type producer strain *Streptomyces tsukubaensis* NRRL18488. For this purpose, CRISPR-Cas9 editing was used as described in 2.2.2.17. The following two protospacer sequences located in the AT domain of module 10 were chosen to build up the single guide RNA (sgRNA):

1) GACGGGCGCTGCAAATCGTT
2) GTCCTCGAATCCATCCCGTT

Module 4 flanked by 500 bp homology arms with adjacent *Eco*RI sites, as prepared for the heterologous module swap approach, was used as homology domain. In order to clone this fragment into the *Stu*I site of the pCRISPR-TT vector, it was necessary to generate blunt ends. Therefore, the Quick Blunting^{TM} Kit (NEB) was used to fill up the sticky ends generated by the *Eco*RI restriction digest. Subsequently, the Quick Ligation^{TM} Kit (NEB) was used for the blunt end ligation, resulting in plasmids pTB75 and pTB76, respectively. The plasmids were used for subsequent conjugation to *Streptomyces tsukubaensis* NRRL18488 to finally induce the Cas9.

2.2.5.2 AT domain swap

The AT domain swap was performed in the wild type strain *Streptomyces tsukubaensis* NRRL18488 using CRISPR-Cas9 editing (2.2.2.17).
Comparable to the module swap approach, it was initially important to define the borders of the AT domain. According to Bayly and Yadav (2017) and Yuzawa *et al.* (2017), it is important to maintain both the native KS-AT linker (KAL) and the post-AT linker (PAL1 & 2) sequences. These linker sequences could be identified by means of the described amino acid consensus sequences which are marked in red in figure 9 (Yuzawa *et al.*, 2017).

GTNAHVILEAPAAPDSPSAASPSVAPREPLFLTERTPLPVSARTPEAVEGQIQRLRA
HLAEHPGDDPRTVAAALFSTRTEFPHRAVLLGEGAVTGTALTRPRTVFVFPGQGS
QWLGMGLKLMAESPVFAARMRECADALAEHTGRDLIAMLEDPAVKSRVDVVHPV
CWAVMMSLAAVWEAAGVRPDAVIGHSQGEIAAACVAGAITLEDGARLVALRSALL
QRELAGHGAMGSIAFPAADVEAAAAQVDNVWVAGRNGTGTTIVSGRPDAVET
LIARYEARGVWVTRLVVDCPTHTPFVDPLYDEFQRIAAATTSRTPRIPWFSTADE
RWIDSPLDDEYWFRNLRNPVGFAAAVAAAREPGDTVFVEVSAHPVLLPAINGTTV
GTLRRGGGADQVVDSLAKAYTAGVAVDWPTVVAAPGTAHDTTRTASGPVPGPA
HDLPTYAFHHERYWI

Figure 9: **Amino acid sequence of the AT domain of module 4 including KAL (upstream) and PAL (downstream) linker sequences.**
Consensus sequences of KAL and PAL linker regions are highlighted in red. The sequence of the AT domain of module 4 is shown in blue.

The corresponding linker sequences in module 10 were identified as GTNAHLVLE (N-terminal end of the AT domain) and LPVYPFQHRHYWL (C-terminal end of the AT domain), respectively. The two protospacer sequences chosen to generate the single guide RNAs for the AT domain swap were the same as for the module swap. They were amplified by PCR and individually cloned into the pCRISPR-TT vector using *Nco*I and *Sna*BI restriction sites (pTB68 & pTB69). The homology domain, consisting of 1000 bp up- and downstream sequences of the AT domain of module 10 as well as the AT domain exchange unit of module 4 (KAL-AT-PAL1-PAL2), was assembled into pBlueScript SK(-) using Gibson Assembly (resulting in pTB70).
After successful assembly of the three fragments into pBlueScript SK(-) and verification by

sequencing, the homology domain was excised from pTB70 using an *Eco*RV restriction digest and cloned into the *Stu*I site of pTB68 and pTB69, respectively. The fully assembled pCRISPR-TT vectors (pTB71 & pTB72) were transformed into *E. coli* ET12567/pUZ8002 for subsequent conjugation.
Cultivation of the mutant strains exhibiting the intended AT domain swap was performed as described in 2.2.1.1. Screening for 9-allyl tacrolimus was accomplished using HPLC, LC-MS and HR-MS measurements.

2.2.5.3 ACP domain swap

In contrast to the module swap and AT domain swap approaches, the ACP domain swap was to result in the production of 9-ethyl tacrolimus. Therefore, the native ACP domain of module 10 was replaced by the ACP domain of the kirromycin PKS module 5 (KirACP5), known for the incorporation of ethylmalonyl-CoA when loaded by the *trans*AT KirCII (Musiol *et al.*, 2011).
The N-terminal end of the native ACP domain of module 10 was identified by the residues EIVRR whereas the C-terminal downstream border was the same as for the module swap: the conserved LEDRL motif. The sequence of KirACP5 was kindly provided by Dr. Ewa Musiol-Kroll (University of Tübingen). A synthetic gene block (plasmid pEX-A258-KirACP5) consisting of KirACP5 flanked by 500 bp homology arms to the up- and downstream sequences of the ACP domain of module 10 was ordered at Eurofins Genomics (Ebersberg, Germany).

ACP domain swap in heterologous host strains

Analogous to the module swap approach, the ACP domain swap was intended to be performed on pAC20N for heterologous production of the 9-ethyl derivative. In the first step, the ACP domain of module 10 had to be replaced by the KirACP5. Therefore, the modified 773 (*aac(3)IV*) resistance cassette with I-*Sce*I restriction site was extended with long primers to target the ACP domain of module 10 and integrated into the BAC using homologous recombination. The modified pAC20N (pTB73) was linearized by I-*Sce*I restriction digest and co-transformed with KirACP5, flanked by 500 bp homology arms, into *E. coli* BW25113/pIJ790 with induced λ-Red/ET genes. Resulting clones were screened for the correct domain swap by colony PCR and verified by sequencing.
The modified pAC20N (pTB74) was integrated into *E. coli* ET12567 using triparental *E. coli* conjugation and afterwards integrated into *Streptomyces coelicolor* M512, M1146, M1152 and M1154, respectively, using conjugation. Spores of the resulting mutant strains were subsequently used for a second conjugation to integrate the plasmid pEM11CII. This plasmid encodes the *trans*AT KirCII which is required for loading the KirACP5 with the ethylmalonyl-CoA extender unit. Cultivation was performed as described in section 2.2.5.1. An overview of the workflow to prepare the ACP domain swap is depicted in figure 10.

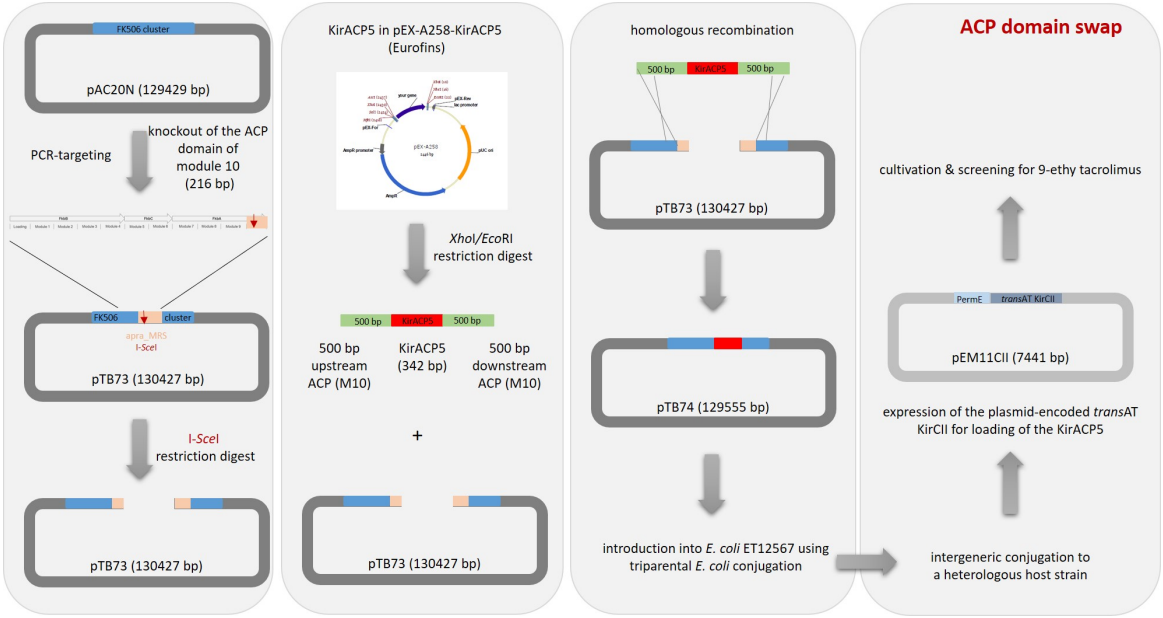

Figure 10: **Working steps to prepare the ACP domain swap on pAC20N.**
First column: preparation of pAC20N through insertion of an I-*Sce*I restriction site-containing apramycin resistance cassette at the position of the ACP domain of module 10 (pTB73). Second column: isolation of KirACP5 flanked by 500 bp homology arms out of pEX-A258-KirACP5 (Eurofins Genomics). Third column: cloning of module 4 into pTB73 using homologous recombination (pTB74). Fourth column: conjugation of pEM11CII into generated mutant strains to achieve the final strains.

ACP domain swap in the natural producer *Streptomyces tsukubaensis* NRRL18488

The second ACP domain swap was performed in the wild type producer strain *Streptomyces tsukubaensis* NRRL18488. For this purpose, CRISPR-Cas9 editing was used as described in 2.2.2.17. The following two protospacer sequences located in the ACP domain of module 10 were chosen to build up the single guide RNA (sgRNA):

1) CGGTGCAGCGCCTGCGCAAC
2) GACTCGACGTTCTTCGCACT

KirACP5 flanked by 500 bp homology arms, ordered as synthetic gene block for the heterologous ACP domain swap approach, was used as homology domain. In order to clone the fragment into the *Stu*I site of the pCRISPR-TT vector, the Quick Blunting^{TM} Kit (NEB) was used. Thereby, the sticky ends generated by the *Xho*I/*Eco*RI restriction digest to excise the flanked KirACP5 from pEX-A258-KirACP5 were filled up. Subsequently, the Quick Ligation^{TM} Kit (NEB) was used for the blunt end ligation, resulting in the plasmids pTB79 and pTB80, respectively. The plasmids were used for conjugation to *Streptomyces tsukubaensis* NRRL18488.

2.2.6 Analytics

2.2.6.1 HPLC

HPLC analytics were routinely carried out to verify and quantify tacrolimus production of the wild type producer strain *Streptomyces tsukubaensis* NRRL18488 and generated mutant strains. Furthermore, HPLC was used to perform the initial screening for the production of tacrologues. Semi-preparative HPLC allowed to purify compounds that were to be used for further analysis. In order to determine the production of tacrolimus and its derivatives, 600 μL of ice-cold methanol was added to 600 μL of culture broth. The mixture was incubated at 30 °C and 200 rpm for one hour. After centrifugation (16100 x g, 10 min), the supernatant was transferred into a new reaction tube and centrifuged as described before. The resulting supernatant was applied onto a Poroshell 120 EC-C18 (150 mm x 4.6 mm, 2.7 μm, Agilent Technologies) reversed-phase HPLC column at 55 °C (instrument: Agilent Technologies 1260 Infinity II). Elution was performed with a gradient of a mobile phase composed of A) 0,1 % *(v/v)* trifluoroacetic acid (TFA) in ddH_2O and B) 20 % *(v/v)* methyl tert-butyl ether (MTBE) in acetonitrile (ACN) according to the following program:

Table 46: **Gradient used for HPLC analytics.**

Time	**Solvent A [%]**	**Solvent B [%]**
0-5 min	60	40
5-35 min	20	80
35-36 min	10	90
36-39 min	10	90
39-40 min	60	40
40-43 min	60	40

Flow rate was maintained at 0.5 mL/min. The peak corresponding to tacrolimus was identified using an external standard (0.5 mM in methanol). The injection volume of the standard was 10 μL, the injection volume of the samples was 80 μL. Detection wavelengths of the UV detector were set to 210 nm, 250 nm and 280 nm. Tacrolimus quantification was carried out at 250 nm.

2.2.6.2 LC-MS

LC-MS measurements were kindly conducted by Andreas Kulik (University of Tübingen). Separation was achieved on a Raptor Fluorophenyl (100 mm x 2.1 mm, 5 μm) column at 40 °C. Elution was accomplished with a gradient of a mobile phase composed of A) 0.1 % formic acid (FA) in ddH_2O and B) 0.06 % formic acid (FA) in acetonitrile (ACN) according to the following program:

Table 47: **Gradient used for LC-MS analytics.**

Time	Solvent A [%]	Solvent B [%]
0 min	70	30
0-15 min	20	80
15-16 min	0	100
16-18 min	0	100

Flow rate was maintained at 0.4 mL/min. The peak corresponding to tacrolimus was identified using an external standard (0.1 mg/mL in methanol). The injection volume of all samples was 2.5 μL. Detection wavelengths of the UV detector were set to 230-600 nm.

2.2.6.3 HR-MS and MS^2

HR-MS measurements were kindly accomplished by Ryan Karongo (University of Tübingen). Separation was conducted on a Kinetex PFP (100 mm x 3 mm, 2.6 μm) column at 30 °C. Elution was performed with a gradient of a mobile phase composed of A) 0.1 % formic acid (FA) in ddH_2O and B) 0.1 % formic acid (FA) in acetonitrile according to the following program:

Table 48: **Gradient used for HR-MS analytics.**

Time	Solvent A [%]	Solvent B [%]
0 min	70	30
0-15.5 min	20	80
15.5-16.5 min	0	100
16.5-18.5 min	0	100
18.5-18.6 min	70	30
18.6-20.6 min	70	30

Flow rate was maintained at 0.8 mL/min with 5.1 μL injection volume. Detection mode was ESI(+) Q-TOF IDA and MRM.

2.2.6.4 NMR

In order to elucidate the structure of the new compound produced by one of the generated ACP domain swap mutant strains, nuclear magnetic resonance (NMR) spectroscopy was required. To obtain a sufficient amount of the respective compound, the mutant strain *Streptomyces tsukubaensis* ACP E2-K7-6/pEM11CII was cultivated on a two liter scale in MGm-2.5 medium. After seven days of cultivation, the culture was extracted with an equal volume of methanol, incubated at 28 °C, 220 rpm for one hour and cells were subsequently detached by centrifugation

(6000 x g, 10 min, 4 °C). The supernatant was transferred into round-bottom flasks and concentrated using a rotary evaporator until a highly viscous extract of 124 g was obtained. 32 g of this extract was used for a reversed-phase (RP) vacuum liquid chromatography (VLC; dimensions: 20 cm x 6.5 cm). Elution was executed using the stepwise gradient depicted in table 49.

Table 49: **Gradient used for VLC.**

Fraction	**Methanol [%]**	**ddH_2O [%]**	**Volume [L]**
1	10	90	1.5
2	30	70	1.0
3	50	50	2.0
4	65	35	1.0
5	80	20	1.0
6	100	0	1.0

Each fraction was concentrated to dryness and resuspended in 4-8 mL of 100 % methanol. Subsequently, every fraction was subjected to LC-MS analysis to identify the extract containing the desired compound. The pure compound was afterwards obtained from fraction 6 by semi-preparative HPLC using a Kinetex®PFP 100 $\AA$ LC column (250 mm x 4.6 mm, 5 μm) with the gradient and conditions described in 2.2.6.1. 8.35 mg of pure compound was obtained after freeze-drying and diluted in 450 μL of deuterated chloroform. The NMR analysis was carried out by Irina Helmle (University of Tübingen). NMR spectra were acquired using a BRUKER Avance III HD 400 MHz NanoBay NMR spectrometer (^{1}H, 400 MHz; ^{13}C, 101 MHz) at 293 K. Chemical shifts were referred to the solvent as internal standard ($CDCl_3$, δ_H/δ_C 7.26/77.0).

3 Results

3.1 DACA

3.1.1 Determination of cell dry weight and tacrolimus production during the 10 L fermentation

In order to obtain a sufficient amount of proteins for the DNA affinity capturing assay, *Streptomyces tsukubaensis* NRRL18488 was cultivated in a 10 L fermenter. Cell dry weight and tacrolimus production were monitored during this cultivation to identify appropriate time points for protein extraction. The resulting growth and production curves are depicted in figure 11. Growth of *Streptomyces tsukubaensis* NRRL18488 in the fermenter started after around 48 hours and was succeeded by an exponential growth phase up to 78 hours of cultivation. After a subsequent switch phase with diminished growth, there was again an increase in cell mass up to finally 10.5 g/L. Tacrolimus production started after approximately 114 hours of growth. Subsequently, there was a continuous increase in tacrolimus production and after 240 hours, 16.7 mg/g was gained, which corresponds to 175.2 mg/L.

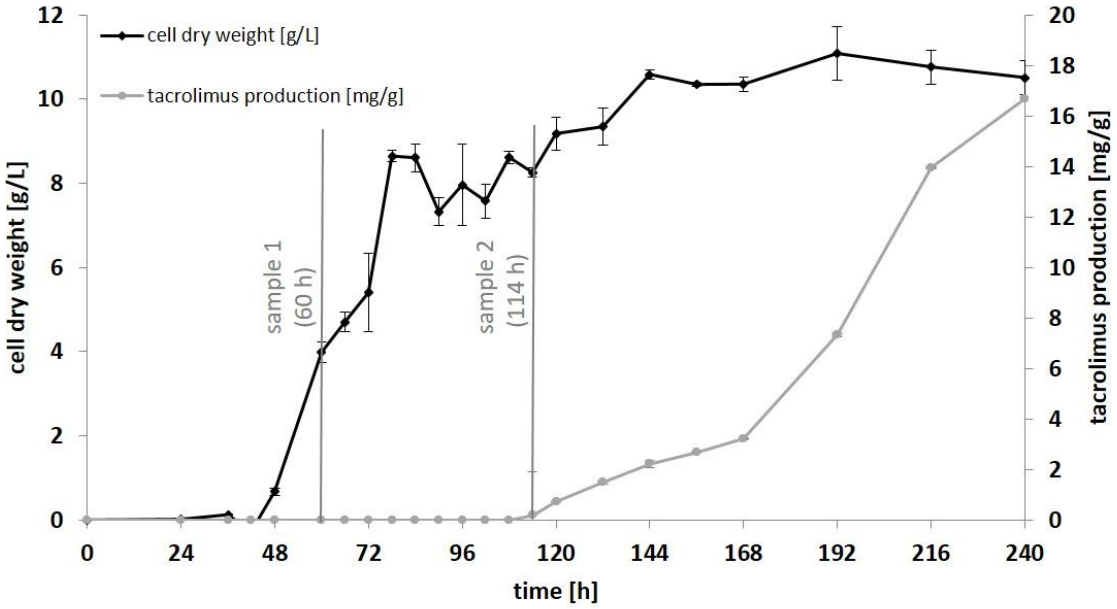

Figure 11: **Cell dry weight and tacrolimus production of *S. tsukubaensis* NRRL18488 monitored during the 10 L fermentation.**

The growth behavior of *Streptomyces tsukubaensis* NRRL18488 in the 10 L fermenter was quite comparable to that observed for common 100 mL scale fermentations (figure 27; appendix), however, the maximum total amount of biomass achieved during the 10 L fermentation was higher compared to smaller scale cultivations (maximum 11.08 g/L after 192 h vs. 7.42 g/L after 144 h). The higher amount of biomass in the fermenter also resulted in a twice as big final tacrolimus yield compared to fermentation on a 100 mL scale (16.67 mg/g vs. 8.17 mg/g).
Based on the results of cell dry weight determination and tacrolimus production during the fermentation of *Streptomyces tsukubaensis* NRRL18488 in the 10 L fermenter, two time points were chosen for protein extraction to perform the subsequent DACA studies. The first selected time point was at 60 hours. At this time point, the culture was in the middle of the exponential growth phase and far away from the onset of tacrolimus production. In contrast, the second time point was chosen to be at 114 hours due to the observed onset of tacrolimus production. It is reasonable to assume that the expression of biosynthetic genes reaches its maximum at this state.

3.1.2 Identification and quantification of DNA-binding proteins via label free mass spectrometry

Following the protein extraction from the cells grown for 60 hours and 114 hours in the 10 L fermenter, the DNA affinity capturing assay was accomplished as described in 2.2.3.6. Captured proteins were precipitated with TCA and subsequently passed to the proteome center of the University of Tübingen to perform the proteome analysis. Prof. Dr. Kay Nieselt (University of Tübingen) kindly provided an annotated protein data base of *Streptomyces tsukubaensis* NRRL18488 for the evaluation of the data achieved by semi-quantitative mass spectrometry. The analysis of the raw data was carried out by Dr. Mirita Franz-Wachtel from the group of Prof. Dr. Boris Macek.
1044 proteins of *Streptomyces tsukubaensis* NRRL18488 could be identified in the DACA with quantities measured as intensities between $9.93 \cdot 10^4$ and $2.11 \cdot 10^9$ (figure 12). The total amount of regulators and hypothetical proteins detected in the DACA was 230, corresponding to 22 % of all proteins. Thereof, 141 were annotated as regulators and 89 as hypothetical proteins. Regarding the value $1.08 \cdot 10^6$ as threshold value to determine high intensities (see below), 104 of these regulators and 49 of the hypothetical proteins depicted high intensities and were considered for further analysis.

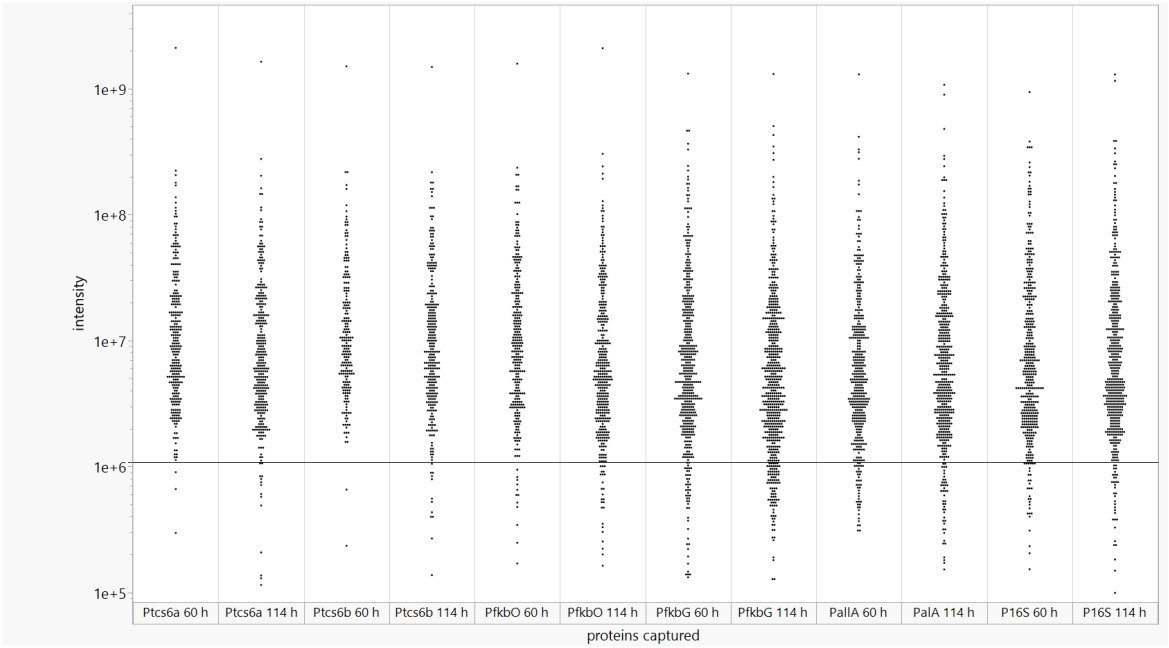

Figure 12: **Scatter plot of the intensities of all identified proteins in the DACA.** The threshold value of $1.08 \cdot 10^6$ as defined in the text is indicated by a horizontal line.

Table 50 indicates the total amount of proteins detected on the individual promoter fragments analyzed in the DACA at the two different time points. The largest promoter fragment Ptcs6b trapped the highest total amount of proteins. A quite similar number of proteins was trapped by the negative control promoter fragment P16S. In contrast, PfkbO, the promoter region controlling the expression of the PKS core genes, had trapped the smallest amount of proteins.

Table 50: **Amount of proteins detected on the different promoter fragments in the DACA.**

Promoter fragment	**Amount of proteins 60 h sample**	**Amount of proteins 114 h sample**	**Total amount of proteins**
Ptcs6a	272	454	726
Ptcs6b	310	563	873
PfkbO	204	398	602
PfkbG	286	470	756
PallA	285	412	697
P16S	366	468	834

3.1.2.1 Positive controls of the DACA

Analogously to the evaluation of the DACA results performed by Bekiesch *et al.* (2016) for the heterologously expressed novobiocin biosynthetic gene cluster, the binding behavior of the positive controls was initially analyzed.

FkbN

The known pathway-specific and positive transcriptional regulator FkbN of tacrolimus biosynthesis was to serve as positive control in the DACA to validate the preliminary procedure. Presumed naturally occurring binding sites of FkbN within the promoter fragments Ptcs6b, PfkbO, PfkbG and PallA (2x) were described by Ordónez-Robles *et al.* (2016). The respective protein (IFCAGPOI_06386) could be identified in the DACA with intensities of $1.08 \cdot 10^6$ at PfkbO and intensities of $5.31 \cdot 10^5$ at P16S in the 114 hours samples. FkbN did not bind to Ptcs6b, PfkbG and PallA in detectable quantities. For the following evaluation of the data, only proteins identified with intensities higher than $1.08 \cdot 10^6$ were considered to be specific regulators. A second threshold value was set similar to Bekiesch *et al.* (2016), defining the specific binding of a protein by the condition that its intensity has to be a least tenfold higher on one promoter region in comparison with all the other ones at least at one time point. Increasing this additional restriction to hundredfold would exclude only one protein compared to the aforementioned criterion of a tenfold higher intensity (IFCAGPOI_06084; Ptcs6a binding).

PhoP

As a second positive control in the DACA served the protein PhoP which is involved in phosphate regulation and which is a known DNA binding protein (Ordóñez-Robles *et al.*, 2017). Ordóñez-Robles *et al.* (2017) predicted putative PhoP binding sites, so-called PHO-boxes, in the whole genome sequence of *Streptomyces tsukubaensis* NRRL18488. One of these putative PHO-boxes is located upstream of the gene *fkbN*, thus in the promoter region Ptcs6. Indeed, the protein PhoP (IFCAGPOI_03863) was found to bind exclusively to Ptcs6b in the 114 hours sample with an intensity of $6.26 \cdot 10^5$.

3.1.2.2 Proteins binding unspecifically to all promoter regions of the tacrolimus biosynthetic gene cluster

116 proteins were detected in the DACA binding in higher quantities ($> 1.08 \cdot 10^6$) to all six promoter fragments at both time points. Among those were 37 unspecifically DNA-binding proteins as e.g. the transcription termination factor RHO1 and the DNA-directed RNA polymerase subunit beta RpoC as well as further polymerases and other proteins. Eight of these 116 proteins have a putative regulatory function.

3.1.2.3 Proteins binding specifically to one promoter region of the tacrolimus biosynthetic gene cluster

Applying the aforementioned selection criteria for specific binding, five proteins were detected binding specifically to Ptcs6a. Four of those proteins were chosen to be further analyzed as they did not bind to the negative control P16S. These were the proteins IFCAGPOI_05107 (TetR family transcriptional regulator), IFCAGPOI_04345 (transcriptional regulator), IFCAGPOI_06084

(GntR family transcriptional regulator) and IFCAGPOI_03331 (two-component sensor histidine kinase) (table 51).
The highest number of specifically binding proteins was detected on the promoter region Ptcs6b. 14 proteins were trapped in total, eleven of which were chosen for further analysis as no binding to P16S could be observed. These were the proteins IFCAGPOI_00860 (transcriptional regulator), IFCAGPOI_01458 (transcriptional regulator), IFCAGPOI_02551 (two-component system DNA-binding response regulator), IFCAGPOI_03512 (single-stranded DNA-binding protein), IFCAGPOI_04383 (hypothetical protein), IFCAGPOI_04468 (DNA-binding response regulator), IFCAGPOI_05876 (YebC/PmpR family DNA binding transcriptional regulator), IFCAGPOI_05926 (transcriptional regulator), IFCAGPOI_05966 (transcription regulator AsnC), IFCAGPOI_05976 (GntR family transcriptional regulator) and IFCAGPOI_06286 (hypothetical protein).
Six proteins showed specific binding properties to the promoter region PfkbO and all of them were chosen for further investigation: IFCAGPOI_00339 (LuxR family transcriptional regulator), IFCAGPOI_01482 (helix-turn-helix transcriptional regulator), IFCAGPOI_03805 (hypothetical protein), IFCAGPOI_05711 (ATP/GTP-binding protein), IFCAGPOI_06136 (TetR family transcriptional regulator) and IFCAGPOI_05636 (GTP-binding protein EngA).
The unidirectional promoter region PfkbG was bound by nine proteins, seven of which did not simultaneously bind to P16S and were therefore further analyzed: IFCAGPOI_02717 (nucleotide-binding protein), IFCAGPOI_03574 (GntR family transcriptional regulator), IFCAGPOI_04736 (LacI family transcriptional regulator), IFCAGPOI_05697 (GntR family transcriptional regulator), IFCAGPOI_06331 (hypothetical protein), IFCAGPOI_01705 (docking protein) and IFCAGPOI_04924 (GTP-binding protein Era).
All of the five proteins binding specifically to PallA were further analyzed: IFCAGPOI_00009 (hypothetical protein), IFCAGPOI_00306 (MarR family transcriptional regulator), IFCAGPOI_05548 (hypothetical protein), IFCAGPOI_06487 (regulatory protein) and IFCAGPOI_06489 (TetR family transcriptional regulator).
Interestingly, all eleven proteins that could be identified on Ptcs6b were extracted from the 114 hours sample. No early stage proteins had specifically bound to this promoter region. Regarding the other promoter regions, the amount of specifically binding proteins detected in the 60 hours sample was comparable to the amount of proteins detected in the 114 hours sample. Only one of the proteins met the classification criteria at both time points, namely IFCAGPOI_04345 (transcriptional regulator) trapped with Ptcs6a.
In addition to these proteins chosen for specificity reasons, seven further putatively regulatory proteins were selected for further analysis as they had bound to two or more promoter regions in high intensities but not to P16S (table 51). These were the proteins IFCAGPOI_04513 (two-component system response regulator), IFCAGPOI_05727 (two-component response regulator), IFCAGPOI_00682 (Crp/Fnr family transcriptional regulator), IFCAGPOI_01589 (response regulator), IFCAGPOI_02857 (transcriptional regulator), IFCAGPOI_03410 (DNA-binding response regulator) and IFCAGPOI_03597 (bifunctional histidine kinase and regulator).

All the aforementioned proteins were to be overexpressed in the wild type producer strain *Streptomyces tsukubaensis* NRRL18488 to elucidate their influence on tacrolimus production. Therefore, the respective genes were cloned into the replicative pUWL-apra-oriT expression vector under control of the strong, constitutive promoter *ermE** and subsequently conjugated to *Streptomyces tsukubaensis* NRRL18488. Designations of the generated plasmids are likewise listed in table 51.

Table 51: **Intensities of proteins binding specifically to the different promoter fragments analyzed in the DACA.**
None of the proteins had bound to the negative control promoter fragment P16S. Names of the corresponding plasmids generated for overexpression studies are listed.

Plasmid		Gene annotation	IFCAGPOI	Ptcs6a		Ptcs6b		PfkbO		PfkG		PallA	
			no. protein	60 h	114 h	60 h	114 h	60 h	114 h	60 h	114 h	60 h	114 h
1	pTB01	TetR family transcriptional regulator	05107	6.03E+06									
2	pTB02	transcriptional regulator	04345	2.56E+06	2.81E+06	2.08E+06				2.13E+06		2.11E+06	
3	pTB03	two-component sensor histidine kinase	03331		7.45E+06								
4	pTB42	GntR family transcriptional regulator	06084		2.72E+07						6.50E+05		
5	pTB04	transcriptional regulator	00860				1.12E+06						
6	pTB05	transcriptional regulator	01458				7.64E+06						
7	pTB06	two-component system DNA-binding response regulator	02551				2.38E+06						
8	pTB07	single-stranded DNA-binding protein	03512				2.47E+06						
9	pTB08	hypothetical protein	04383				1.10E+06						
10	pTB09	DNA-binding response regulator	04468				1.16E+06						
11	pTB10	YebC/PmpR family DNA-binding transcriptional regulator	05876				1.27E+06						
12	pTB11	transcriptional regulator	05926				1.11E+06						
13	pTB12	transcription regulator AsnC	05966				1.57E+07						
14	pTB13	GntR family transcriptional regulator	05976				1.09E+07						
15	pTB14	hypothetical protein	06286				2.35E+06						
16	pTB15	LuxR family transcriptional regulator	00339						6.35E+06				
17	pTB16	helix-turn-helix transcriptional regulator	01482					1.78E+07					
18	pTB17	hypothetical protein	03805					1.58E+06					
19	pTB18	TetR family transcriptional regulator	06136					1.88E+06					
20	pTB19	ATP/GTP-binding protein	05711						1.14E+06				
21	pTB39	GTP-binding protein EngA	05636						3.93E+06				
22	pTB20	docking protein	01705								1.43E+06		
23	pTB21	nucleotide-binding protein	02717								1.17E+06		
24	pTB22	GntR family transcriptional regulator	03574							1.32E+06			
25	pTB23	LacI family transcriptional regulator	04736							3.44E+06			
26	pTB24	GntR family transcriptional regulator	05697							1.17E+06			
27	pTB25	hypothetical protein	06331								1.63E+06		
28	pTB38	GTP-binding protein Era	04924								1.71E+06		
29	pTB26	hypothetical protein	00009										3.58E+06
30	pTB27	MarR family transcriptional regulator	00306									1.36E+06	
31	pTB28	hypothetical protein	05548									1.86E+06	
32	pTB29	regulatory protein	06487									1.80E+06	
33	pTB30	TetR family transcriptional regulator	06489										1.57E+06

	Plasmid	**Gene annotation**	**IFCAGPOI**	Ptcs6a		Ptcs6b		PfkbO		PfkG		PallA	
			no. protein	60 h	114 h	60 h	114 h	60 h	114 h	60 h	114 h	60 h	114 h
34	pTB31	two-component system response regulator	04513		1.07E+06		3.27E+06		1.14E+06		1.46E+06		
35	pTB32	two-component response regulator	05727				6.42E+06				3.54E+06		1.99E+06
36	pTB33	Crp/Fnr family transcriptional regulator	00682				1.16E+07		1.16E+07		1.13E+07		
37	pTB34	response regulator	01589				5.81E+06				7.65E+06		
38	pTB35	transcriptional regulator	02857				2.04E+06				2.11E+06		
39	pTB36	DNA-binding response regulator	03410				1.54E+06				1.79E+06		
40	pTB37	bifunctional histidine kinase and regulator	03597		2.55E+06		2.15E+06						

3.1.2.4 Proteins of the tacrolimus biosynthetic gene cluster

Having a look at the proteins encoded in the tacrolimus biosynthetic gene cluster, it became obvious that most of these proteins could be detected in the DACA (table 52). Eight proteins were not trapped by any promoter fragment, among those the proteins AllM, AllN, AllO, FkbI, FkbJ, FkbL, Tcs6 and the second pathway-specific regulator FkbR. As expected, the proteins were predominantly detected in the 114 hours sample as they are required for the biosynthesis which evidently only starts after 114 hours.
The proteins FkbD and AllA could additionally be detected in nearly every 60 hours sample at every promoter fragment in quite high intensities ($1 \cdot 10^7$-range).
In order to figure out a putatively regulatory role of AllA, which is known to be involved in allylmalonyl-CoA precursor biosynthesis, this protein was additionally chosen to be analyzed in further detail (plasmid pTB40).
Likewise, the known cluster-located positive regulator FkbN and one of the seven phosphopantethenyl transferases present in *Streptomyces tsukubaensis* NRRL18488 were chosen for overexpression.

Table 52: **Proteins of the tacrolimus biosynthetic gene cluster and their intensities on the different promoter fragments analyzed in the DACA.**

Some of the proteins are listed several times due to the fact that they possess multiple annotation numbers. The gene encoding Tcs6, which is located in the intergenic region between *fkbR* and *fkbQ*, had not been annotated and could therefore not be detected in the DACA. Specific intensities as defined in the text are shaded in grey.

Protein	IFCAGPOI	Ptcs6a		Ptcs6b		PfkbO		PfkG		PallA		P16S	
name	no. protein	60 h	114 h	60 h	114 h	60 h	114 h	60 h	114 h	60 h	114 h	60 h	114 h
FkbR	06384												
Tcs6	not annotated												
FkbQ	06385		3.61E+06		3.02E+06		3.40E+06		4.01E+06		2.74E+06		3.97E+06
FkbN	06386						1.08E+06						6.60E+01
FkbM	06387						2.40E+06						
FkbD	06388	2.00E+07	4.15E+07	2.19E+07	4.53E+07	1.77E+07	6.97E+07	1.37E+07	3.55E+07	1.08E+07	3.39E+07	1.98E+07	5.02E+07
FkbA	06389		2.69E+06		3.75E+06		3.05E+06				2.44E+06		
FkbA	06390				2.36E+06								
FkbA	06393		2.31E+06		2.83E+06		3.42E+06		1.59E+06		2.83E+06		
FkbA	06394						1.13E+06						
FkbA	06395				1.18E+06								
FkbP	06395		3.67E+06		5.83E+06		5.39E+06		4.06E+06		3.63E+06		3.21E+06
FkbP	06397	2.40E+06	6.33E+06	2.38E+06	6.37E+06		8.20E+06		5.97E+06		5.44E+06	2.25E+06	6.86E+06
FkbO	06398		4.07E+06		3.78E+06		4.89E+06		4.84E+06		2.98E+06		4.27E+06
FkbB	06399				2.01E+06								
FkbB	06400												
FkbB	06401				4.06E+06		5.09E+06				2.07E+06		2.58E+06
FkbB	06402		5.24E+05										
FkbC	06403						7.69E+05						
FkbC	06404		2.91E+06		4.09E+06		3.01E+06						
FkbC	06405										4.30E+05		
FkbL	06406												
FkbK	06407		2.89E+06		2.78E+06		2.98E+06		2.69E+06		2.21E+06		4.01E+06
FkbJ	06408												
FkbI	06409												
FkbH	06410										8.49E+05		
FkbG	06411				6.64E+05								
AllS	06413										8.49E+05		
AllO	06414												
AllP	06415				6.61E+05								
AllN	06416												
AllM	06417												
AllD	06418								1.16E+06				
AllR	06419		8.22E+06		6.63E+06		8.86E+06		5.59E+06		6.37E+06		6.57E+06
AllK	06420		3.73E+06		3.58E+06		3.39E+06		2.34E+06		2.64E+06		4.43E+06

Protein name	**IFCAGPOI no. protein**	Ptcs6a		Ptcs6b		PfkbO		PfkG		PallA		P16S	
		60 h	114 h	60 h	114 h	60 h	114 h	60 h	114 h	60 h	114 h	60 h	114 h
AllA	06421	6.18E+05	3.60E+07	1.32E+07	3.94E+07		5.34E+07	4.96E+06	3.15E+07	8.01E+06	3.69E+07	1.05E+07	4.28E+07

3.2 Overexpression of putative regulatory proteins of tacrolimus biosynthesis

3.2.1 Non-integrative overexpression of putative regulatory proteins

The implemented DACA studies allowed to identify 40 putatively regulatory proteins of tacrolimus biosynthesis (table 51). To investigate the impact of an overexpression of these proteins and further three candidates (3.1.2.4) on tacrolimus production, all the respective genes were amplified by PCR and cloned into the vector pUWL-apra-oriT under control of the constitutive *ermE** promoter, resulting in plasmids pTB01-pTB43.
As the amplification of the genes encoding the proteins IFCAGPOI_06487, IFCAGPOI_03597 and IFCAGPOI_05636 was not successful and chemical synthesis of these genes was likewise not possible, plasmids pTB29, pTB37 and pTB39 could not be prepared and the respective proteins could not be included in the overexpression study.
All generated mutant strains were submitted to an initial high-throughput screening approach to figure out the effect of the overexpressed proteins on tacrolimus production. This screening was kindly performed by SINTEF (Trondheim, Norway). Each of the three individual exconjugants of a certain mutant strain was cultivated in triplicate on a 1 mL scale. Results of these cultivations are depicted in figure 13a. On average, overexpression of the putatively regulatory proteins resulted in a 1.4-fold increase in tacrolimus production. 14 of the generated mutant strains showed a significantly increased tacrolimus production compared to the reference strain *Streptomyces tsukubaensis* NRRL18488 harboring the empty vector pUWL-apra-oriT. 50 % of the proteins binding to Ptcs6a, 54.5 % of the proteins binding to Ptcs6b, 20 % of the proteins trapped with PkfbO and 57.1 % of the proteins binding to PfkbG significantly increased tacrolimus production following their overexpression. None of the proteins trapped with PallA significantly increased tacrolimus production upon overexpression.
Especially the strains *Streptomyces tsukubaensis*/pTB03, pTB08 and pTB20, overexpressing a two-component sensor histidine kinase, a hypothetical protein and a docking protein, respectively, were outstanding due to their high production yields (2.3-, 1.9- and 2.2-fold increase compared to the reference strain, respectively). Interestingly, the strain *Streptomyces tsukubaensis*/pTB40, overexpressing the cluster located protein AllA, showed a significantly decreased production compared to the control strain on a 1 mL scale cultivation. However, due to the fact that AllA is required for precursor biosynthesis (Mo *et al.*, 2011), a knockout of this protein was no option.

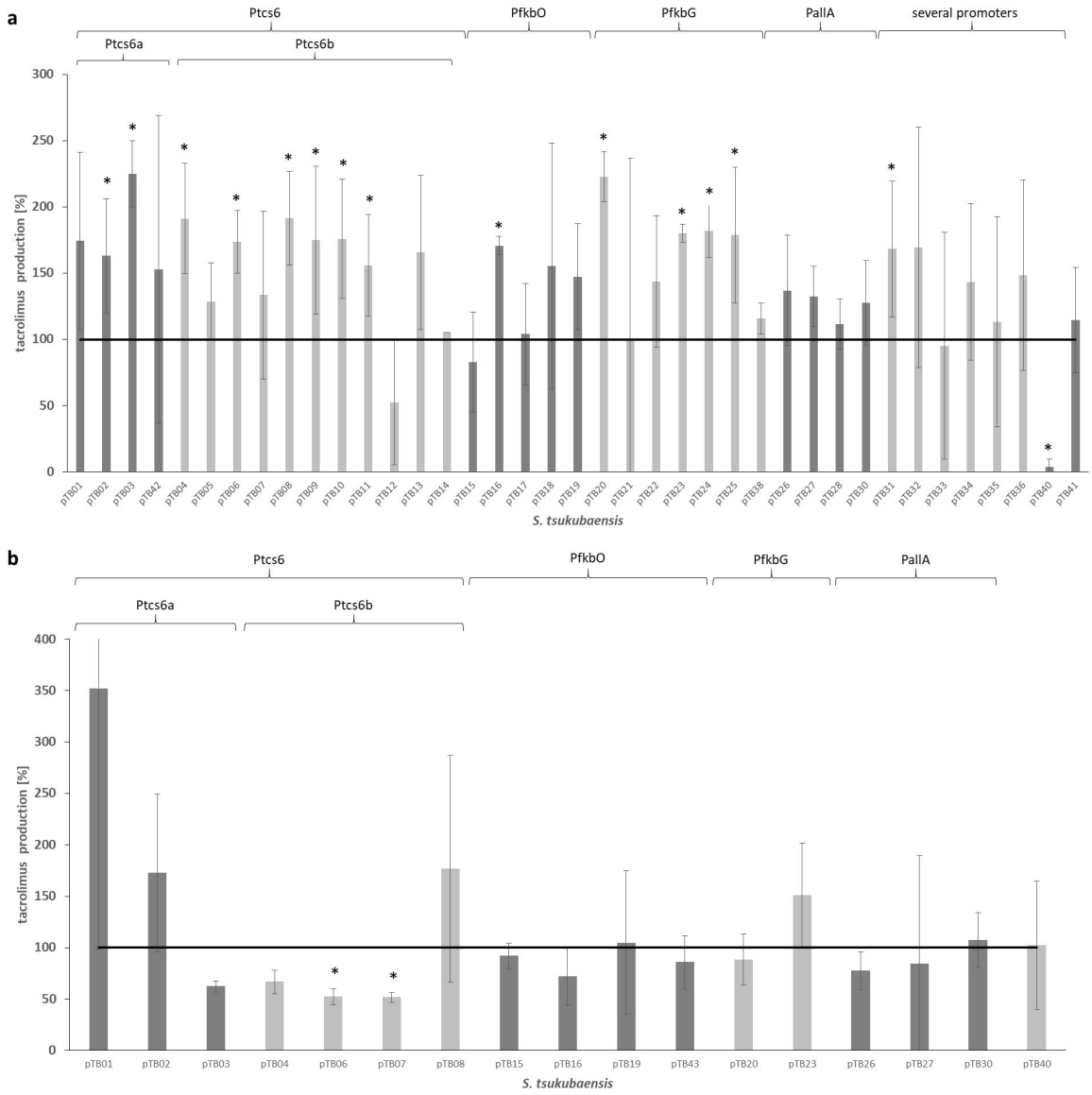

Figure 13: **Tacrolimus production of the generated mutant strains overexpressing regulatory proteins.**

a Tacrolimus production of all generated *S. tsukubaensis* NRRL18488 mutant strains overexpressing regulatory proteins obtained on 1 mL scale fermentations. All yields are normalized to the reference strain *S. tsukubaensis*/pUWL-apra-oriT. Production values represent the maximum mean tacrolimus production yield achieved for three biological replicates, each cultivated in triplicate (data generated by SINTEF). **b** Tacrolimus production of selected *S. tsukubaensis* NRRL18488 mutant strains overexpressing regulatory proteins obtained on 100 mL scale fermentations. Production values represent the maximum mean tacrolimus production yield achieved for three biological replicates. The 100 mL scale cultivation additionally included the strain *S. tsukubaensis*/pTB43 overexpressing the known pathway-specific regulator FkbN. Statistically significant differences compared to *S. tsukubaensis*/pUWL-apra-oriT are marked with asterisks.

Simultaneously with the screening of the mutant strains overexpressing regulatory proteins performed by SINTEF, 17 selected strains were additionally cultivated on a 100 mL scale, each over a period of 14 days. The maximum mean tacrolimus production yield achieved for three individual exconjugants is shown in figure 13b. A significantly increased production of tacrolimus could not be detected for any of the analyzed strains, however it became obvious that the strains *Streptomyces tsukubaensis*/pTB01, pTB02, pTB08 and pTB23 are quite good tacrolimus producers (3.5-, 1.7-, 1.8- and 1.5-fold production increase, respectively). According to the annotation, these strains overexpress a TetR family transcriptional regulator, a transcriptional regulator, a hypothetical protein and a LacI family transcriptional regulator. Noticeably, production yields obtained by the mutant strain *Streptomyces tsukubaensis*/pTB40 were increased compared to the reference strain rather than being reduced as it had been observed on small-scale cultivation. The observations indicate that tacrolimus production yields are not fully transferable between different scales of cultivation.

3.2.2 Comparison of non-integrative and integrative overexpression of selected putative regulatory proteins

With regard to the intention of combining the genes encoding some of the best positive regulators of tacrolimus biosynthesis on a single vector for simultaneous overexpression (see 3.3), it was necessary to select some of the regulators identified in the DACA. FkbN (IFCAGPOI_06386), the known pathway-specific positive regulator of tacrolimus biosynthesis, was to be included in further studies anyway. For the choice of the remaining regulators it was important to consider that they bind to different promoter regions within the tacrolimus biosynthetic gene cluster in order to prevent steric interference of the proteins on their target sequences. Due to the limited comparability of the tacrolimus production values obtained in microfermentation and 100 mL fermentation, the selection of appropriate regulators was not straightforward. Yet, finally two Ptcs6 binders (IFCAGPOI_05107 and IFCAGPOI_03331), one PfkbO binder (IFCAGPOI_01482), one PfkbG binder (IFCAGPOI_04736) and one PallA binder (IFCAGPOI_06489) were chosen. As it was intended to use an integrative vector for simultaneous overexpression of these regulators, it was obvious to firstly investigate whether tacrolimus production is distinctly affected following non-integrative and integrative overexpression of a certain regulator, respectively. Therefore, all six regulators were initially cloned individually into the mrsMR02 destination vector, which was meant to be used to assemble all regulators afterwards.
Due to the conflicting production yields obtained upon overexpression of the cluster-located protein AllA (IFCAGPOI_06421) in the two aforementioned cultivations, there was an interest in further studying the effect of this protein on tacrolimus production. Therefore, the protein IFCAGPOI_06421 was additionally included in this part of the study to evaluate the effect of its integrative and non-integrative overexpression.
In the course of his Master thesis, Alexander Hoffreiter prepared the vectors mrsAH01-mrsAH05, harboring the regulators IFCAGPOI_06489, IFCAGPOI_05107,

IFCAGPOI_03331, IFCAGPOI_01482 and IFCAGPOI_04736, respectively. The remaining two vectors, mrsHK01 and mrsHK02 with the genes encoding IFCAGPOI_06386 and IFCAGPOI_06421, were prepared by Panagiota-Channa Koutsandrea who continued to work on the project during her Master thesis. Due to the difficulty of introducing the latter two proteins via λ-Red/ET-mediated homologous recombination into the mrsMR02 destination vector, traditional cloning was used instead. Therefore, the vector was digested with *Pac*I and subsequently ligated with the respective entry plasmid insert fragment, thereby removing the multiple recombineering site (MRS). All seven destination vectors harboring the individual gene fragments and the empty vector mrsMR02 were conjugated to the wild type strain *Streptomyces tsukubaensis* NRRL18488. After verification of the resulting exconjugants by colony PCR, a comprehensive cultivation in 24-square deepwell plates was performed to compare the tacrolimus production yields obtained by integrative and non-integrative overexpression of the respective regulators and to elucidate the effect of inducing the integrative systems with anhydrotetracycline (aTc). Results of this cultivation are depicted in figure 14. Interestingly, the formation of extensive aggregates could be observed during these cultivations which is in accordance with the observations made by SINTEF during the small-scale cultivations (figure 28; appendix).

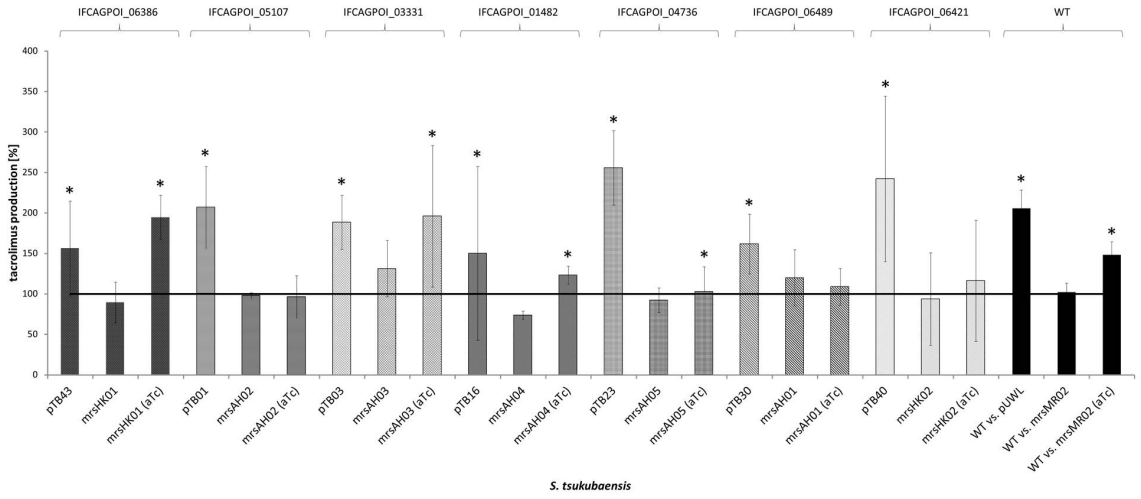

Figure 14: **Comparison of integrative versus non-integrative overexpression of seven regulators of tacrolimus biosynthesis.**
Three different types of overexpression were analyzed for each regulator: non-integrative overexpression (pTB constructs) and integrative overexpression (mrs constructs) in a non-induced and induced (aTc) state, respectively. All production yields are normalized to the production of the respective reference strains, *S. tsukubaensis*/pUWL-apra-oriT and *S. tsukubaensis*/mrsMR02 (without and with aTc), respectively. Production values represent the mean tacrolimus production yield achieved for three biological replicates, each cultivated in triplicate on 3 mL scale. A comparison of the wild type (*S. tsukubaensis* NRRL18488) production yields with the yields of the respective reference strains is additionally included. Statistically significant differences compared to the reference strains are marked with asterisks. Data generated in cooperation with Panagiota-Channa Koutsandrea.

Overall, the impact of overexpressing the respective regulators on tacrolimus production was moderate. Nonetheless, most of the analyzed strains depicted elevated production values compared to the respective reference strains, some of them being even significantly increased. As expected, based on the preceding studies, non-integrative overexpression of the selected regulators increased tacrolimus production compared to the reference strain *Streptomyces tsukubaensis*/pUWL-apra-oriT. For each regulator, the increase in tacrolimus production was significant, ranging from a 1.5-fold yield improvement caused by IFCAGPOI_01482 to a 2.6-fold raise following overexpression of IFCAGPOI_04736. A comparison of the fold-change production values achieved on different scales of cultivation reveals a considerable influence of the culture volume on the production behavior of a certain mutant strain (table 53). However, a general correlation between observed production yields and culture volume cannot be deduced.

Table 53: **Effect of an overexpression of selected regulators on tacrolimus production depending on cultivation scale.**
The impact of the cultivation volume on tacrolimus production of mutant strains non-integratively overexpressing regulatory proteins is shown. Values represent the fold-change in tacrolimus production compared to the reference strain *S. tsukubaensis*/pUWL-apra-oriT. Cultivations on 1 mL scale were kindly performed by SINTEF.

***S. tsukubaensis*/**	**Regulator**	**1 mL scale**	**3 mL scale**	**100 mL scale**
pTB43	IFCAGPOI_06386	n/a	1.56	0.86
pTB01	IFCAGPOI_05107	1.75	2.07	3.52
pTB03	IFCAGPOI_03331	2.25	1.88	0.62
pTB16	IFCAGPOI_01482	1.71	1.50	0.72
pTB23	IFCAGPOI_04736	1.80	2.56	1.51
pTB30	IFCAGPOI_06489	1.28	1.61	1.07
pTB40	IFCAGPOI_06421	0.04	2.42	1.02

Regarding the regulators IFCAGPOI_06386 and IFCAGPOI_03331, an induced integrative overexpression of the regulators resulted in higher tacrolimus production yields compared to non-integrative overexpression. Using the induced integrative system, FK506 production could be further raised by 38 % and 8 % compared to the constitutive overexpression. Except for IFCAGPOI_05107 and IFCAGPOI_06489, the induction of the integrative systems increased production compared to the non-induced integrative systems that only depicted leaky expressions. However, the difference between induced and non-induced integrative systems for the two mentioned regulators was only minor (1.6 % and 9.2 % difference, respectively). An induction of the *tcp830* promoters with anhydrotetracycline resulted in 1.1- to 2.2-fold elevated tacrolimus yields compared to non-induced systems. Tacrolimus production of mutant strains with non-induced integrative overexpression of regulators was generally comparable to the production of the respective reference strain not overexpressing any regulator. Taking non-integrative and integrative systems together, the best production values were achieved for the mutant strain *Streptomyces*

tsukubaensis/pTB03, overexpressing IFCAGPOI_03331, a two-component sensor histidine kinase.

3.2.3 Impact of cultivation scale on tacrolimus production

As already briefly mentioned in section 3.2.2, the culture volume has a noticeable effect on tacrolimus yields. In cooperation with SINTEF it was possible to test four different scales of cultivation in the course of this study. While cultivations on a 3 mL and a 100 mL scale were routinely carried out in-house, SINTEF has the equipment for small-scale and large-scale fermentations and kindly carried out cultivations on a 1 mL and a 1 L scale of selected mutant strains. In order to convey an idea of the absolute production yields achieved for selected mutant strains, table 54 depicts production values in mg/L of some of the non-integrative overexpression systems on different scales of cultivation.

Table 54: **Absolute tacrolimus production yields achieved by different mutant strains on various scales of cultivation.**
The impact of cultivation scale on tacrolimus production of chosen mutant strains non-integratively overexpressing regulatory proteins is shown. Values represent the maximum mean tacrolimus production [mg/L] achieved by three individual exconjugants, each cultivated in triplicate (exception: no technical replicates on 100 mL scale and two technical replicates on 1 L scale). Cultivations on 1 mL and 1 L scale were kindly performed by SINTEF.

Regulator	**1 mL scale**	**3 mL scale**	**100 mL scale**	**1 L**
IFCAGPOI_06386	n/a	34.29	76.77	n/a
IFCAGPOI_05107	12.17	56.88	201.29	n/a
IFCAGPOI_03331	15.99	55.50	39.69	87
IFCAGPOI_04383	14.18	n/a	102.96	32
IFCAGPOI_01482	13.19	40.95	50.08	104
IFCAGPOI_04736	14.35	71.49	108.75	55
IFCAGPOI_06489	9.95	44.57	60.67	121
IFCAGPOI_06421	0.37	61.11	65.30	0.4
S. tsukubaensis WT	n/a	60.43	78.65	97

Regarding table 54, it becomes obvious that, overall, tacrolimus production raises with increasing culture volume. Only the mutant strains overexpressing IFCAGPOI_04383 and IFCAGPOI_04736 show a different result with reduced production values on a 1 L scale compared to a 100 mL scale. Considering the wild type producer strain *Streptomyces tsukubaensis* NRRL18488 it becomes apparent that this strain is naturally producing considerable amounts of tacrolimus. Within the scope of the DACA studies, *Streptomyces tsukubaensis* NRRL18488 was additionally cultivated in a 10 L fermenter implying optimized aeration conditions. After ten days of cultivation, tacrolimus yields were determined as 175.2 mg/L, thus even exceeding the

high value obtained on a 1 L scale. Regarding the three individual exconjugants of *Streptomyces tsukubaensis*/pTB40, overexpressing IFCAGPOI_06421, it is assumed that the mutant strains did somehow lose their capability to produce tacrolimus during their travel to Norway as the production yields obtained by SINTEF are not at all in accordance with those obtained in-house.

3.3 Simultaneous overexpression of several regulatory proteins

In order to investigate the combined effect of several positive regulators on tacrolimus production, the idea was to assemble the encoding regulator genes on a single overexpression construct. The artificial gene operon assembly system AGOS (Basitta *et al.*, 2017), a tool originally developed to assemble gene operons into a destination vector, seemed to be a suitable method to meet the requirements of a combined overexpression. Using this tool allowed to equip each regulator gene with its own *tcp830* promoter, a ribosomal binding site (RBS) and a terminator.
The existing AGOS kit has seven entry plasmids to target seven different integration sites in the multiple recombineering site of the mrsMR02 destination vector. Six of the regulators which had been investigated in detail, regarding different expression systems (see 3.2.2), were chosen to be combined on mrsMR02 to study their common effect on production. IFCAGPOI_06421 was excluded from this study due to its binding to all of the tested promoter fragments which could possibly result in a steric hindrance at the promoter regions.
The results of the comparative study of integrative versus non-integrative overexpression described above were promising in that a combination of several regulators on an integrative vector, combined with the possibility to induce their transcription, might lead to tacrolimus producer strains exhibiting higher yields compared to the wild type producer. The stepwise assembly of the individual gene fragments into the mrsMR02 destination vector was performed by Panagiota-Channa Koutsandrea during her Master thesis. For a successful assembly it was necessary to retransform the DNA isolated out of clones resulting from a targeting reaction as the λ-Red/ET-mediated homologous recombination always resulted in a mixture of the desired cosmid and the preceding, non-modified vector.
Due to the good production yields obtained by *Streptomyces tsukubaensis* NRRL18488 integratively overexpressing IFCAGPOI_03331 (mrsAH03; Ptcs6a binder), this vector was chosen as starting vector for the second assembly reaction. The IFCAGPOI_06489 gene fragment was used for the second targeting reaction as all related production values in the previous study were beyond the reference value. The vector containing two regulators was designated as mrsHK03. Afterwards, the second Ptcs6a binder, IFCAGPOI_05107, was introduced into the vector, generating mrsHK04. The following targeting reactions included the gene fragments of IFCAGPOI_04736 (PfkbG binder) and IFCAGPOI_01482 (PfkbO binder). Finally, the pathway-specific regulator FkbN (IFCAGPOI_06386) was introduced successfully using homologous recombination and the final construct (mrsHK07) was achieved. mrsHK07 as well as all intermediate cosmids generated during the stepwise assembly were individually conjugated to *Streptomyces tsukubaensis* NRRL18488 to analyze the effect of combined overexpression on

tacrolimus production.

While it was possible to get three individual exconjugants harboring mrsHK03, the vector containing two regulators, only one exconjugant harboring mrsHK04 was gained. Although conjugation was repeated several times under various conditions, no exconjugants were obtained following conjugation of mrsHK04, mrsHK05, mrsHK06 and mrsHK07. Therefore, only four strains with combined overexpression could be analyzed in tacrolimus production studies. The generated mutant strains were each cultivated in triplicate in 24-square deepwell plates for five and seven days, respectively. Tacrolimus yields obtained during these cultivations are depicted in figure 15.

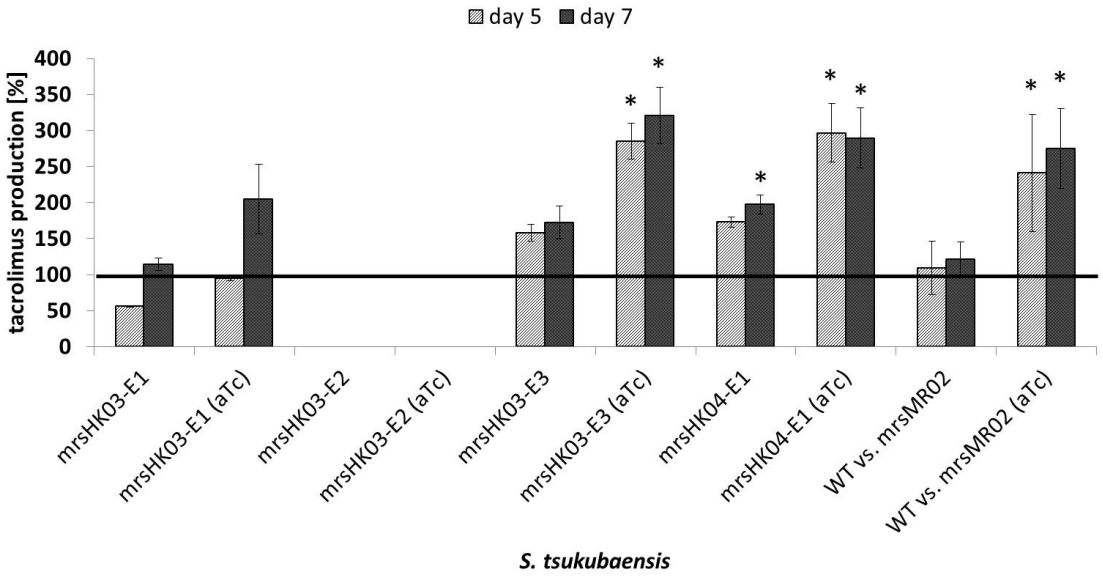

Figure 15: **Simultaneous overexpression of two and three positive regulators of tacrolimus biosynthesis.**

Three individual exconjugants of *S. tsukubaensis*/mrsHK03, overexpressing regulators IFCAGPOI_03331 and IFCAGPOI_06489, were analyzed as well as one exconjugant of *S. tsukubaensis*/mrsHK04, additionally overexpressing IFCAGPOI_05107. Each mutant was analyzed in a non-induced and induced (aTc) state, respectively. All production yields are normalized to the production of the respective reference strain, *S. tsukubaensis*/mrsMR02 (without and with aTc), respectively. Production values represent the mean tacrolimus production yield achieved for three technical replicates, cultivated on 3 mL scale for 3 and 5 days, respectively. A comparison of the wild type (*S. tsukubaensis* NRRL18488) production yields to the yields of the respective reference strains is additionally included. Statistically significant differences compared to the reference strains are marked with asterisks. Data generated by Panagiota-Channa Koutsandrea.

Generally, production yields obtained after seven days of cultivation were slightly higher compared to those determined after five days. Interestingly, the three individual exconjugants of *Streptomyces tsukubaensis*/mrsHK03 differed a lot in their production behavior. Whilst exconjugant 2 did not produce tacrolimus at all, albeit depicting a comparable growth behavior, exconjugant 1 displayed a 2-fold increased production compared to the reference strain in the induced state after seven days of cultivation. Exconjugant 3, however, depicted a significantly increased tacrolimus production upon induction, both after five and seven days. FK506 yields were increased 3.2-fold after seven days which represents the maximum value observed in this study. The production behavior of *Streptomyces tsukubaensis*/mrsHK04 was fairly similar to the third exconjugant of *Streptomyces tsukubaensis*/mrsHK03, also depicting significantly increased yields in the induced state at both time points and even the non-induced mutant depicted a significant increase after seven days. In accordance with the previous studies, a comparison of the wild type producer *Streptomyces tsukubaensis* NRRL18488 to the reference strains illustrates the significantly decreased production of *Streptomyces tsukubaensis*/mrsMR02.

In order to investigate the combined effect of all regulators and considering the common difficulty of conjugating large vectors to *Streptomyces tsukubaensis* NRRL18488, it was anticipated introducing mrsHK07 into a heterologous tacrolimus producer strain. For this purpose, *Streptomyces coelicolor* M512 and M1146 harboring pAC20N were chosen. Generated by Jones *et al.* (2013), these mutant strains have been shown to produce tiny amounts of tacrolimus in previous studies (0.16 mg/L and 0.75 mg/L, respectively). As the *attB* attachment site of these host strains is already occupied by pAC20N and due to the fact that mrsHK07 also targets this locus because of its *attP* site, it was necessary to select for both inserts, pAC20N and mrsHK07, upon the second homologous recombination. In order to do so, the progenitor of mrsHK07, mrsHK07-apra, which still contains the apramycin resistance cassette, had to be used to enable a simultaneous selection for pAC20N (thiostrepton) and mrsHK07-apra (apramycin). Conjugation to the *Streptomyces coelicolor* strains was straightforward, verified by colony PCR and afterwards six individual exconjugants were analyzed for both strains, respectively.

Unfortunately, the introduction of mrsHK07-apra into the heterologous producer strains and the induction of the expression with anhydrotetracycline did not increase their tacrolimus production. Regarding the generated *Streptomyces coelicolor* M512 strains, tacrolimus production was not at all detectable, only in one of the two original exconjugants of *Streptomyces coelicolor* M512/pAC20N (0.004 mg/L). Tacrolimus production was detectable in minor amounts in extracts resulting from *Streptomyces coelicolor* M1146/pAC20N exconjugant number 3 (0.125 mg/L). Two out of the six generated exconjugants of *Streptomyces coelicolor* M1146/pAC20N/mrsHK07-apra also produced tiny quantities of FK506, however being lower than the reference strain (0.029 mg/L and 0.023 mg/L).

3.4 PKS engineering

The intention to biosynthetically generate a tacrologue depicting an allyl side chain in position 9 of the molecule brought up the idea of PKS engineering. As module 4 of the tacrolimus PKS system naturally introduces allylmalonyl-CoA as extender unit, it seemed plausible to replace the natural module 10 by module 4 in order to introduce allylmalonyl-CoA instead of malonyl-CoA in the final step of the PKS assembly line.
As depicted in table 55, module 4 and module 10 differ in the composition of their domains. Compared to module 10, module 4 has two additional domains, a dehydratase (DH) and a ß-ketoacyl reductase (KR). As a consequence, module 10 misses 1679 bp compared to module 4. Swapping module 10 with module 4 thus means a magnification of the PKS system. There is no similarity between these two modules on the DNA level, however, the amino acid sequences show a similarity of 50 %.

Table 55: **Comparison of module 4 and module 10 of the FK506 cluster.**
Module 10 misses two domains compared to module 4, however, these domains have been predicted to be not active and nonfunctional, respectively (Mo *et al.*, 2011).

Domain	**Module 4**	**Module 10**	**Similarity DNA sequence**	**Similarity amino acid sequence**
KS	1257 bp	1284 bp	no similarity	68 %
AT	831 bp	867 bp	no similarity	33 %
DH	483 bp	-	-	-
KR	? bp	-	-	-
ACP	210 bp	216 bp	no similarity	40 %
whole module	4598 bp	2919 bp	no similarity	50 %

The alternative approach of swapping only the AT domain meant to exchange the domain showing the lowest similarity between module 4 and module 10. As depicted in figure 16, the first catalytic center is quite conserved for both domains (GHSxGE), however, the second catalytic center of the two domains differs: the AT domain of module 4 shows the motif CPTH which results in the specific incorporation of allylmalonyl-CoA, while the AT domain of module 10 harbors the malonyl-CoA specific HAFH motif, respectively (Jiang *et al.*, 2015; Del Vecchio *et al.*, 2003).

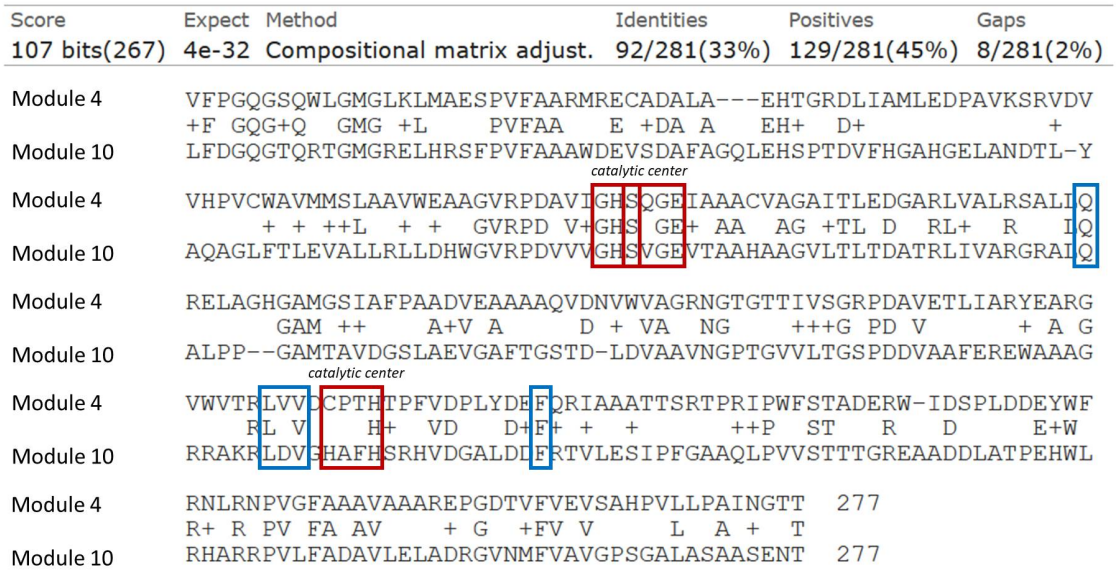

Figure 16: **Amino acid sequence alignment of the AT domains of module 4 and module 10.** Residues of the catalytic centers are marked in red. Residues responsible for the incorporation of allylmalonyl-CoA and malonyl-CoA, respectively, are highlighted in blue.

A further extender unit which can be naturally introduced by PKS systems is ethylmalonyl-CoA. As an ethyl group in position 9 would likewise represent a magnification of the side chain compared to the tacrolimus molecule, a further PKS engineering approach was included, intending to generate 9-ethyl tacrolimus. Using the known *trans*AT KirCII in combination with the KirACP5 (Musiol *et al.*, 2011) seemed to be a promising approach to generate this derivative. A comparison of the native ACP domain of module 10 and the KirACP5 revealed no similarity on the DNA level, however, the amino acid sequences show 33 % similarity (table 56).

Table 56: **Comparison of the ACP domains of module 10 of the tacrolimus BGC and module 5 of the kirromycin BGC (KirACP5).**

	ACP(M10)	**KirACP5**	**Similarity**
nucleotide sequence	216 bp	342 bp	no similarity
amino acid sequence	72 residues	114 residues	33 %

The *trans*AT KirCII originating from the kirromycin biosynthetic gene cluster was likewise compared with the natural AT domain of module 10 which has not been deleted for this approach. Thereby, it became obvious that the *trans*AT KirCII domain is larger than the cluster-located *cis*AT domain (1338 bp vs. 867 bp). Moreover, the *trans*AT KirCII reveals the VASH motif which is responsible for its ethylmalonyl-CoA selectivity.

3.4.1 Module swap

3.4.1.1 Module swap in heterologous host strains

Screening for modified pAC20N clones with module 4 at the position of module 10 (pTB67) was complicated by the difficulty of designing specific screening primers. Three clones (1, 21 & 22) that seemed to be promising regarding their observed DNA restriction pattern were thus haphazardly used for conjugation to the heterologous host strains *Streptomyces coelicolor* and *Streptomyces albus* J1074. Additionally, one of these modified pAC20N (pTB67-22) was given to QBiC (University of Tübingen) for Nanopore sequencing. With the aid of Shrikant Mantri and Prof. Dr. Nadine Ziemert (University of Tübingen) the Nanopore data was analyzed. It became obvious that the sequenced pTB67-22 lacks a sequence of around 80 kb corresponding to almost the whole FK506 biosynthetic gene cluster.
In order to confirm this predicted deletion, PCR reactions with various primer pairs were performed. Using the primers that were required to amplify the cluster-located promoter regions for the DACA studies and pTB67-22 as template DNA resulted in the amplification of Ptcs6a, PfkbG and PallA. Sequencing of these amplificates confirmed the correctness of the amplified fragments Ptcs6a and PallA. The promoter fragment Ptcs6a is located in the predicted deletion, thus an amplification should not have been possible assuming that the Nanopore sequencing is correct. This suggests that at least parts of the cluster should still be present on pTB67-22 or else there is a mixture of the size-reduced BAC and the desired pTB67.
However, using primers specifically designed to test for the predicted deletion (primer pairs 20 & 21, table 8) led to an opposite result: the border regions of the predicted deletion could not be amplified. In contrast, this was possible when using the original pAC20N as template DNA. Additionally, an amplification was successful using primers binding upstream and downstream of the deletion site (figure 29; appendix). These PCR reactions indeed confirmed the deletion on pTB67-22. Though, the expected band for a deletion was not visible using genomic DNA of some of the generated heterologous *Streptomyces* mutant strains as PCR template.
To further confirm the predicted deletion on pTB67-22, a *Pci*I restriction digest was performed. As this enzyme cuts once in module 10, the restriction pattern of the correct pTB67-22 was to miss one DNA fragment compared to the restriction pattern of pAC20N. Indeed, the restriction patterns of pAC20N and pTB67-22 differed and the sizes of the observed fragments corresponded to the expectations, although the three upper fragments of pTB67-22 could not be separated properly (figure 30; appendix).
The restriction pattern thus indicates that the generated pTB67-22 carries an intact tacrolimus biosynthetic gene cluster. Further evidence thereof was given by LC-MS analysis of culture extracts resulting from the generated mutant strains which allowed to identify masses corresponding to tacrolimus (*m/z* 826.5 $[M+Na]^+$; figure 17). The detection of tacrolimus would nevertheless indicate that either the module swap was not successful or that the promiscuous AT domain of module 4 introduces the original extender unit in position 9 of the molecule.

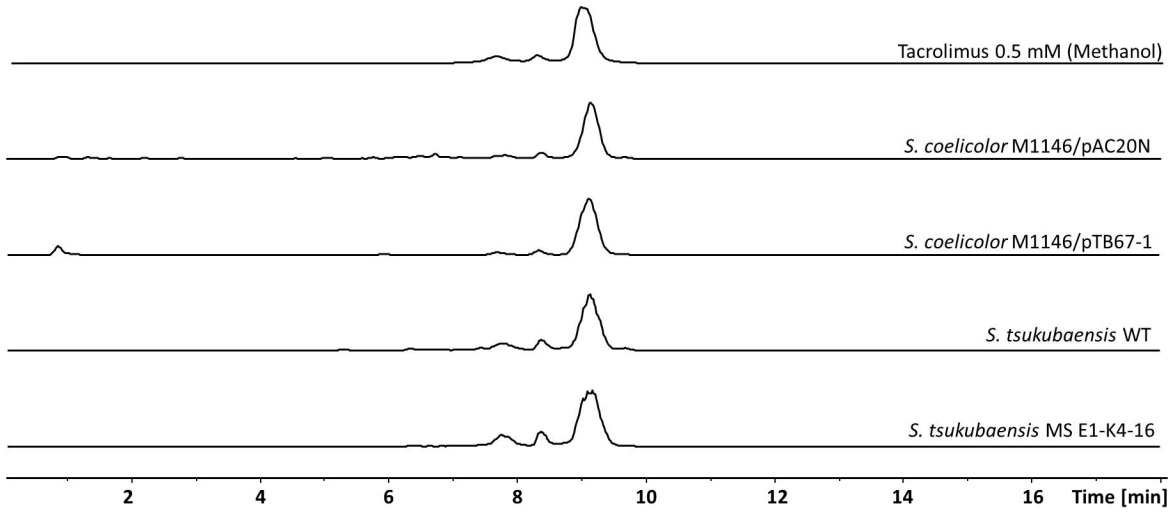

Figure 17: **Representative extracted ion chromatograms of extracts resulting from module swap mutant strains and controls.**
Extracted ion chromatograms of *m/z* 826.5 $[M+Na]^+$ (tacrolimus). The expected mass for the sodium adduct of tacrolimus can be detected both in tacrolimus producer strains (*S. coelicolor* M1146/pAC20N and *S. tsukubaensis* WT) and in strains expected to produce the 9-allyl derivative of tacrolimus (e.g. *S. coelicolor* M1146/pTB67-1 and *S. tsukubaensis* MS E1-K4-16).

None of the total ion chromatograms obtained following LC-MS analysis of the generated *Streptomyces coelicolor* and *Streptomyces albus* module swap mutant strains revealed new peaks. Likewise, the extraction of masses corresponding to hydrogen, sodium or potassium adducts of the expected 9-allyl derivative did not indicate that the module swap in the heterologous host strains was successful.
HPLC analysis of the extracts obtained from the heterologous module swap mutant strains was less expressive than LC-MS analysis as the observed peaks were extremely tiny. Nonetheless, it was possible to make out differences between heterologous host strains harboring the original pAC20N and those harboring the modified pAC20N (pTB67). The strains *Streptomyces coelicolor* M512 and M1146 harboring pTB67-1 both showed a remarkably increased peak eluting approximatively 3.5 minutes later than the tacrolimus standard compared to the strains with the original pAC20N. The strains *Streptomyces coelicolor* M1146, M1152 and M1154 harboring pTB67-21 and pTB67-22, respectively, did not show this remarkable increase. Regarding *Streptomyces albus* J1074 as heterologous host strain of pTB67-21 and pTB67-22, the mentioned peak was detectable in all three exconjugants of *Streptomyces albus* J1074/pTB67-21. However, considering that these peaks were extremely tiny, a purification of the corresponding compound for further analysis was not possible.

3.4.1.2 Module swap in the natural producer *Streptomyces tsukubaensis* NRRL18488

Analogously to the heterologous module swap approach, the proof of the successful module swap in the genome of *Streptomyces tsukubaensis* NRRL18488 was quite challenging due to the difficulty of designing specific verification primers. Six potential module swap mutant strains that could be partly verified by a PCR reaction amplifying the downstream border region of the new module 10 were cultivated and culture extracts were analyzed regarding the production of the expected 9-allyl derivative. After HPLC and LC-MS analysis, it became obvious that the module swap in the natural producer strain did likewise not result in the production of the desired 9-allyl derivative. However, also in this case the production of tacrolimus was still detectable (figure 17).

3.4.2 AT domain swap

The undesired deletion on pAC20N following the homologous recombination event to introduce module 4 at the position of module 10 revealed that this method is not suitable to double a certain module or domain on this BAC vector. Therefore, the AT domain swap was not to be performed on pAC20N for heterologous production of the derivative. Instead, the swap was accomplished in the genome of the wild type producer *Streptomyces tsukubaensis* NRRL18488. Following CRISPR-Cas9 editing, the successful AT domain swap could be verified by PCR and sequencing in seven independent mutant strains.

After cultivation of the AT domain swap mutant strains and analysis of the culture supernatants using HPLC, it became obvious that there were still peaks corresponding to tacrolimus as compared to the wild type strain and the tacrolimus standard. A further verification of the generated mutant strains by PCR using primers specific for the AT domain of module 10 resulted in an amplification of the AT domain of module 10, indicating that the CRISPR-Cas9 editing had not lead to a clean genotype. After further rounds of streaking spore dilutions of the generated mutant strains, the complete absence of the AT domain of module 10 could be confirmed by PCR for one of the mutant strains *Streptomyces tsukubaensis* AT E3-K1-7. However, upon cultivation of this mutant, the peak corresponding to tacrolimus could still be detected, although much smaller than before.

LC-MS analysis of culture extracts originating from the AT domain swap mutant strains also confirmed that tacrolimus was still produced. The extracted ion chromatograms for the mass of the sodium adduct of tacrolimus (m/z 826.5 $[M+Na]^+$) looked comparable to that of the wild type producer for all extracts originating from the generated mutant strains (figure 18). An extraction for the mass of the sodium adduct of the desired 9-allyl derivative (m/z 852.5 $[M+Na]^+$) did not result in a clear peak. Likewise, the extraction for masses corresponding to hydrogen or potassium adducts of the expected 9-allyl derivative did not confirm the production of a new derivative.

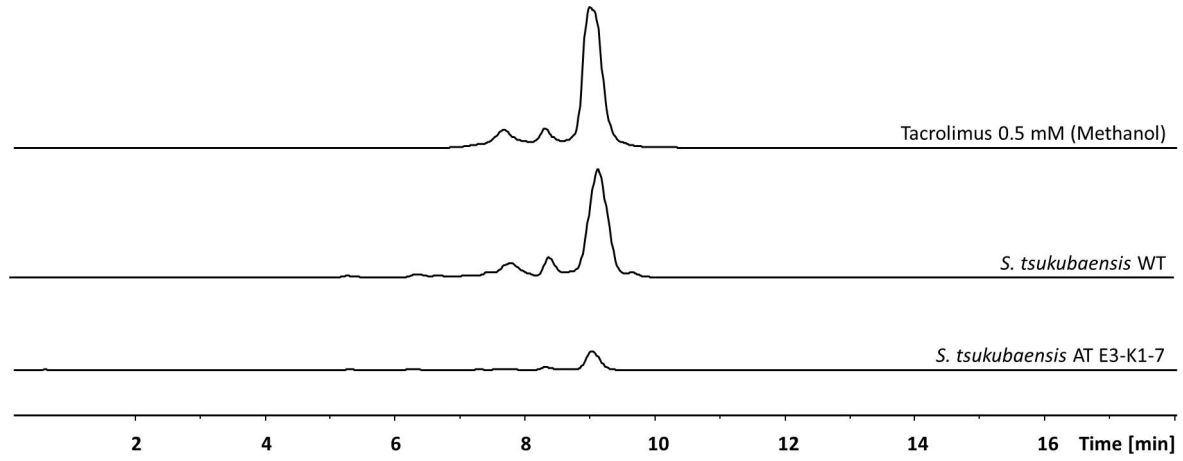

Figure 18: **Extracted ion chromatogram of an extract resulting from an AT domain swap mutant strain compared to the controls.**
Extracted ion chromatograms of *m/z* 826.5 $[M+Na]^+$ (tacrolimus). The depicted mutant strain *S. tsukubaensis* AT E3-K1-7 was achieved after several rounds of streaking dilutions of spores in order to select spores with a clean genotype. Compared to the wild type producer *S. tsukubaensis* NRRL18488, tacrolimus production is extremely reduced.

In addition to HPLC and LC-MS analysis, the extract originating from *Streptomyces tsukubaensis* AT E3-K1-7 was subjected to an HR-MS analysis. Thereby, masses of *m/z* 830.5048, *m/z* 830.5414 and *m/z* 830.5658 could be detected with low intensities. These are indeed quite similar to the expected mass of the 9-allyl derivative (*m/z* 830.5418 $[M+H]^+$). However, after calculating the respective mass deviations (-44.55 ppm, -0.48 ppm, +28.89 ppm), it became obvious that the masses cannot be ascribed to the expected derivative.

3.4.3 ACP domain swap

3.4.3.1 ACP domain swap in heterologous host strains

As the KirACP5 domain is not present in the natural tacrolimus biosynthetic gene cluster, it was reasonable to reuse the method of homologous recombination and to perform the ACP domain swap on pAC20N for heterologous production of the 9-ethyl derivative. The successful insertion of the KirACP5 at the position of the ACP domain of module 10 could be easily verified by PCR and thus Nanopore sequencing of the modified pAC20N (pTB74) was not performed in this case. HPLC analysis of culture extracts resulting from cultivations of the ACP domain swap mutant strains revealed that tacrolimus was no longer produced. However, no new peak could be detected instead. The extracts were further submitted to LC-MS analysis which confirmed that tacrolimus production was abolished in the ACP domain swap mutant strains (figure 19). Nevertheless, also LC-MS analysis could not reveal the production of a new derivative. Extracting for the expected mass of 9-ethyl tacrolimus (*m/z* 818.5 $[M+H]^+$, *m/z* 840.5 $[M+Na]^+$ and *m/z* 856.5 $[M+K]^+$) did not result in a signal.

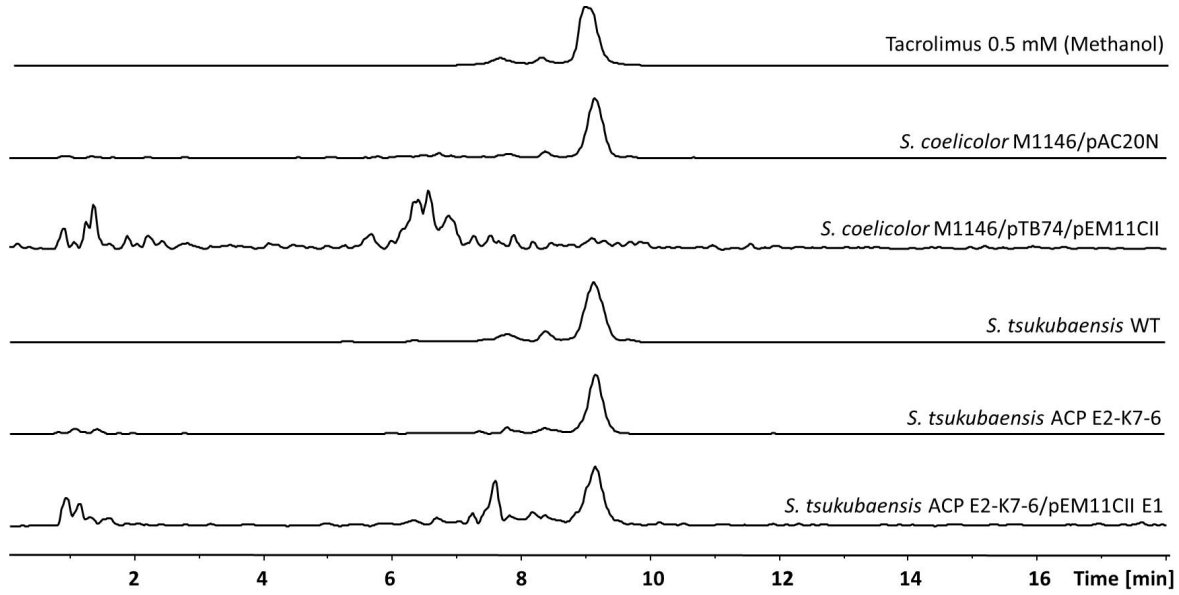

Figure 19: **Representative extracted ion chromatograms of extracts resulting from selected ACP domain swap mutant strains and controls.**
Extracted ion chromatograms of *m/z* 826.5 $[M+Na]^+$ (tacrolimus). Tacrolimus production can no longer be detected in extracts of heterologous ACP domain swap mutant strains (e.g. *S. coelicolor* M1146/pTB74/pEM11CII). The peak appearing in extracts of *S. tsukubaensis* ACP E2-K7-6/pEM11CII can not be assigned to a mass of *m/z* 826.5, but to a new mass of *m/z* 798.3 (see 3.4.3.2).

3.4.3.2 ACP domain swap in the natural producer *Streptomyces tsukubaensis* NRRL18488

It is well known that the engineering of polyketide synthases often extremely reduces yields of new products. Considering the fact that heterologous production of the natural compound tacrolimus is low anyway (Jones *et al.*, 2013), the detection of a putative new derivative following PKS engineering might be hampered. Therefore, an ACP domain swap in the native producer strain *Streptomyces tsukubaensis* NRRL18488 was additionally taken into account as the wild type is a quite good producer and a reduced production could still be detectable. The established method of CRISPR-Cas9 editing was used for this purpose. Four individual ACP domain swap mutant strains were generated, verified by PCR and sequencing and cultivated.
In accordance with the heterologous ACP domain swap mutant strains, HPLC analysis revealed that tacrolimus production was abolished in the generated mutant strains. The extracted ion chromatogram of *m/z* 826.5 $[M+Na]^+$ (tacrolimus) only showed a peak for mutant strain *Streptomyces tsukubaensis* ACP E2-K7-6/pEM11CII (figure 19), however, the corresponding mass *m/z* 826.5 could not be detected. In contrast, a mass of *m/z* 798.3 was detectable. Interestingly, the mentioned ACP domain swap mutant strain displayed a new peak in the HPLC chromatogram, eluting approximately five minutes prior to the standard (detection wavelength 210 nm) (figure 31; appendix). This dominant new peak also appeared in the total

ion chromatogram of the performed LC-MS analysis and could likewise be assigned to a mass of *m/z* 798.3 $[M+Na]^+$ (figure 20). A corresponding mass of *m/z* 774.3 $[M-H]^-$ could be detected in the negative mode which confirmed the new mass to be *m/z* 775.3. Noticeably, the new compound was also produced by *Streptomyces tsukubaensis* ACP E2-K7-6 not harboring pEM11CII, the plasmid encoding the *trans*AT KirCII. Yields of the new compound were found to vary between 100 mg/L and 120 mg/L, dependent on the period of cultivation.

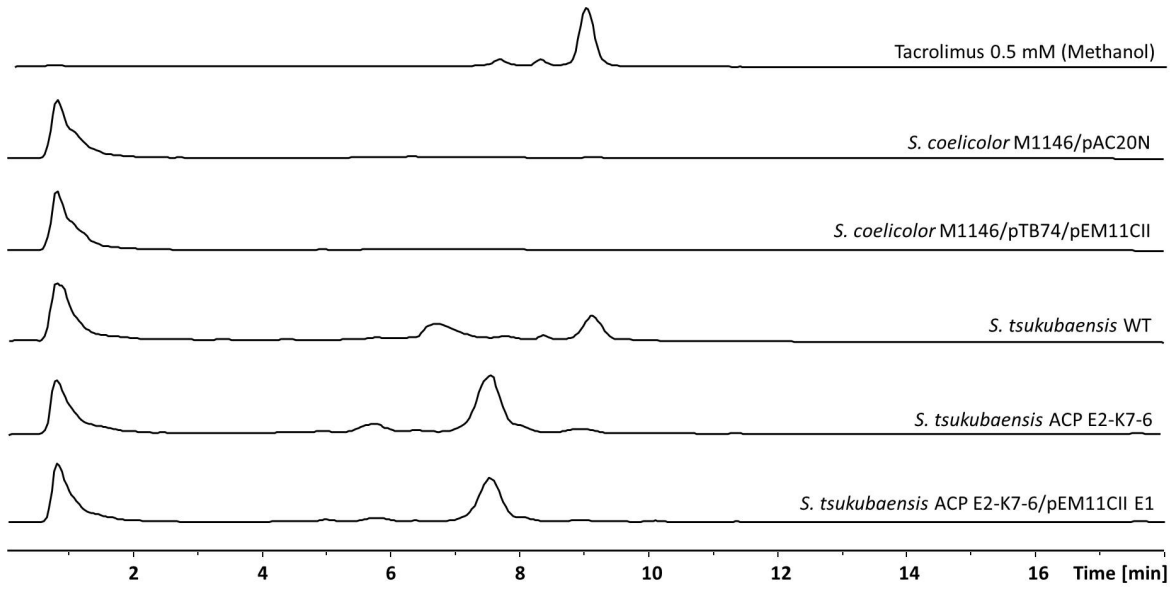

Figure 20: **Total ion chromatograms of extracts resulting from selected ACP domain swap mutant strains and controls.**
Tacrolimus production can no longer be detected in any ACP domain swap mutant strain, neither in heterologous mutants (e.g. *S. coelicolor* M1146/pTB74/pEM11CII) nor in *S. tsukubaensis* ACP domain swap mutants. Mutant strain *Streptomyces tsukubaensis* ACP E2-K7-6/pEM11CII exhibits a new peak eluting after approximately 7.5 minutes and thus 1.6 minutes prior to tacrolimus (retention time 9.1 minutes). The new peak reveals a mass of *m/z* 798.3 $[M+Na]^+$.

As the exact mass of the expected 9-ethyl derivative is *m/z* 817.5340, it could be excluded that the new compound of mutant strain *Streptomyces tsukubaensis* ACP E2-K7-6/pEM11CII revealed the expected structure. In order to get an indication of the structure of the produced compound, HR-MS/MS analysis was performed.
The mass of the new compound was identified to be *m/z* 774.4796 $[M-H]^-$ (figure 32; appendix) which could be related to a structure with a molecular formula of $C_{43}H_{69}NO_{11}$ (Δppm=0.52). A possible corresponding compound, 9-deoxo-31-*O*-demethyl-FK506 (*m/z* 775.4871), has been described as an intermediate in tacrolimus biosynthesis (Motamedi *et al.*, 1996). Likewise, the known compound 9-deoxo-prolyl-FK506 (Shinde *et al.*, 2015) reveals an appropriate mass. To elucidate the actual structure of the unknown compound, NMR spectroscopy was performed.
Following a 2 L cultivation of *Streptomyces tsukubaensis* ACP E2-K7-6/pEM11CII, 130 g of

crude extract was obtained. 30 g thereof was subjected to preparative reversed-phase vacuum liquid chromatography (VLC), followed by semi-preparative HPLC to finally yield 8.3 mg of pure compound. This amount of compound was sufficient to measure a full set of 1D- and 2D-NMR spectra which was accomplished by Irina Helmle.

Prof. Dr. Harald Groß carried out the *de novo* structure elucidation employing the above mentioned NMR data set. Both the ^{1}H and ^{13}C NMR spectra showed the characteristic signals of the tacrolimus molecule when compared with the spectra of an additionally measured tacrolimus standard (figure 21). However, careful comparison of the ^{13}C NMR spectra indicated that the unknown compound misses the C-9-carbonyl (δ_C 196.1/C-9) which is typical of tacrolimus (Mierke *et al.*, 1991). The corresponding chemical shift of the new compound was determined as δ_C 37.2/C-9 (δ_H 2.50+2.68/H-9). Furthermore, the chemical shift δ_C 74.3/C-31 (δ_H 3.46/H-31) observed for the unknown compound differs from the respective chemical shift δ_C 84.2/C-31 (δ_H 2.97/H-31) of tacrolimus. Moreover, the signal at δ_C 56.6/C-45 (δ_H 3.35/H-45) which is observable in the spectrum of the tacrolimus standard cannot be detected in the spectrum of the isolated compound.

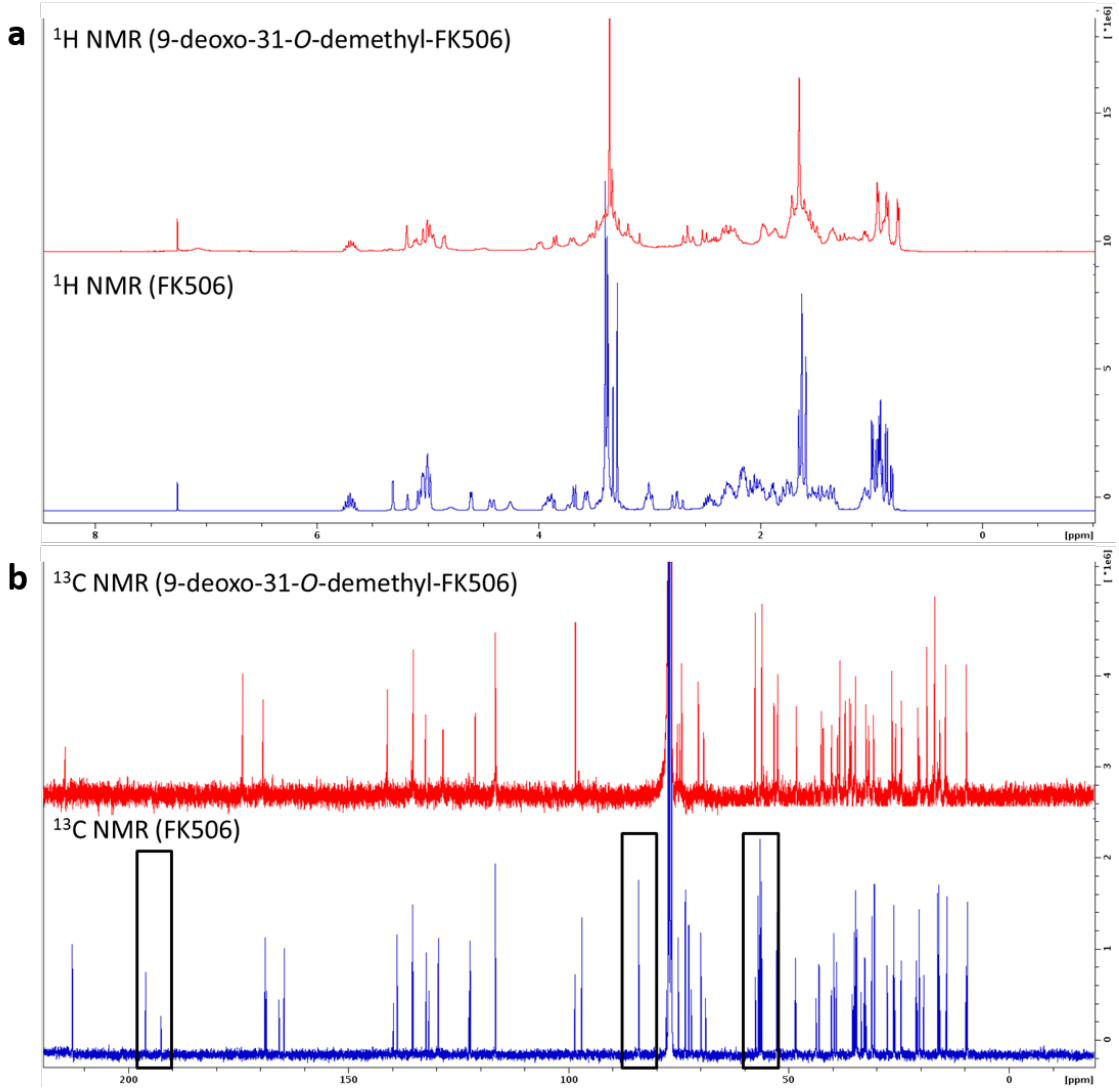

Figure 21: **^{1}H NMR and ^{13}C NMR spectra of the new compound (9-deoxo-31-*O*-demethyl-FK506) and FK506.**
a ^{1}H NMR spectra and **b** ^{13}C NMR spectra of the new compound identified as 9-deoxo-31-*O*-demethyl-FK506 (red) and an additionally measured FK506 standard (blue). Signals appearing only in the FK506 standard are highlighted by the black frames: δ_C 196.1/C-9, δ_C 84.2/C-31 and δ_C 56.6/C-45.

The chemical shifts determined for the purified compound are comparable to the NMR data published by Ban *et al.* (2013) for 9-deoxo-31-*O*-demethyl-FK506 (figure 22), a natural intermediate in tacrolimus biosynthesis. Reference values according to Ban *et al.* (2013) are depicted in table 57 (δ_C 37.5/C-9 (δ_H 2.49+2.67/H-9) and δ_C 75.6/C-31 (δ_H 3.31/H-31)). The values for C-31 and C-32 were assigned differently in the *de novo* structure elucidation of this study which results in elevated deviations $\Delta(\delta_C)$.

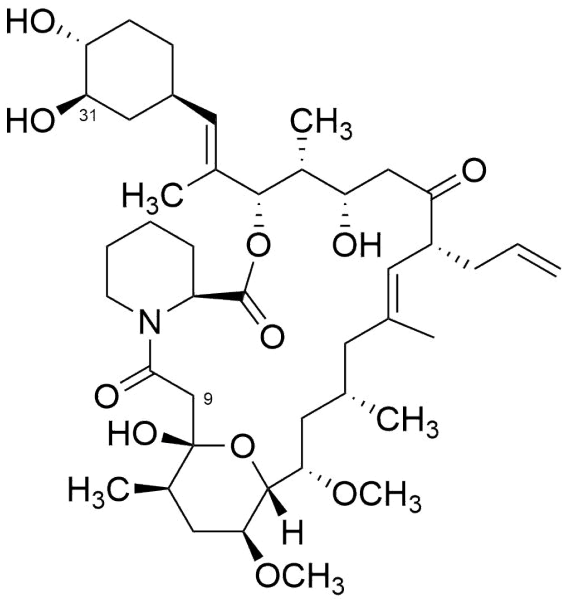

Figure 22: **Chemical structure of the compound isolated from *Streptomyces tsukubaensis* ACP E2-K7-6/pEM11CII.**
Chemical structure of 9-deoxo-31-*O*-demethyl-FK506 ($C_{43}H_{69}NO_{11}$) proven by NMR spectroscopy.

A subsequently performed HR-MS analysis of the purified compound allowed to deduce the chemical formulas $C_{44}H_{70}NO_{13}$ (*m/z* 820.4856 [M+HCOO]$^-$) and $C_{43}H_{68}NO_{11}$ (*m/z* 774.4799 [M-H]$^-$), respectively, and consequently corroborated the NMR findings (figure 23).

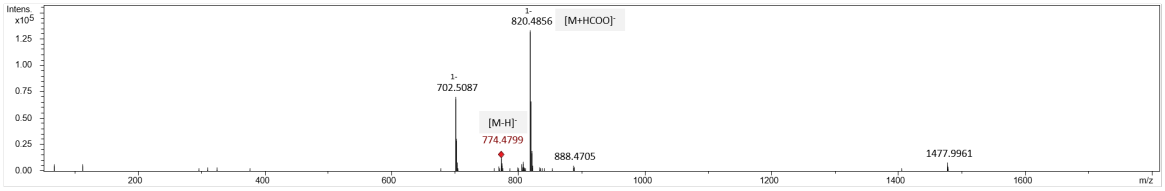

Figure 23: **HR-MS analysis of the purified compound isolated from *Streptomyces tsukubaensis* ACP E2-K7-6/pEM11CII.**
The observed masses of *m/z* 820.4856 [M+HCOO]$^-$ and *m/z* 774.4799 [M-H]$^-$ can be assigned to the chemical formulas $C_{44}H_{70}NO_{13}$ and $C_{43}H_{68}NO_{11}$, respectively (Δppm=1.1 and 0.9).

Table 57: **^{1}H and ^{13}C NMR data of 9-deoxo-31-*O*-demethyl-FK506 in $CDCl_3$.**

Values represent chemical shifts δ in ppm which were referred to the solvent $CDCl_3$ as internal standard (δ_H/δ_C 7.26/77.0).

Chemical shifts of 9-deoxo-31-*O*-demethyl-FK506 were determined by Ban *et al.* (2013) using tetramethylsilane as an internal reference.

Position	Isolated compound		9-deoxo-31-*O*-demethyl-FK506		
	δ_H	δ_C	δ_H	δ_C	$\Delta(\delta_C)$
1		169.4		169.6	0.2
2	4.86	52.6	4.85	52.8	0.2
3	1.71	26.6	1.70	26.8	0.2
	2.24		2.23		
4	1.22	20.7	1.21	20.9	0.2
	1.72		1.70		
5	1.52	24.4	1.51	24.6	0.2
	1.69		1.68		
6	3.19	42.6	3.20	42.8	0.2
	3.70		3.69		
7					
8		174.0		174.3	0.3
9	2.50	37.2	2.49	37.5	0.3
	2.68		2.67		
10		98.5		98.7	0.2
11	1.67	38.4	1.54	38.6	0.2
12	1.56	32.5	1.52	32.8	0.3
	1.97		1.96		
13	3.42	74.3	3.42	74.5	0.2
14	3.85	70.6	3.85	70.8	0.2
15	3.53	76.8	3.52	77.1	0.3
16	1.35	36.2	1.33	36.5	0.3
	1.49		1.48		
17	1.65	25.8	1.68	26.0	0.2
18	1.67	48.3	1.63	48.5	0.2
	2.32		2.30		
19		141.2		141.3	0.1
20	5.11	121.3	5.10	121.5	0.2
21	3.32	53.4	3.31	53.6	0.2
22		214.4		214.5	0.1
23	2.24	42.2	2.23	42.5	0.3
	2.63		2.63		
24	3.99	69.4	3.99	69.6	0.2
25	1.86	40.3	1.85	40.5	0.2
26	5.18	76.6	5.18	76.8	0.2
27		132.6		132.6	0.0
28	4.98	128.6	4.96	128.9	0.3
29	2.33	34.9	2.32	35.1	0.2
30	1.15	38.9	1.11	39.1	0.2
	1.89		1.87		
31	3.46	74.3	3.31	75.6	**1.3**
32	3.37	75.4	3.41	75.0	0.4
33	1.35	31.9	1.32	32.2	0.3
	1.97		1.96		
34	1.06	30.8	1.04	31.2	0.4
	1.62		1.60		
35	2.27	35.9	2.21	36.1	0.2
	2.41		2.40		
36	5.70	135.4	5.71	135.6	0.2
37	5.00	116.7	5.00	116.8	0.1
38	0.94	16.9	0.94	17.1	0.2
39	0.76	18.7	0.76	18.9	0.2
40	1.65	15.7	1.65	16.0	0.3
41	0.85	9.8	0.86	10.0	0.2
42	1.65	14.4	1.66	14.6	0.2
43	3.36	56.2	3.36	56.3	0.1
44	3.36	57.7	3.36	57.9	0.2

4 Discussion

4.1 DACA

4.1.1 Fermentation

The growth and tacrolimus production behavior of *Streptomyces tsukubaensis* NRRL18488 observed during the 10 L fermentation within the DACA studies was overall comparable to the results obtained in preliminary tests on a 100 mL scale (see figure 27; appendix). However, the maximum cell dry weight achieved in the fermenter exceeded the one obtained on a 100 mL scale (11.08 g/L vs. 7.42 g/L). Accordingly, tacrolimus production was much higher in the fermenter (175.2 mg/L vs. 46.5 mg/L after 240 h). The observation that tacrolimus production heavily depends on the culture volume is consistent with all further production studies described throughout this work and has to be considered when comparing absolute production yields with those described in literature. Furthermore, it was observed that tacrolimus is not stable in cultures which results in a beginning degradation of the compound after several days of cultivation. Taking the two parameters of cultivation scale and degradation into consideration, it is overall quite challenging to determine an appropriate time point to quantify the maximum production of a tacrolimus producer strain. Generally, cultivation in the fermenter obviously provides the most favorable conditions among the ones examined during this thesis, very likely due to optimized aeration and a controlled, constant pH-value.

4.1.2 Positive controls of the DACA

FkbN

According to the expectation, the pathway-specific positive regulator of tacrolimus biosynthesis, FkbN, could be detected on PfkbO, the bidirectional promoter region controlling the expression of the polyketide synthase core genes, *fkbA*, *fkbB* and *fkbC*, respectively. Missing detection of FkbN in the 60 hours sample was expected as the expression of biosynthetic genes during the exponential growth phase is unlikely. However, contrary to the anticipations based on theoretically predicted FkbN binding sites (Ordónez-Robles *et al.*, 2016), the positive regulator FkbN did not bind to Ptcs6b, PfkbG and PallA, but to P16S which has no predicted binding motifs for this protein. There might be several reasons for the observed binding properties of FkbN. On the one hand, it has been described in literature that an inactivation of the protein FkbN does not prevent the transcription of the genes *tcs6*, *fkbG* and *allA* as their transcription also depends on an FkbN-independent promoter (Goranovič *et al.*, 2012; Ordónez-Robles *et al.*,

2016). Thus, the protein FkbN might not be detected on the respective promoter as it is just not required for the expression of these genes. Or else, only very few FkbN proteins had bound to the promoter region, resulting in intensities too low to be detected by semi-quantitative mass spectrometry. On the other hand, the binding sites within the tacrolimus biosynthetic gene cluster were only predicted theoretically but have not yet been verified experimentally, thus their location is only based on assumptions. In order to reliably confirm the predicted binding sites, it will be necessary to perform protein-DNA interaction assays, using e.g. surface plasmon resonance.
The unexpected detection of FkbN on P16S, though in a lower intensity, can be explained by the fact that two sections of the P16S sequence bear in part analogy to the predicted FkbN binding site sequence (Ordónez-Robles *et al.*, 2016). As the genome sequence of *Streptomyces tsukubaensis* NRRL18488 is very rich in GC (71.9 %), the predicted motif comprising many guanine and cytosine residues is quite abundant and not very specific. Therefore, probably a few bases are sufficient to be recognized and bound by FkbN, which could explain why this protein was found to bind to the negative control fragment.

PhoP

Fortunately, the second positive control protein PhoP (IFCAGPOI_03863) fully met the expectations as it was found to bind exclusively to Ptcs6b in the 114 hours sample with an intensity of $6.26 \cdot 10^5$. PhoP is part of the PhoR-PhoP two-component system that is required for the expression of genes belonging to the phosphate (*pho*) regulon (Sola-Landa *et al.*, 2003). Under phosphate-limiting conditions, the sensor kinase PhoR is self-phosphorylated and transfers the phosphate group to the DNA binding response regulator PhoB. PhoB, in turn, binds to consensus phosphate boxes in the promoter regions of genes in the *pho* regulon, so called PHO boxes (Makino *et al.*, 1988). Ordóñez-Robles *et al.* (2017) predicted putative PHO boxes in the genome of *Streptomyces tsukubaensis* NRRL18488 and identified one of them located upstream of the gene *fkbN*. The detection of PhoP on Ptcs6b thus confirms the theoretically predicted binding site and supports the hypothesis that inorganic phosphate might control the expression of *fkbN* (Martínez-Castro *et al.*, 2013; Ordóñez-Robles *et al.*, 2017). Furthermore, the detection of this protein nicely validates the described DACA procedure and confirms the significance of this assay.

4.1.3 Proteins of the tacrolimus biosynthetic gene cluster

What was quite interesting to note when looking at the proteins of the tacrolimus biosynthetic gene cluster was the fact that the cluster proteins FkbO and AllA could be detected on almost every promoter fragment in the 60 hours sample in quite high intensities ($1 \cdot 10^7$-range), contrary to the other cluster proteins that were mostly detectable in the 114 hours sample.
While this might be explained for FkbO by the fact that it is a cytochrome P450 enzyme which could be involved in more unspecific hydroxylation reactions besides tacrolimus biosynthesis, the

occurrence of AllA in the 60 hours sample is more surprising. The gene *allA* encodes an acyltransferase and an ACP domain and has been described to be involved in allylmalonyl-CoA precursor biosynthesis (Goranovič *et al.*, 2010). It has been shown that a deletion of *allA* extinguishes tacrolimus production due to the missing generation of the allylmalonyl-CoA extender unit (Mo *et al.*, 2011). In order to figure out a further, putatively regulatory role of AllA, the protein was additionally chosen to be analyzed in further detail by overexpression. Remarkably, the protein AllA has also been striking in a first proteomic approach with *Streptomyces tsukubaensis* NRRL18488 published by Wang, Liu, Huang, Jin, Wang and Wen (2017). Described as hypothetical protein, AllA could be detected in higher quantities in a strain showing 88 % enhanced tacrolimus production upon feeding with soybean oil. It is likely that an increased demand for the extender unit allylmalonyl-CoA during tacrolimus production raises the expression of AllA for further precursor supply. However, this would also require the expression of three further proteins involved in allylmalonyl-CoA biosynthesis: AllK, AllR and AllD. Unspecific accretion of AllA to DNA might explain why it could be identified on all the tested promoter fragments in the DACA.

4.2 Overexpression of putative regulatory proteins of tacrolimus biosynthesis

4.2.1 Non-integrative overexpression of putative regulatory proteins

Microfermentation of the generated mutant strains of *Streptomyces tsukubaensis* NRRL18488 overexpressing 40 different putative regulators of tacrolimus biosynthesis was carried out by SINTEF. This high-throughput screening revealed that 14 of those regulators significantly increased tacrolimus production in *Streptomyces tsukubaensis* NRRL18488 upon overexpression. The respective strains and the annotations of the corresponding proteins are summarized in table 58.

Table 58: **Mutant strains revealing significantly increased tacrolimus production in microfermentation.**

Strain	Annotation of the overexpressed protein	Promoter	Fold increase
S. tsukubaensis/pTB02	transcriptional regulator	Ptcs6a	1.63
S. tsukubaensis/pTB03	two-component sensor histidine kinase	Ptcs6a	2.25
S. tsukubaensis/pTB04	transcriptional regulator	Ptcs6b	1.91
S. tsukubaensis/pTB06	two-component system DNA-binding response regulator	Ptcs6b	1.74
S. tsukubaensis/pTB08	hypothetical protein	Ptcs6b	1.92
S. tsukubaensis/pTB09	DNA-binding response regulator	Ptcs6b	1.75
S. tsukubaensis/pTB10	YebC/PmpR family DNA-binding transcriptional regulator	Ptcs6b	1.76
S. tsukubaensis/pTB11	transcriptional regulator	Ptcs6b	1.56
S. tsukubaensis/pTB16	helix-turn-helix transcriptional regulator	PfkbO	1.71
S. tsukubaensis/pTB20	docking protein	PfkbG	2.23
S. tsukubaensis/pTB23	LacI family transcriptional regulator	PfkbG	1.80
S. tsukubaensis/pTB24	GntR family transcriptional regulator	PfkbG	1.82
S. tsukubaensis/pTB25	hypothetical protein	PfkbG	1.79
S. tsukubaensis/pTB31	two-component system response regulator	several	1.68

Proteins revealing a positive impact on tacrolimus biosynthesis had bound to Ptcs6, PfkbO and PfkbG, thus to three out of the four cluster-located promoter regions that had been analyzed in the DACA. None of the proteins found on PallA noticeably increased tacrolimus production. The promoter region PallA controls the expression of the genes located in the so-called *all* subcluster, which is involved in allylmalonyl-CoA precursor biosynthesis. Chen *et al.* (2012) could show that an overexpression of the genes *allAKRD* significantly improved tacrolimus production yields. Obviously, the proteins of the DACA binding specifically to this promoter region did not cause a sufficient overexpression of the respective genes, as otherwise a significant increase in tacrolimus production could have been expected.

Half of the proteins which significantly increased tacrolimus production have been annotated as transcriptional regulators, thus a regulatory function of these proteins was anticipated. Two of the strains listed in table 58, *Streptomyces tsukubaensis*/pTB09 and pTB16, overexpress proteins that are located in putative biosynthetic gene clusters predicted by antiSMASH, namely a possible lad-

derane cluster with similarity to an asukamycin biosynthetic gene cluster (IFCAGPOI_04468) and a putative cluster with similarity to an oligomycin biosynthetic gene cluster (IFCAGPOI_01482). Possibly, these regulatory proteins act as global regulators and consequently do not only affect the biosynthesis of the cluster-related antibiotics but also tacrolimus biosynthesis. Likewise, it is also possible that regulators located within another biosynthetic gene cluster reduce tacrolimus production upon their overexpression due to a potential competition for precursor molecules which are required both for the biosynthesis of tacrolimus and the regulator-related natural product. Considering that nine of the regulators that didn't significantly increase FK506 production following their overexpression are located in predicted biosynthetic gene clusters, the latter hypothesis is not that unlikely.

During microfermentations performed by SINTEF and 3 mL cultivations performed in-house, the formation of extensive aggregates could be observed. As this was not the case for cultivations on larger scale, this observation might be related to a reduced mixing of the smaller culture volumes. It is known that production of secondary metabolites is dependent on the structural morphology of the producer strain, as aggregates can restrict an efficient transfer of nutrients and gases to the center of the pellets and thereby lower the maximal obtainable production (Celler *et al.*, 2012). The observed aggregates might therefore explain the high variations that could be observed not only between different exconjugants but sometimes also between the technical replicates of an individual exconjugant. Furthermore, the aggregates might be in charge of the generally lower tacrolimus production yields achieved following small-scale cultivations.

In addition to the microfermentation performed by SINTEF, 17 selected mutant strains and the empty vector reference strain were cultivated on a 100 mL scale. Except for mutant strains *Streptomyces tsukubaensis*/pTB08 and pTB23, which showed high production both on a 1 mL and a 100 mL scale, the production behavior of the strains observed in microfermentation and 100 mL fermentation was not that comparable. Regarding the large-scale fermentation, it was especially mutant strain *Streptomyces tsukubaensis*/pTB01 that turned out to be an interesting candidate in view of increased tacrolimus production, although high variations between the three individual exconjugants were observed. At the same time, the elevated production seen for mutant strain *Streptomyces tsukubaensis*/pTB03 in microfermentation could not be observed on a larger scale.

Overall, production on a 100 mL scale was much higher than on a 1 mL scale. The higher production yields obtained in 500 mL Erlenmeyer flasks with 100 mL of medium can once more be explained by an improved oxygen supply through a better mixing of the cultures. A further fact that could account for the huge difference in tacrolimus production could be the extraction procedure. SINTEF freeze-dried the samples for two days, extracted them with DMSO for one hour and analyzed the extracts obtained after centrifugation. Extraction of the samples from the 100 mL fermentation was performed according to the TacroDrugs standard operating procedure, meaning that samples were mixed with an equal volume of methanol and incubated for one hour under shaking. The supernatant obtained after two centrifugation steps was directly analyzed via HPLC. This extraction procedure was validated by comparing data obtained for a 100 mL

cultivation of the wild type strain *Streptomyces tsukubaensis* NRRL18488 (figure 27) with data described in literature. Martínez-Castro *et al.* (2013) cultivated the same strain under the same conditions and used an equivalent extraction protocol. The published production values bear a striking similarity to the data obtained in this study.

None of the mutant strains cultivated on a 100 mL scale significantly increased tacrolimus production compared to the reference strain. In contrast, two strains, namely *Streptomyces tsukubaensis*/pTB06 and pTB07, depicted a significantly decreased production. Considering that the strain *Streptomyces tsukubaensis*/pTB06 depicted a significantly increased tacrolimus production on a 1 mL scale reveals once more the discrepancy observed between the two types of cultivation. Although not showing a significantly increased production on a 1 mL scale fermentation, the mutant strain *Streptomyces tsukubaensis*/pTB30 produced quite well on a 100 mL scale. The overexpressed protein is located in a fatty acid type 1 PKS/NRPS cluster with similarity to an abyssomycin biosynthetic gene cluster. There might be a putative cross regulation of this type 1 PKS/NRPS cluster and the tacrolimus type 1 PKS/NRPS biosynthetic gene cluster.

A further putative cross regulation was assumed for protein IFCAGPOI_00339 which is located in the hypothetical type 1 PKS bafilomycin biosynthetic gene cluster. Therefore, the mutant strain *Streptomyces tsukubaensis*/pTB15 has been analyzed on a 100 mL scale fermentation. However, neither in the large-scale fermentation nor in microfermentation this strain showed striking production values. In accordance with tacrolimus biosynthesis, the biosynthesis of bafilomycin comprises the incorporation of two methoxymalonyl-CoA extender units (Nara *et al.*, 2017). Overexpression of the cluster-specific LuxR family transcriptional regulator originating from the bafilomycin biosynthetic gene cluster might thus only trigger bafilomycin production and impair FK506 biosynthesis by withdrawing the mentioned precursor molecules.

Regardless of the DACA studies, a phosphopantetheinyl transferase (PPTase) was overexpressed in the wild type producer strain as these proteins have been described to be involved in post-translational modification of PKS systems (Wang *et al.*, 2016). Thus, these proteins could likewise affect tacrolimus production. The genome of *Streptomyces tsukubaensis* NRRL18488 harbors seven different PPTase genes, however, no PPTase could be detected in the DACA. Thus, the PPTase IFCAGPOI_01486 was chosen for overexpression as it shows the highest similarity (72 %) to an already characterized PPTase from *Streptomyces verticillus* (Sánchez *et al.*, 2001). Tacrolimus production of the strain *Streptomyces tsukubaensis*/pTB41, overexpressing the respective protein, was only slightly increased compared to the reference strain, however, the difference was not significant. Probably, one of the other six PPTases of *Streptomyces tsukubaensis* NRRL18488 might have revealed a more obvious effect on tacrolimus production following its overexpression.

Overall, the percentage increase in tacrolimus production upon overexpression of regulatory proteins identified in the DACA corresponded considerably to the values described in literature for attempts to increase yields on a regulatory level (see section 1.4). As mentioned earlier, overexpression of individual genes potentially affecting FK506 production caused 1.2- to 2-fold

increments in tacrolimus production. Even upon overexpression of the pathway-specific regulator FkbN, production could not be raised more than 2-fold (Mo *et al.*, 2012). Higher yield improvements up to 7-fold (Turło *et al.*, 2012) could only be achieved by feeding precursors of tacrolimus biosynthesis which indicates that transcription is not the only limiting factor in the biosynthesis of tacrolimus. Additionally, the observed changes in production following overexpression of proteins identified in the DACA are altogether quite comparable with those described in a similar study, aiming to identify regulatory proteins of novobiocin biosynthesis (Bekiesch *et al.*, 2016). The best regulator ($BxlR_{Sc}$=Sco4754) identified in the mentioned heterologous approach caused a 1.76-fold increase in novobiocin production upon its overexpression. Considering that the best regulator IFCAGPOI_03331 identified in *Streptomyces tsukubaensis* NRRL18488 increased tacrolimus production even 2.25-fold when overexpressed, attaches even more importance to the present study performed in the native producer strain. Moreover, the binding of putatively regulatory proteins to the promoter fragments in the tacrolimus biosynthetic gene cluster was found to be far more specific in contrast to the findings of Bekiesch *et al.* (2016) where most of the regulators were discovered to simultaneously bind to several promoter regions. This observation might be indicative of evolutionarily caused optimized binding capabilities of regulators to their respective DNA sequences.

4.2.2 Comparison of non-integrative and integrative overexpression of selected putative regulatory proteins

Based on the results of the high-throughput screening approach including all generated *Streptomyces tsukubaensis* NRRL18488 mutant strains, seven regulators have been chosen for further investigation. The aim was to compare the effect of a non-integrative versus an integrative overexpression of the respective regulators. Whilst non-integrative overexpression using a replicative plasmid with *ermE** promoter results in a high copy number of the overexpressed regulators, integrative overexpression under control of the tetracycline-inducible *tcp830* promoter involves single-copy transcription in the induced state. A leaky transcription in the absence of the inductor anhydrotetracycline has been observed in previous studies and can be ascribed to a partial repression of the *tcp830* promoter by the innate tetracycline-responsive repressor (Dangel *et al.*, 2010). By including both replicative and integrative overexpression, this study thus allowed to reveal a putative dose-response effect of certain regulatory proteins.

The non-induced integrative overexpression of regulators corresponded more or less to the expectations as the production behavior of the respective strains was quite comparable to the reference strain harboring the empty vector. Two out of the seven regulators included in this study resulted in maximum tacrolimus yields following induced integrative overexpression while for the other five regulators the replicative overexpression was fostered. Interestingly, the cluster-specific regulator FkbN is one of the two regulators whose overexpression is remarkably favored in the induced integrative system. From an evolutionary point of view this might be explained by an evolved strong interaction of this regulator with the corresponding promoter region within the

same biosynthetic gene cluster. Accordingly, regulators originating from different biosynthetic gene clusters or other genomic regions might depict a weaker interaction with the respective promoter and therefore require higher copy numbers to compensate this effect. However, to confirm this hypothesis, it would be absolutely necessary to perform protein-DNA interaction assays to quantify the binding strength of each regulator to its promoter.

Due to its known function as cluster-specific, positive regulator, FkbN was included in this study. This LuxR family transcriptional regulator has been studied in detail and its positive impact on tacrolimus production is unquestioned (Goranovič *et al.*, 2012; Mo *et al.*, 2012). Putative binding sites of FkbN within the genome of *Streptomyces tsukubaensis* NRRL18488 have been predicted theoretically and it became obvious that FkbN only weakly self-regulates its own expression (Ordóñez-Robles *et al.*, 2017). As mentioned before, this is consistent with the results of the DACA as FkbN could not be detected on Ptcs6, the promoter region located upstream of FkbN. Due to its large size, FkbN belongs to the LAL subfamily of LuxR regulators which is known to contain activators of polyketide biosynthesis. Most LuxR-type regulators are cluster-specific and activate the expression of the respective compound (Romero-Rodríguez *et al.*, 2015). The positive impact of FkbN on tacrolimus production could be confirmed in this study where FkbN resulted in a 56 % increase in tacrolimus production upon non-integrative overexpression and even a 94 % increase following an induced non-integrative overexpression. The observed values correspond to those described by Mo *et al.* (2012) and Goranovič *et al.* (2012) who both used the integrative pSET152 vector for overexpression and achieved an increase in production of ∼100 % and 55 %, respectively.

Furthermore, two TetR family regulators, namely IFCAGPOI_05107 and IFCAGPOI_06489, were chosen for further investigation. The TetR (tetracycline repressor) family of transcription factors is the third most frequently identified transcription factor family observed in bacteria (Ramos *et al.*, 2005). Generally, these regulators are described as proteins repressing transcription upon binding to the operator (Romero-Rodríguez *et al.*, 2015). However, there are also examples in which members of this transcription factor family positively influence the production of secondary metabolites, for example the protein SlgR1 which regulates streptolydigin biosynthesis in *Streptomyces lydicus* (Gómez *et al.*, 2012) or Gel19 that has a positive impact on geldanamycin production in *Streptomyces hygroscopocus* JCM4427 (Woncheol *et al.*, 2010). In this study, the TetR family transcriptional regulators IFCAGPOI_05107 and IFCAGPOI_06489 did neither reveal a positive nor a negative effect on tacrolimus production upon integrative overexpression. Nevertheless, using the non-integrative vector for overexpression of these two proteins significantly increased tacrolimus production compared to the control strains, which indicates that they are most likely positive global regulators of tacrolimus biosynthesis.

Another protein that has been further investigated in detail was the two-component sensor histidine kinase IFCAGPOI_03331. It has already been described in literature that response regulators of histidine kinases can either exert a positive or a negative effect on the biosynthesis of secondary metabolites. Regarding trioxacarcin biosynthesis in *Streptomyces bottropensis*, it could be shown that the two-component response regulator Txn11 activates the biosynthesis of

this metabolite (Yang *et al.*, 2015). In contrast, a two-component system histidine kinase reduced rapamycin production upon overexpression in *Streptomyces rapamycinicus* (Yoo *et al.*, 2015). The two-component sensor histidine kinase of *Streptomyces tsukubaensis* NRRL18488, which has been chosen for this study based on the results of the DACA, is located in a section of the genome that is poorly characterized regarding the annotation of the respective neighbor proteins. Most of them are just annotated as hypothetical proteins. Therefore, it is likely that this histidine kinase is involved in the regulation of the biosynthesis of an as yet unknown compound and further acts as global regulator, thus also influences tacrolimus biosynthesis. Overall, the protein IFCAGPOI_03331 proved to be one of the best regulators of this study, revealing significantly increased production yields compared to the reference strains using non-integrative and induced integrative overexpression.

Furthermore, the protein IFCAGPOI_01482 was investigated. This helix-turn-helix transcriptional regulator is located in a putative oligomycin biosynthetic gene cluster where it controls the expression of several ABC transporter-related proteins. A BLAST analysis of the amino acid sequence of this regulator revealed a similarity to LuxR-type family transcriptional regulators. As described previously, these regulators are mostly cluster-specific. Missing cluster-specificity for the tacrolimus biosynthetic gene cluster might explain why the overexpression of this protein revealed only a minor effect compared to the other regulators investigated in this study. Actually, due to the binding of this regulator to the promoter region PfkbO, which controls the expression of the polyketide synthase core genes, a noticeable effect on tacrolimus production had been anticipated.

Additionally, a LacI family transcriptional regulator, IFCAGPOI_04736, was studied. Comparable to the TetR family transcriptional regulators, LacI family regulators have been described as repressor proteins. These regulators often control carbohydrate catabolic pathways and are thus associated with carbon catabolite repression (Romero-Rodríguez *et al.*, 2015). A genomic approach including 270 bacterial genomes revealed that nearly 90 % of the LacI family transcriptional regulators are local regulators controlling sugar-utilizing pathways. Only 10 % of these regulators thus act as global regulators (Ravcheev *et al.*, 2014). Indeed, an integrative overexpression of the LacI-type regulator IFCAGPOI_04736 in this study revealed no remarkable effect on tacrolimus production. However, following non-integrative overexpression of the respective protein, a significant increase in production was observed, indicating that a high copy number of this regulator type positively affects tacrolimus production.

Generally, the advantage of an integrative overexpression of regulators over non-integrative overexpression is the missing necessity to conduct selection for a plasmid during fermentation. A putative impact of the antibiotic on growth and production behavior of the mutant strain has consequently not be taken into account. Nevertheless, this study revealed that non-integrative overexpression might be beneficial in some cases, depending on the dose-response effect of a certain regulator. Using plasmid-based systems further allows overexpressions in mutant strains where natural attachment sites required for integrative vectors are already occupied and thus no longer available for further integrations.

4.3 Simultaneous overexpression of several regulatory proteins

The artificial gene operon assembly system (AGOS) has been successfully used to assemble the complete novobiocin gene cluster on a single vector (Basitta *et al.*, 2017). Due to the possibility of consecutively adding individual gene operons, this approach seemed to be a suitable method to simultaneously overexpress several positive regulators of tacrolimus biosynthesis, each equipped with a *tcp830* promoter, a ribosomal binding site and a terminator. Furthermore, the stepwise integration of the genes would allow to generate different combinations of the six regulators chosen for overexpression.

Combining the best regulator of the 3 mL scale studies, IFCAGPOI_03331, with regulator IFCAGPOI_06489 resulted in a maximum 3.21-fold yield improvement after induction with anhydrotetracylin. Compared to the 1.96-fold and 1.20-fold increases achieved following individual overexpression of these two regulators, this actually represents a remarkable improvement and exceeds all other yield optimizations achieved in the course of this study. It cannot be excluded that a combination of two other regulators might have resulted in an even higher yield improvement. However, as the size of the construct is a very crucial parameter regarding successful conjugation, it was intended to keep the vector preferably small as long as possible. This meant introducing the regulator genes depicting lower amounts of base pairs first.

Unfortunately, the commonly known difficulty of introducing large vectors into *Streptomyces tsukubaensis* NRRL18488 prohibited the generation of the strain *Streptomyces tsukubaensis*/mrsHK07, simultaneously overexpressing all six regulators. Nevertheless, considering the data achieved for the strains overexpressing two or three regulators, it is doubtful anyway whether all six regulators would actually considerably increase tacrolimus production following their combined overexpression. Since two of the exconjugants overexpressing two regulators were not outstanding and the third exconjugant revealed only slightly increased production yields compared to the one available exconjugant overexpressing three regulators, it is reasonable to assume that manipulating regulation alone might not be enough to trigger tacrolimus production. According to several studies described in literature, it will be necessary to combine regulatory approaches with feeding strategies or other methods of improved precursor supply to prevent biosynthetic building blocks from becoming a bottleneck for the biosynthesis of natural products as tacrolimus. Metabolic engineering approaches as described by Huang, Li, Xia, Wen and Jia (2013) might therefore be of increasing importance in the future in order to determine potential genetic targets that allow to improve tacrolimus yields.

Taking a close look at literature reveals that studies focusing on simultaneous overexpression of several regulatory genes in *Streptomycetes* are quite rare. Malla *et al.* (2010) pursued an approach rather similar to the one described in this study. They intended to improve the production of doxorubicin by *Streptomyces peuceticus* by mutually overexpressing different pathway-specific and global regulators. However, in contrast to this study, the choice of the respective regulators was not based on DACA studies but on various preceding regulation studies. The authors could show that different combinations of the regulatory genes *dnrN*, *dnrI*, *afsR* and *metK1-sp*

resulted in highly different doxorubicin production yields. The combination of AfsR/MetK1-sp had no significant effect on doxorubicin, but combined overexpression of DnrN/DnrI resulted in a 1.2-fold increment. While a simultaneous overexpression of DnrN/DnrI/MetKI-sp resulted only in a 1.4-fold increase in doxorubicin production, the combination of the three regulators DnrN/DnrI/AfsR maximized doxorubicin production (4.3-fold increment). In contrast, the combination of DnrN/DnrI/AfsR/MetK1-sp was not found to affect the production of doxorubicin significantly.

Regarding ascomycin biosynthesis, Wang *et al.* (2019) published a comprehensive approach with individual and common overexpression of the genes *aroA* (encoding a 3-deoxo-7-phosphoheptulonate synthase), *fkbN* and *luxR* (encoding a pleiotropic regulator). Following individual overexpression of these genes, they achieved 1.32-, 2.55- and 2.58-fold production enhancements in comparison with that of the control strain. Applying combined overexpression of AroA/LuxR, AroA/FkbN and FkbN/LuxR, they detected 2.92-, 3.04- and 3.40-fold increases compared to the control. These values thus coincide with those obtained for a combined overexpression of two regulators in this study. Following simultaneous overexpression of all three proteins, ascomycin yields were 4.12-fold higher than the control yield, which indicates that it is indeed possible to further enhance the production of natural compounds when considering both precursor metabolic and transcriptional regulatory pathways. Nevertheless, it should also be stated that cell growth was apparently affected by the combined gene overexpression as reflected by declines in final biomass concentrations. Again, this observation is consistent with the present study as cell dry weight for exconjugants 1 and 2 of *Streptomyces tsukubaensis*/mrsHK03 was diminished compared to the control strains.

4.4 PKS engineering

None of the performed PKS engineering approaches resulted in the production of the desired derivatives 9-allyl tacrolimus and 9-ethyl tacrolimus, although various strategies were used and a lot of individual mutant strains were analyzed.

Regarding the heterologous module swap approach, missing production of 9-allyl tacrolimus can be easily explained by the result of the Nanopore sequencing which revealed that nearly the complete tacrolimus biosynthetic gene cluster had been deleted. Most likely, an undesired homologous recombination event, resulting in the homologous recombination between the natural module 4 and the PCR-amplified module 4 (4599 bp), was favored over the desired recombination event which was to introduce module 4 at the position of module 10. However, the predicted deletion is still in question as restriction digest, PCR and cultivation lead to conflicting results. The module swap performed in the native producer strain *Streptomyces tsukubaensis* NRRL18488 has not been verified by sequencing. Moreover, it was difficult to confirm the correct swap by PCR. According to LC-MS analysis, the generated module swap mutant strains are still able to produce tacrolimus.

The same result was obtained for the AT domain swap mutant strains generated with *Streptomyces tsukubaensis* NRRL18488 as parental strain. In the case of the AT domain swap approach, colony PCR followed by sequencing could reliably confirm the successful AT domain swap. Furthermore, a clean genotype was obtained after several rounds of dilution spreading of the mutant spores. Nevertheless, tacrolimus production was still detectable. These observations raise suspicion that the promiscuous nature of the AT domain of module 4 hampers a specific modification of the tacrolimus molecule. Mo *et al.* (2011) described that tacrolimus producer strains naturally biosynthesize tiny amounts of derivatives due to the incorporation of either methylmalonyl-CoA, ethylmalonyl-CoA or propylmalonyl-CoA, respectively, by the AT domain of module 4 instead of the original extender unit allylmalonyl-CoA. Furthermore, they could show that the production of these natural derivatives can be significantly increased following genetic manipulations within the biosynthetic gene cluster, e.g. a deletion of the gene *allK*. AllK, as well as AllA, AllR and AllD, are involved in allylmalonyl-CoA precursor biosynthesis (Mo *et al.*, 2011). Both Chen *et al.* (2012) and Mo *et al.* (2016) identified allylmalonyl-CoA as limiting factor in tacrolimus biosynthesis. Thus, it is possible that an insufficient allylmalonyl-CoA precursor supply impedes the incorporation of a second allylmalonyl-CoA extender unit by the second AT domain of module 4 located within the manipulated module 10. Consequently, the promiscuous AT domain of module 4 is forced to take another precursor molecule, presumably malonyl-CoA. Regarding further studies on this project, it will be worthwhile investigating the effect of an overexpression of the *all* subcluster in the generated mutant strains. Alternatively, the feeding of allylmalonyl-CoA to the mutant strains could compensate a putative precursor shortage.

Besides the possibility that a lack of allylmalonyl-CoA as precursor molecule is responsible for the missing production of the 9-allyl derivative, it is also likely that steric hindrance prevents the biosynthesis of the desired derivative as the natural carbonyl group in position 9 of the

tacrolimus molecule is much smaller in size than the requested allyl group. An allyl residue in position 9 might impede the closure of the macrocyclic ring and coincidentally impair FkbD, the enzyme which normally catalyzes the C-9-oxydation.
Additionally, regarding the AT domain swap approach, it cannot be excluded that the natural ACP domain of module 10 continues to introduce malonyl-CoA as extender unit due to a transacylation by another catalytically active malonyl-CoA-specific AT domain of the tacrolimus PKS. Regarding the 6-deoxyerythronolide B synthase (DEBS), a corresponding reaction has been observed following an inactivation of the AT domain of module 1 of the DEBS PKS. The natural PKS product 6-deoxyerythronolide B (6-dEB) was still detectable after *in vitro* assays with the modified PKS in the absence of a complemented AT domain which made the authors hypothesize a transacylation reaction catalyzed by one of the other five AT domains located within the same cluster (Dunn *et al.*, 2014).
The idea of the performed ACP domain swap (ACP(M10) vs. KirACP5) in combination with the expression of the *trans*AT KirCII was to introduce an ethyl group in position 9 of the tacrolimus molecule. As producer strains of tacrolimus also synthesize FK506-related macrolides such as ascomycin in trace amounts (Park *et al.*, 2009), it was supposed that *Streptomyces tsukubaensis* NRRL18488 should be able to produce the extender unit ethylmalonyl-CoA which is required for the *trans*AT KirCII-KirACP5 strategy. Ascomycin production and consequently the presence of the ethylmalonyl-CoA extender unit was also observed during heterologous tacrolimus production in *Streptomyces coelicolor* M1146 (Jones *et al.*, 2013).
However, LC-MS analysis revealed that the desired 9-ethyl derivative is not produced in any of the two approaches, although tacrolimus production is abolished both in heterologous ACP domain swap mutant strains and the *Streptomyces tsukubaensis* NRRL18488 mutant strains. The observation of missing tacrolimus production is in striking contrast to the AT domain swap approach and the module swap approach, which still resulted in tacrolimus production in both kinds of mutant stains. Furthermore, this finding might support the hypothesis of the promiscuous AT domain of module 4 or the alternatively transacylated ACP domain of module 10, leading unexpectedly to a continued incorporation of malonyl-CoA in the last step of the PKS assembly line.
As the successful replacement of the ACP domain of module 10 with the KirACP5 domain on pAC20N could be verified by colony PCR and sequencing of the PCR product, Nanopore sequencing of the modified BAC used in the heterologous ACP domain swap approach was not absolutely necessary, especially as a wrong homologous recombination event was less likely in this case due to the fact that the KirACP5 domain originates from a foreign bacterial strain. Beyond that, also the ACP domain swap generated in *Streptomyces tsukubaensis* NRRL18488 could be verified by PCR and sequencing of the PCR products and the presence of the plasmid pEM11CII was likewise confirmed in all generated mutant strains. Therefore, missing detection of the expected derivative might thus be ascribed to an extremely low production rate. Dunn *et al.* (2014) used the KirCII to complement an AT-null 6-deoxyerythronolide B synthase (DEBS) assembly line and detected only a minor production of the expected derivative *in vitro*. At

the same time, they identified methylmalonate as preferred extender unit for KirCII under the assay conditions. In many cases described in literature the production of target compounds from engineered PKS systems was lowered to about 3-5 % compared to the production of the wild type PKS product (Rowe *et al.*, 2001). As heterologous production of tacrolimus is quite low anyway (Jones *et al.*, 2013), it is reasonable to assume that the production of the 9-ethyl derivative is even lower and therefore no longer detectable in heterologous host strains. A low production might not be that crucial in *Streptomyces tsukubaensis* ACP domain swap mutant strains, whereas limited transferability of the *trans*AT KirCII-KirACP5 system to the tacrolimus biosynthetic gene cluster could account for the missing production of 9-ethyl tacrolimus. Apart from the mentioned *in vitro* complementation approach including the DEBS assembly line (Dunn *et al.*, 2014), the *trans*AT KirCII has so far only been applied in the natural kirromycin biosynthetic gene cluster (Musiol *et al.*, 2011).
Furthermore, it cannot be excluded that the missing production of the 9-ethyl derivative is due to a shortage of the ethylmalonyl-CoA extender unit. Therefore, it could be helpful to feed the required precursor molecule to the generated mutant strains. In accordance with the study described by Musiol-Kroll *et al.* (2017), this could be realized by feeding ethylmalonic acid to ACP domain swap mutant strains overexpressing the malonyl-CoA synthetase T207G/M306I MatB. The MatB enzyme is able to activate non-natural extender units in a two-step reaction mechanism (Hughes and Keatinge-Clay, 2011). As the *trans*AT KirCII was found to be quite promiscuous, accepting also allylmalonyl-CoA and propargylmalonyl-CoA as substrates (Musiol-Kroll *et al.*, 2017), a feeding approach would putatively allow to generate even more derivatives than initially intended.

Interestingly, ACP domain swap mutant strain *Streptomyces tsukubaensis* ACP E2-K7-6/ pEM11CII produced an unexpected compound. Following NMR spectroscopy, this compound was identified as 9-deoxo-31-*O*-demethyl-FK506. The compound is a well known intermediate in tacrolimus biosynthesis. It occurs before the proteins FkbD (cytochrome P450 hydroxylase) and FkbM (*S*-adenosylmethionine (SAM)-dependent methyltransferase) catalyze C-9-oxidation and 31-*O*-methylation. The compound was initially described by Motamedi *et al.* (1996) in an *fkbD* deletion strain. The authors hypothesized that the gene disruption has a polar effect on the synthesis of FkbM, located just downstream. In order to exclude that the CRISPR-Cas9 editing used to exchange the ACP domain of module 10 unintentionally resulted in a further modification of the adjacent *fkbD* gene, *fkbD* was amplified from DNA of the respective mutant strain and confirmed by sequencing of the PCR product. Consequently, there has to be another reason for the observed accumulation of the tacrolimus intermediate. Putatively, the ACP domain swap, which resulted in a magnification of module 10 by 126 bp, has a polar effect on both downstream genes, *fkbD* and *fkbM*.
The detection of 9-deoxo-31-*O*-demethyl-FK506 further illustrates that the new KirACP5 domain, contrary to expectations, introduces malonyl-CoA instead of ethylmalonyl-CoA. Moreover, it has to be stated that the control strain not harboring pEM11CII, the *trans*AT KirCII encoding plas-

mid, likewise produces this compound. This observation raises the suspicion that the KirACP5 might be unexpectedly loaded by the original AT domain of module 10 which naturally selects malonyl-CoA. In order to preclude this possibility, it could be helpful to delete the respective AT domain of module 10 in the mutant strain, similar to Dunn *et al.* (2014) who also used the *trans*AT KirCII-KirACP5 system for an *in vitro* approach with the DEBS PKS.
Just as tacrolimus, 9-deoxo-31-*O*-demethyl-FK506 was shown to exert immunosuppressive activity *in vitro*, albeit with a 70-fold reduced potency. Nevertheless, the compound could in principle be used as starting material for chemical synthesis of C-9-derivatives.

Several PKS engineering approaches aiming to produce derivatives of natural products or novel compounds have been described in literature. However, PKS engineering is still a challenging and risky procedure as many approaches simply fail or result in drastically reduced yields (Weissman, 2016). Various possible reasons for this observation have been proposed, including reduced stability of the new PKS, hampered reactions within a module and deteriorated processing of the new chemical structure by succeeding modules (Gokhale *et al.*, 1999).
Many publications mention the importance of maintaining interfaces between different domains or modules intact. Gokhale *et al.* (1999) defined two types of linkers: intermodular linkers, which separate covalently connected modules, and interpolypeptide linkers, located upstream of NH_2-terminal and downstream of COOH-terminal modules. The latter have also been described as docking domains (Broadhurst *et al.*, 2003). Furthermore, boundaries within a module have been described, such as the KS-AT linker (KAL) and post-AT linkers (PAL1 and PAL2), which are important to consider when exchanging for example AT domains (Yuzawa *et al.*, 2017).
These above-mentioned linker regions have been taken into consideration when the cloning procedures for the PKS engineering approaches of this study were designed.
For the module swap approach, this meant to preserve the intermodular linker located between the ACP domain of module 9 and the KS domain of module 10. Gokhale *et al.* (1999) have described a consensus sequence for those linkers which could also be identified in the respective sequence section of *Streptomyces tsukubaensis* NRRL18488. The linker sequence comprises 22 amino acids (66 bp), including a conserved proline residue, and is part of the 85 bp sequence section between the ACP domain of module 9 and the KS domain of module 10 (figure 24). This linker sequence was completely maintained in the module swap approach.

Intermodular linker sequence between module 9 and module 10
CGCTCCCGCCACCCGGTCCGCGGCGGACTCCGTGCCCGCCCCGGCCGTACGG
GACCGGGACCGGGACCGGGACCGGGACCGGGAC

Corresponding amino acid sequence with conserved proline residue marked in bold
APATRSAADSVPA**P**AVRDRDRDRDRDRD

Figure 24: **Intermodular linker sequence located between module 9 and module 10.**

However, Zhang *et al.* (2017) published updated module boundaries which considerably differ from the previous definitions. According to the new findings, a complete module exhibits the domain order AT+DH+ER+KR+ACP+KS with a central ACP domain. Regarding the performed module swap in *Streptomyces tuskubaensis* NRRL18488, this would have meant to remove the KS domain at the beginning of the second module 4 and to attach the KS domain of the following module 5. However, up to now, the benefit of using the updated module boundaries is hard to assess as respective publications are rare. Miyazawa *et al.* (2020) have only lately published a successful approach of engineering the venemycin PKS by using the updated module boundaries. The interpolypeptide linker located downstream of module 10 corresponds to the docking domain between the last module of the PKS system and the TE (thioesterase) domain. These linkers have been described to contain many charged residues such as lysine (K), arginine (R), histidine (H), aspartic acid (D) and glutamic acid (E) (Gokhale *et al.*, 1999) which can also be detected in the corresponding sequence section of *Streptomyces tsukubaensis* NRRL18488 (figure 25). However, in contrast to most of the polyketide synthases described in literature, the thioesterase of the tacrolimus biosynthetic gene cluster is not located just downstream of the last module of the PKS, but is rather a free standing protein encoded by *fkbQ*. Therefore, it seemed to be particularly important to conserve this docking domain in order to preserve the region required for the correct protein interaction. Consequently, the end of the ACP domain of module 10 with the conserved LEDRL motif, as predicted by antiSMASH, was chosen as downstream border for module 10.

Interpolypeptide linker sequence downstream of module 10
GGCGACGGCGCGGACGACGACCCGCCCACCGTGCTCGAACTCCTGACGGAGAT
GGAGTCGCTCGACGCCGCGGACATCGCGGCGACACCCGCCCCGGAGCGTGCG
GCCATCGCCGATCTCCTCGACACTCTCTCCCGCGTCTGGAAGGACCACCGATGA

Corresponding amino acid sequence
GDGADDDPPTVLELLTEMESLDAADIAATPAPERAAIADLLDTLSRVWKDHR-

Figure 25: **Interpolypeptide linker sequence located downstream of module 10.**

Regarding the AT domain swap, it was necessary to consider the interdomain linkers connecting the KS and AT domains (linker KAL) and the post-AT linker sequences (linker PAL1 and PAL2). Yuzawa *et al.* (2017) presented a detailed investigation of different combinations of these interdomain linkers with the respective AT domain. They stated that both the KAL and PAL1 linker sequences of an AT domain have to be included in order to achieve stable and active proteins. At the same time, the authors noted that it is crucial to preserve the native KS-PAL2 interaction, however, they did not investigate a mutant enzyme where KAL-AT-PAL1-PAL2 had been swapped. They rather demonstrated that exchanging the KAL-AT-PAL1 unit and the AT-PAL1 unit was successful, respectively. Therefore, this study aimed to use KAL-AT4-PAL1-PAL2 as exchange unit, thereby maintaining the native KS-PAL2 interaction of module 4. A comparison of the PAL2 sequences of module 4 and module 10 revealed that they are quite similar anyway. Seven of the 13 residues are homologous and the remaining six residues show similar properties: two hydrophobic residues, one polar residue and two charged residues each, respectively (figure 26).

PAL2 sequence of module 4
L P T **Y** A **F** H **H** E R **Y W** I

PAL2 sequence of module 10
L P V **Y** P **F** Q **H** R H **Y W** L

Figure 26: **Post-AT linker sequences of module 4 and module 10.**
Conserved residues are printed in bold.

When comparing the HPLC chromatograms of extracts from the generated AT domain swap mutant strains with those of the wild type strain *Streptomyces tsukubaensis* NRRL18488, it became apparent that the peak corresponding to tacrolimus got smaller. Thus, the production pathway of the natural compound seems to be somehow impaired in the mutant strains, albeit not destroyed. Similar to the module swap approaches, many AT domain swaps described in literature have generally led to reduced polyketide production. Hans *et al.* (2003) postulated that domain swaps might alter modules at sites not included in the swapping process which consequently harms interactions existing between KS and ACP domains. This in turn impairs the hybrid module to catalyze chain elongation. Furthermore, the size of the swapped region might be a critical parameter in AT domain swaps (Yuzawa *et al.*, 2017). Regarding the AT domain swap performed in *Streptomyces tsukubaensis* NRRL18488, the original KAL-AT-PAL1-PAL2 region of module 10 comprising 1527 bp was replaced with the KAL-AT-PAL1-PAL2 unit of module 4 that consists of only 1353 bp. The generated size reduction of module 10 by 174 bp might probably have a negative effect on intermodular interactions.

An alternative to the AT domain swap, which intends to introduce an allyl group in position 9 of the tacrolimus molecule, might be site-directed mutagenesis of the AT domain of module 10. Shen

et al. (2018) identified five amino acid residues in the AT domain of module 4 of *Streptomyces tsukubaensis* YN06 that are essential for the introduction of the allylmalonyl-CoA extender unit. These residues, Q119, L185, V186, V187 and F203, respectively, are also present in the AT domain of module 10, except for V186 which is an aspartic acid (D) (figure 16). Regarding further studies on this project, it would thus be an idea to mutate this single residue (D186V) and to exchange the HAFH motif within the AT domain of module 10 for the CPTH motif observed in the AT domain of module 4. A large benefit of site-directed mutagenesis approaches is the fact that structural disturbances in the PKS remain minimal. Point mutations within PKS systems have been proven to remarkably affect the selectivity or specificity of domains and can furthermore impair the communication between different domains (Drufva *et al.*, 2020). However, performing such mutations in native producer strains will be far more laborious than modifying enzymes used for *in vitro* assays as performed by Shen *et al.* (2018).

5 Bibliography

Annaval, T., Paris, C., Leadlay, P. F., Jacob, C. and Weissman, K. J. (2015), 'Evaluating ketoreductase exchanges as a means of rationally altering polyketide stereochemistry', *ChemBioChem* **16**(9), 1357–1364.

Balsevich, G., Häusl, A. S., Meyer, C. W., Karamihalev, S., Feng, X., Pöhlmann, M. L., Dournes, C., Uribe-Marino, A., Santarelli, S., Labermaier, C., Hafner, K., Mao, T., Breitsamer, M., Theodoropoulou, M., Namendorf, C., Uhr, M., Paez-Pereda, M., Winter, G., Hausch, F., Chen, A., Tschöp, M. H., Rein, T., Gassen, N. C. and Schmidt, M. V. (2017), 'Stress-responsive FKBP51 regulates AKT2-AS160 signaling and metabolic function', *Nature Communications* **8**(1725).

Ban, Y. H., Park, S. R. and Yoon, Y. J. (2016), 'The biosynthetic pathway of FK506 and its engineering: from past achievements to future prospects', *Journal of Industrial Microbiology and Biotechnology* **43**(2-3), 389–400.

Ban, Y. H., Shinde, P. B., Hwang, J. Y., Song, M. C., Kim, D. H., Lim, S. K., Sohng, J. K. and Yoon, Y. J. (2013), 'Characterization of FK506 biosynthetic intermediates involved in post-PKS elaboration', *Journal of Natural Products* **76**(6), 1091–1098.

Barreiro, C. and Martínez-Castro, M. (2014), 'Trends in the biosynthesis and production of the immunosuppressant tacrolimus (FK506)', *Applied Microbiology and Biotechnology* **98**(2), 497–507.

Barreiro, C., Prieto, C., Sola-Landa, A., Solera, E., Martínez-Castro, M., Pérez-Redondo, R., García-Estrada, C., Aparicio, J. F., Fernández-Martínez, L. T., Santos-Aberturas, J., Salehi-Najafabadi, Z., Rodríguez-García, A., Tauch, A. and Martín, J. F. (2012), 'Draft genome of Streptomyces tsukubaensis NRRL 18488, the producer of the clinically important immunosuppressant tacrolimus (FK506)', *Journal of Bacteriology* **194**(14), 3756–3757.

Basitta, P., Westrich, L., Rösch, M., Kulik, A., Gust, B. and Apel, A. K. (2017), 'AGOS: A plug-and-play method for the assembly of artificial gene operons into functional biosynthetic gene clusters', *ACS Synthetic Biology* **6**(5), 817–825.

Bauer, J. S., Fillinger, S., Förstner, K., Herbig, A., Jones, A. C., Flinspach, K., Sharma, C., Gross, H., Nieselt, K. and Apel, A. K. (2017), 'dRNA-seq transcriptional profiling of the FK506 biosynthetic gene cluster in Streptomyces tsukubaensis NRRL18488 and general analysis of the transcriptome', *RNA Biology* **14**(11), 1617–1626.

Baughman, G., Wiederrecht, G. J., Campbell, N. F., Martin, M. M. and Bourgeois, S. (1995), 'FKBP51, a novel T-cell-specific immunophilin capable of calcineurin inhibition.', *Molecular and Cellular Biology* **15**(8), 4395–4402.

Bayly, C. L. and Yadav, V. G. (2017), 'Towards precision engineering of canonical polyketide synthase domains: recent advances and future prospects', *Molecules* **22**(235).

Bekiesch, P., Franz-Wachtel, M., Kulik, A., Brocker, M., Forchhammer, K., Gust, B. and Apel, A. K. (2016), 'DNA affinity capturing identifies new regulators of the heterologously expressed novobiocin gene cluster in Streptomyces coelicolor M512', *Applied Microbiology and Biotechnology* **100**(10), 4495–4509.

Bennett, P. M., Grinsted, J. and Richmond, M. H. (1977), 'Transposition of TnA does not generate deletions', *MGG Molecular & General Genetics* **154**(2), 205–211.

Blažič, M., Starcevic, A., Lisfi, M., Baranasic, D., Goranovič, D., Fujs, Š., Kuščer, E., Kosec, G., Petković, H., Cullum, J., Hranueli, D. and Zucko, J. (2012), 'Annotation of the modular polyketide synthase and nonribosomal peptide synthetase gene clusters in the genome of Streptomyces tsukubaensis NRRL18488', *Applied and Environmental Microbiology* **78**(23), 8183–8190.

Bradford, M. M. (1976), 'A rapid and sensitive method for the quantitation of microgram quantities of protein utilizing the principle of protein-dye binding.', *Analytical Biochemistry* **72**, 248–254.

Broadhurst, R., Nietlispach, D., Wheatcroft, M. P., Leadlay, P. F. and Weissman, K. J. (2003), 'The structure of docking domains in modular polyketide synthases', *Chemistry & Biology* **10**(8), 723–731.

Celler, K., Picioreanu, C., van Loosdrecht, M. C. M. and van Wezel, G. P. (2012), 'Structured morphological modeling as a framework for rational strain design of Streptomyces species', *Antonie van Leeuwenhoek* **102**, 409–423.

Chen, C., Zhao, X., Chen, L., Jin, Y., Zhao, Z. K. and Suh, J.-W. (2015), 'Effect of overexpression of endogenous and exogenous Streptomyces antibiotic regulatory proteins on tacrolimus (FK506) production in Streptomyces sp. KCCM11116P', *RSC Advances* **5**(21), 15756–15762.

Chen, D., Zhang, Q., Zhang, Q., Cen, P., Xu, Z. and Liu, W. (2012), 'Improvement of FK506 production in Streptomyces tsukubaensis by genetic enhancement of the supply of unusual polyketide extender units via utilization of two distinct site-specific recombination systems', *Applied and Environmental Microbiology* **78**(15), 5093–5103.

Cioffi, D. L., Hubler, T. R. and Scammell, J. G. (2011), 'Organization and function of the FKBP52 and FKBP51 genes', *Current Opinion in Pharmacology* **11**(4), 308–313.

Cobb, R. E., Wang, Y. and Zhao, H. (2015), 'High-efficiency multiplex genome editing of Streptomyces species using an engineered CRISPR/Cas system', *ACS Synthetic Biology* **4**, 723–728.

Dangel, V., Westrich, L., Smith, M. C., Heide, L. and Gust, B. (2010), 'Use of an inducible promoter for antibiotic production in a heterologous host', *Applied Microbiology and Biotechnology* **87**(1), 261–269.

Datsenko, K. A. and Wanner, B. L. (2000), 'One-step inactivation of chromosomal genes in Escherichia coli K-12 using PCR products', *Proceedings of the National Academy of Sciences of the United States of America* **97**(12), 6640–6645.

de Paulis, A., Cirillo, R., Ciccarelli, A., Condorelli, M. and Marone, G. (1991), 'FK-506, a potent novel inhibitor of the release of proinflammatory mediators from human Fc epsilon RI+ cells.', *Journal of Immunology* **146**(7), 2374–2381.

Del Vecchio, F., Petkovic, H., Kendrew, S. G., Low, L., Wilkinson, B., Lill, R., Cortés, J., Rudd, B. A., Staunton, J. and Leadlay, P. F. (2003), 'Active-site residue, domain and module swaps in modular polyketide synthases', *Journal of Industrial Microbiology and Biotechnology* **30**(8), 489–494.

Dilworth, D., Gudavicius, G., Xu, X., Boyce, A. K., O'Sullivan, C., Serpa, J. J., Bilenky, M., Petrochenko, E. V., Borchers, C. H., Hirst, M., Swayne, L. A., Howard, P. and Nelson, C. J. (2018), 'The prolyl isomerase FKBP25 regulates microtubule polymerization impacting cell cycle progression and genomic stability', *Nucleic Acids Research* **46**(5), 2459–2478.

Drufva, E. E., Hix, E. G. and Bailey, C. B. (2020), 'Site directed mutagenesis as a precision tool to enable synthetic biology with engineered modular polyketide synthases', *Synthetic and Systems Biotechnology* **5**(2), 62–80.

Du, W., Huang, D., Xia, M., Wen, J. and Huang, M. (2014), 'Improved FK506 production by the precursors and product-tolerant mutant of Streptomyces tsukubaensis based on genome shuffling and dynamic fed-batch strategies', *Journal of Industrial Microbiology and Biotechnology* **41**(7), 1131–1143.

Dunn, B. J., Watts, K. R., Robbins, T., Cane, D. E. and Khosla, C. (2014), 'Comparative analysis of the substrate specificity of trans - versus cis- acyltransferases of assembly line polyketide synthases', *Biochemistry* **53**(23), 3796–3806.

Erb, A., Luzhetskyy, A., Hardter, U. and Bechthold, A. (2009), 'Cloning and sequencing of the biosynthetic gene cluster for saquayamycin Z and galtamycin B and the elucidation of the assembly of their saccharide chains', *ChemBioChem* **10**(8), 1392–1401.

Fisch, K. M., Bakeer, W., Yakasai, A. A., Song, Z., Pedrick, J., Wasil, Z., Bailey, A. M., Lazarus, C. M., Simpson, T. J. and Cox, R. J. (2011), 'Rational domain swaps decipher programming

in fungal highly reducing polyketide synthases and resurrect an extinct metabolite', *Journal of the American Chemical Society* **133**(41), 16635–16641.

Floriano, B. and Bibb, M. (1996), 'afsR is a pleiotropic but conditionally required regulatory gene for antibiotic production in Streptomyces coelicolor A3(2)', *Molecular Microbiology* **21**(2), 385–396.

Fu, L. F., Tao, Y., Jin, M. Y. and Jiang, H. (2016), 'Improvement of FK506 production by synthetic biology approaches', *Biotechnology Letters* **38**(12), 2015–2021.

Gaali, S., Gopalakrishnan, R., Wang, Y., Kozany, C. and Hausch, F. (2011), 'The chemical biology of immunophilin ligands', *Current Medicinal Chemistry* **18**, 5355–5379.

Gajzlerska, W., Kurkowiak, J. and Turło, J. (2015), 'Use of three-carbon chain compounds as biosynthesis precursors to enhance tacrolimus production in Streptomyces tsukubaensis', *New Biotechnology* **32**(1), 32–39.

Gokhale, R. S., Tsuji, S. Y., Cane, D. E. and Khosla, C. (1999), 'Dissecting and exploiting intermodular communication in polyketide synthases', *Science* **284**(5413), 482–485.

Gold, B. G., Densmore, V., Shou, W., Matzuk, M. M. and Gordon, H. S. (1999), 'Immunophilin FK506-binding protein 52 (not FK506-binding protein 12) mediates the neurotrophic action of FK506', *Journal of Pharmacology and Experimental Therapeutics* **289**(3), 1202–1210.

Gómez, C., Olano, C., Méndez, C. and Salas, J. A. (2012), 'Three pathway-specific regulators control streptolydigin biosynthesis in Streptomyces lydicus', *Microbiology* **158**(10), 2504–2514.

Gomez-Escribano, J. P. and Bibb, M. J. (2011), 'Engineering Streptomyces coelicolor for heterologous expression of secondary metabolite gene clusters', *Microbial Biotechnology* **4**(2), 207–215.

Goranovič, D., Blažič, M., Magdevska, V., Horvat, J., Kuščer, E., Polak, T., Santos-Aberturas, J., Martínez-Castro, M., Barreiro, C., Mrak, P., Kopitar, G., Kosec, G., Fujs, Š., Martín, J. F. and Petković, H. (2012), 'FK506 biosynthesis is regulated by two positive regulatory elements in Streptomyces tsukubaensis', *BMC Microbiology* **12**(238).

Goranovič, D., Kosec, G., Mrak, P., Fujs, Š., Horvat, J., Kuščer, E., Kopitar, G. and Petković, H. (2010), 'Origin of the allyl group in FK506 biosynthesis', *Journal of Biological Chemistry* **285**(19), 14292–14300.

Griffith, J. P., Kim, J. L., Kim, E. E., Sintchak, M. D., Thomson, J. A., Fitzgibbon, M. J., Fleming, M. A., Caron, P. R., Hsiao, K. and Navia, M. A. (1995), 'X-ray structure of calcineurin inhibited by the immunophilin-immunosuppressant FKBP12-FK506 complex', *Cell* **82**(3), 507–522.

Gust, B., Challis, G. L., Fowler, K., Kieser, T. and Chater, K. F. (2003), 'PCR-targeted Streptomyces gene replacement identifies a protein domain needed for biosynthesis of the

sesquiterpene soil odor geosmin.', *Proceedings of the National Academy of Sciences of the United States of America* **100**(4), 1541–1546.

Hans, M., Hornung, A., Dziarnowski, A., Cane, D. E. and Khosla, C. (2003), 'Mechanistic analysis of acyl transferase domain exchange in polyketide synthase modules', *Journal of the American Chemical Society* **125**(18), 5366–5374.

Huang, D., Li, S., Xia, M., Wen, J. and Jia, X. (2013), 'Genome-scale metabolic network guided engineering of Streptomyces tsukubaensis for FK506 production improvement', *Microbial Cell Factories* **12**(52).

Huang, D., Xia, M., Li, S., Wen, J. and Jia, X. (2013), 'Enhancement of FK506 production by engineering secondary pathways of Streptomyces tsukubaensis and exogenous feeding strategies', *Journal of Industrial Microbiology and Biotechnology* **40**(9), 1023–1037.

Huang, H., Zheng, G., Jiang, W., Hu, H. and Lu, Y. (2015), 'One-step high-efficiency CRISPR/Cas9-mediated genome editing in Streptomyces', *Acta Biochimica et Biophysica Sinica* **47**(4), 231–243.

Hughes, A. J. and Keatinge-Clay, A. (2011), 'Enzymatic extender unit generation for in vitro polyketide synthase reactions: Structural and functional showcasing of Streptomyces coelicolor MatB', *Chemistry and Biology* **18**(2), 165–176.

Jiang, H., Wang, Y. Y., Guo, Y. Y., Shen, J. J., Zhang, X. S., Luo, H. D., Ren, N. N., Jiang, X. H. and Li, Y. Q. (2015), 'An acyltransferase domain of FK506 polyketide synthase recognizing both an acyl carrier protein and coenzyme A as acyl donors to transfer allylmalonyl and ethylmalonyl units', *FEBS Journal* **282**(13), 2527–2539.

Jones, A. C., Gust, B., Kulik, A., Heide, L., Buttner, M. J. and Bibb, M. J. (2013), 'Phage P1-derived artificial chromosomes facilitate heterologous expression of the FK506 gene cluster', *PLoS ONE* **8**(7).

Kieser, T., Bibb, M. J., Buttner, M. J., Chater, K. F. and Hopwood, D. A. (2000), 'Practical Streptomyces Genetics'.

Kino, T. and Goto, T. (1993), 'Discovery of FK-506 and update', *Annals New York Academy of Sciences* **685**, 13–21.

Kino, T., Hatanaka, H., Miyata, S., Inamura, N., Nishiyama, M., Yajima, T., Goto, T., Okuhara, M., Kohsaka, M., Aoki, H. and Ochiai, T. (1987), 'FK-506, a novel immunosuppressant isolated from a Streptomyces II. Immunosuppressive effect of FK-506 in vitro', *The Journal of Antibiotics* **40**(9), 1256–1265.

Lau, J., Fu, H., Cane, D. E. and Khosla, C. (1999), 'Dissecting the role of acyltransferase domains of modular polyketide synthases in the choice and stereochemical fate of extender units', *Biochemistry* **38**(5), 1643–1651.

Lee, Y., Lee, K.-t., Lee, J., Beom, Y., Hwangbo, A., Jung, J. A. and Song, C. (2018), 'In vitro and in vivo assessment of FK506 analogs as novel antifungal drug candidates', *Antimicrobial Agents and Chemotherapy* **62**(11), 1–17.

Liu, J., Farmer, J. D., Lane, W. S., Friedman, J., Weissman, I. and Schreiber, S. L. (1991), 'Calcineurin is a common target of cyclophilin-cyclosporin A and FKBP-FK506 complexes', *Cell* **66**(4), 807–815.

Ma, D., Wang, C., Chen, H. and Wen, J. (2018), 'Manipulating the expression of SARP family regulator BulZ and its target gene product to increase tacrolimus production', *Applied Microbiology and Biotechnology* **102**(11), 4887–4900.

MacNeil, D. J., Gewain, K. M., Ruby, C. L., Dezeny, G., Gibbons, P. H. and MacNeil, T. (1992), 'Analysis of Streptomyces avermitilis genes required for avermectin biosynthesis utilizing a novel integration vector', *Gene* **111**, 61–68.

Maiarù, M., Tochiki, K. K., Cox, M. B., Annan, L. V., Bell, C. G., Feng, X., Hausch, F. and Géranton, S. M. (2016), 'The stress regulator FKBP51 drives chronic pain by modulating spinal glucocorticoid signaling', *Science Translational Medicine* **8**(325).

Makino, K., Shinagawa, H., Amemura, M., Kimura, S., Nakata, A. and Ishihama, A. (1988), 'Regulation of the phosphate regulon of Escherichia coli. Activation of pstS transcription by PhoB protein in vitro', *Journal of Molecular Biology* **203**(1), 85–95.

Malla, S., Niraula, N. P., Liou, K. and Sohng, J. K. (2010), 'Improvement in doxorubicin productivity by overexpression of regulatory genes in Streptomyces peucetius', *Research in Microbiology* **161**(2), 109–117.

Marks, A. R. (1996), 'Cellular functions of immunophilins', *Physiological Reviews* **76**(3), 631–649.

Martínez-Castro, M., Salehi-Najafabadi, Z., Romero, F., Pérez-Sanchiz, R., Fernández-Chimeno, R. I., Martín, J. F. and Barreiro, C. (2013), 'Taxonomy and chemically semi-defined media for the analysis of the tacrolimus producer 'Streptomyces tsukubaensis'', *Applied Microbiology and Biotechnology* **97**(5), 2139–2152.

Mierke, D. F., Schmieder, P., Karuso, P. and Kessler, H. (1991), '97. Conformational analysis of the cis- and trans-isomers of FK506 by NMR and molecular dynamics', *Helvetica Chimica Acta* **74**, 1027–1047.

Miyazawa, T., Hirsch, M., Zhang, Z. and Keatinge-Clay, A. T. (2020), 'An in vitro platform for engineering and harnessing modular polyketide synthases', *Nature Communications* **11**(80), 1–7.

Mo, S., Ban, Y. H., Park, J. W., Yoo, Y. J. and Yoon, Y. J. (2009), 'Enhanced FK506 production in Streptomyces clavuligerus CKD1119 by engineering the supply of methylmalonyl-CoA precursor', *Journal of Industrial Microbiology and Biotechnology* **36**(12), 1473–1482.

Mo, S. J., Lee, S.-K., Jin, Y.-Y. and Suh, J.-W. (2016), 'Improvement of FK506 production in the high-yielding strain Streptomyces sp. RM7011 by engineering the supply of allylmalonyl-CoA through a combination of genetic and chemical approach', *Journal of Microbiology and Biotechnology* **26**(2), 233–240.

Mo, S. J., Yoo, Y. J., Ban, Y. H., Lee, S. K., Kim, E., Suh, J. W. and Yoon, Y. J. (2012), 'Roles of fkbN in positive regulation and tcs7 in negative regulation of FK506 biosynthesis in Streptomyces sp. strain KCTC 11604BP', *Applied and Environmental Microbiology* **78**(7), 2249–2255.

Mo, S., Kim, D. H., Lee, J. H., Park, J. W., Basnet, D. B., Ban, Y. H., Yoo, Y. J., Chen, S. W., Park, S. R., Choi, E. A., Kim, E., Jin, Y. Y., Lee, S. K., Park, J. Y., Liu, Y., Lee, M. O., Lee, K. S., Kim, S. J., Kim, D., Park, B. C., Lee, S. G., Kwon, H. J., Suh, J. W., Moore, B. S., Lim, S. K. and Yoon, Y. J. (2011), 'Biosynthesis of the allylmalonyl-CoA extender unit for the FK506 polyketide synthase proceeds through a dedicated polyketide synthase and facilitates the mutasynthesis of analogues', *Journal of the American Chemical Society* **133**(4), 976–985.

Moss, S. J., Stanley-Smith, A. E., Schell, U., Coates, N. J., Foster, T. A., Gaisser, S., Gregory, M. A., Martin, C. J., Nur-E-Alam, M., Piraee, M., Radzom, M., Suthar, D., Thexton, D. G., Warneck, T. D., Zhang, M. Q. and Wilkinson, B. (2013), 'Novel FK506 and FK520 analogues via mutasynthesis: Mutasynthon scope and product characteristics', *MedChemComm* **4**(2), 324–331.

Motamedi, H. and Shafiee, A. (1998), 'The biosynthetic gene cluster for the macrolactone ring of the immunosuppressant FK506', *European Journal of Biochemistry* **256**(3), 528–534.

Motamedi, H., Shafiee, A., Cai, S. J., Streicher, S. L., Arison, B. H. and Miller, R. R. (1996), 'Characterization of methyltransferase and hydroxylase genes involved in the biosynthesis of the immunosuppressants FK506 and FK520', *Journal of Bacteriology* **178**(17), 5243–5248.

Musiol, E. M., Härtner, T., Kulik, A., Moldenhauer, J., Piel, J., Wohlleben, W. and Weber, T. (2011), 'Supramolecular templating in kirromycin biosynthesis: The acyltransferase KirCII loads ethylmalonyl-CoA extender onto a specific ACP of the trans-AT PKS', *Chemistry and Biology* **18**(4), 438–444.

Musiol-Kroll, E. M. and Wohlleben, W. (2018), 'Acyltransferases as tools for polyketide synthase engineering', *Antibiotics* **7**(62).

Musiol-Kroll, E. M., Zubeil, F., Schafhauser, T., Härtner, T., Kulik, A., McArthur, J., Koryakina, I., Wohlleben, W., Grond, S., Williams, G. J., Lee, S. Y. and Weber, T. (2017), 'Polyketide bioderivatization using the promiscuous acyltransferase KirCII', *ACS Synthetic Biology* **6**(3), 421–427.

Nara, A., Hashimoto, T., Komatsu, M., Nishiyama, M., Kuzuyama, T. and Ikeda, H. (2017), 'Characterization of bafilomycin biosynthesis in Kitasatospora setae KM-6054 and comparative analysis of gene clusters in Actinomycetales microorganisms', *Journal of Antibiotics* **70**(5), 616–624.

Ng, Y. Z., Baldera-Aguayo, P. A. and Cornish, V. W. (2017), 'Fluorescence polarization assay for small molecule screening of FK506 biosynthesized in 96-well microtiter plates', *Biochemistry* **56**, 5260–5268.

Oliynyk, M., Brown, M. J., Cortés, J., Staunton, J. and Leadlay, P. F. (1996), 'A hybrid modular polyketide synthase obtained by domain swapping', *Chemistry and Biology* **3**(10), 833–839.

Ordónez-Robles, M., Rodríguez-García, A. and Martín, J. F. (2016), 'Target genes of the Streptomyces tsukubaensis FkbN regulator include most of the tacrolimus biosynthesis genes, a phosphopantetheinyl transferase and other PKS genes', *Applied Microbiology and Biotechnology* **100**(18), 8091–8103.

Ordóñez-Robles, M., Santos-Beneit, F., Rodríguez-García, A. and Martín, J. F. (2017), 'Analysis of the Pho regulon in Streptomyces tsukubaensis', *Microbiological Research* **205**, 80–87.

Organ, H. M., Holmes, M. A., Pisano, J. M., Staruch, M. J., Wyvratt, M. J., Dumont, F. J. and Sinclair, P. J. (1993), 'Novel derivatives at the C21 position of the FK-506 macrocycle', *Bioorganic and Medicinal Chemistry Letters* **3**(4), 657–662.

Park, J. W., Mo, S. J., Park, S. R., Ban, Y. H., Yoo, Y. J. and Yoon, Y. J. (2009), 'Liquid chromatography-mass spectrometry characterization of FK506 biosynthetic intermediates in Streptomyces clavuligerus KCTC 10561BP', *Analytical Biochemistry* **393**(1), 1–7.

Periyasamy, S., Warrier, M., Tillekeratne, M. P., Shou, W. and Sanchez, E. R. (2007), 'The immunophilin ligands cyclosporin A and FK506 suppress prostate cancer cell growth by androgen receptor-dependent and -independent mechanisms', *Endocrinology* **148**(10), 4716–4726.

Peters, D. H., Fitton, A., Plosker, G. L. and Faulds, D. (1993), 'Tacrolimus: A review of its pharmacology, and therapeutic potential in hepatic and renal transplantation', *Drugs* **46**(4), 746–794.

Ramos, J. L., Martínez-Bueno, M., Molina-Henares, A. J., Terán, W., Watanabe, K., Zhang, X., Gallegos, M. T., Brennan, R. and Tobes, R. (2005), 'The TetR family of transcriptional repressors', *Microbiology and Molecular Biology Reviews* **69**(2), 326–356.

Ranganathan, A., Timoney, M., Bycroft, M., Cortés, J., Thomas, I. P., Wilkinson, B., Kellenberger, L., Hanefeld, U., Galloway, I. S., Staunton, J. and Leadlay, P. F. (1999), 'Knowledge-based design of bimodular and trimodular polyketide synthases based on domain and module swaps: A route to simple statin analogues', *Chemistry and Biology* **6**(10), 731–741.

Ravcheev, D. A., Khoroshkin, M. S., Laikova, O. N., Tsoy, O. V., Sernova, N. V., Petrova, S. A., Rakhmaninova, A. B., Novichkov, P. S., Gelfand, M. S. and Rodionov, D. A. (2014), 'Comparative genomics and evolution of regulons of the LacI-family transcription factors', *Frontiers in Microbiology* **5**(294).

Revill, W. P., Voda, J., Reeves, C. R., Chung, L., Schirmer, A., Ashley, G., Carney, J. R., Fardis, M., Carreras, C. W., Zhou, Y., Feng, L., Tucker, E., Robinson, D. and Gold, B. G. (2002), 'Genetically engineered analogs of ascomycin for nerve regeneration', *Journal of Pharmacology and Experimental Therapeutics* **302**(3), 1278–1285.

Romero-Rodríguez, A., Robledo-Casados, I. and Sánchez, S. (2015), 'An overview on transcriptional regulators in Streptomyces', *Biochimica et Biophysica Acta* **1849**(8), 1017–1039.

Rowe, C. J., Böhm, I. U., Thomas, I. P., Wilkinson, B., Rudd, B. A., Foster, G., Blackaby, A. P., Sidebottom, P. J., Roddis, Y., Buss, A. D., Staunton, J. and Leadlay, P. F. (2001), 'Engineering a polyketide with a longer chain by insertion of an extra module into the erythromycin-producing polyketide synthase', *Chemistry and Biology* **8**(5), 475–485.

Ruan, X., Pereda, A., Stassi, D. L., Zeidner, D., Summers, R. G., Jackson, M., Shivakumar, A., Kakavas, S., Staver, M. J., Donadio, S. and Katz, L. (1997), 'Acyltransferase domain substitutions in erythromycin polyketide synthase yield novel erythromycin derivatives.', *Journal of Bacteriology* **179**(20), 6416–6425.

Rudolph, M. M., Vockenhuber, M. P. and Suess, B. (2013), 'Synthetic riboswitches for the conditional control of gene expression in Streptomyces coelicolor', *Microbiology (United Kingdom)* **159**, 1416–1422.

Salehi-Najafabadi, Z., Barreiro, C., Rodríguez-García, A., Cruz, A., López, G. E. and Martín, J. F. (2014), 'The gamma-butyrolactone receptors BulR1 and BulR2 of Streptomyces tsukubaensis: Tacrolimus (FK506) and butyrolactone synthetases production control', *Applied Microbiology and Biotechnology* **98**(11), 4919–4936.

Sánchez, C., Du, L., Edwards, D. J., Toney, M. D. and Shen, B. (2001), 'Cloning and characterization of a phosphopantetheinyl transferase from Streptomyces verticillus ATCC15003, the producer of the hybrid peptide-polyketide antitumor drug bleomycin', *Chemistry and Biology* **8**(7), 725–738.

Schmidt, M. V., Paez-Pereda, M., Holsboer, F. and Hausch, F. (2012), 'The prospect of FKBP51 as a drug target', *ChemMedChem* **7**(8), 1351–1359.

Shen, J. J., Chen, F., Wang, X. X., Liu, X. F., Chen, X. A., Mao, X. M. and Li, Y. Q. (2018), 'Substrate specificity of acyltransferase domains for efficient transfer of acyl groups', *Frontiers in Microbiology* **9**(1840).

Shinde, P. B., Ban, Y. H., Hwang, J. Y., Cho, Y., Chen, Y. A., Cheong, E., Nam, S. J., Kwon, H. J. and Yoon, Y. J. (2015), 'A non-immunosuppressive FK506 analogue with neuroregenerative activity produced from a genetically engineered Streptomyces strain', *RSC Advances* **5**(9), 6823–6828.

Snyder, S. H., Sabatini, D. M., Lai, M. M., Steiner, J. P., Hamilton, G. S. and Suzdak, P. D. (1998), 'Neural action of immunophilin ligands', *Trends in Pharmacological Sciences* **19**(1), 21–26.

Sola-Landa, A., Moura, R. S. and Martin, J. F. (2003), 'The two-component PhoR-PhoP system controls both primary metabolism and secondary metabolite biosynthesis in Streptomyces lividans', *Proceedings of the National Academy of Sciences of the United States of America* **100**(10), 6133–6138.

Song, K., Wei, L., Liu, J., Wang, J., Qi, H. and Wen, J. (2017), 'Engineering of the LysR family transcriptional regulator FkbR1 and its target gene to improve ascomycin production', *Applied Microbiology and Biotechnology* **101**(11), 4581–4592.

Storer, C. L., Dickey, C. A., Galigniana, M. D., Rein, T. and Cox, M. B. (2011), 'FKBP51 and FKBP52 in signaling and disease', *Trends in Endocrinology and Metabolism* **22**(12), 481–490.

Tong, Y., Charusanti, P., Zhang, L., Weber, T. and Lee, S. Y. (2015), 'CRISPR-Cas9 based engineering of Actinomycetal genomes', *ACS Synthetic Biology* **4**, 1020–1029.

Turło, J., Gajzlerska, W., Klimaszewska, M., Król, M., Dawidowski, M. and Gutkowska, B. (2012), 'Enhancement of tacrolimus productivity in Streptomyces tsukubaensis by the use of novel precursors for biosynthesis', *Enzyme and Microbial Technology* **51**(6-7), 388–395.

Wang, C., Liu, J., Liu, H., Liang, S. and Wen, J. (2017), 'Combining metabolomics and network analysis to improve tacrolimus production in Streptomyces tsukubaensis using different exogenous feedings', *Journal of Industrial Microbiology and Biotechnology* **44**(11), 1527–1540.

Wang, C., Liu, J., Liu, H., Wang, J. and Wen, J. (2017), 'A genome-scale dynamic flux balance analysis model of Streptomyces tsukubaensis NRRL18488 to predict the targets for increasing FK506 production', *Biochemical Engineering Journal* **123**, 45–56.

Wang, C., Wang, J., Yuan, J., Jiang, L., Jiang, X., Yang, B., Zhao, G., Liu, B. and Huang, D. (2019), 'Generation of Streptomyces hygroscopicus cell factories with enhanced ascomycin production by combined elicitation and pathway-engineering strategies', *Biotechnology and Bioengineering* **116**(12), 3382–3395.

Wang, J., Liu, H., Huang, D., Jin, L., Wang, C. and Wen, J. (2017), 'Comparative proteomic and metabolomic analysis of Streptomyces tsukubaensis reveals the metabolic mechanism of FK506 overproduction by feeding soybean oil', *Applied Microbiology and Biotechnology* **101**, 2447–2465.

Wang, Y.-Y., Zhang, X.-S., Luo, H.-D., Ren, N.-N., Jiang, X.-H., Jiang, H. and Li, Y.-Q. (2016), 'Characterization of discrete phosphopantetheinyl transferases in Streptomyces tsukubaensis L19 unveils a complicate phosphopantetheinylation network', *Scientific Reports* **6**(24255), 1–10.

Weissman, K. J. (2016), 'Genetic engineering of modular PKSs : from combinatorial biosynthesis to synthetic biology', *Natural Product Reports* **33**, 203–230.

Woncheol, K., Lee, J. J., Paik, S.-G. and Hong, Y.-S. (2010), 'Identification of three positive regulators in the geldanamycin PKS gene cluster of Streptomyces hygroscopicus JCM4427', *Journal of Microbiology and Biotechnology* **20**(11), 1484–1490.

Yang, K., Qi, L. H., Zhang, M., Hou, X. F., Pan, H. X., Tang, G. L., Wang, W. and Yuan, H. (2015), 'The SARP family regulator Txn9 and two-component response regulator Txn11 are key activators for trioxacarcin biosynthesis in Streptomyces bottropensis', *Current Microbiology* **71**(4), 458–464.

Yong, J. H. and Byeon, W. H. (2005), 'Alternative production of avermectin components in Streptomyces avermitilis by gene replacement', *Journal of Microbiology* **43**(3), 277–284.

Yoo, Y. J., yeon Hwang, J., luyung Shin, H., Cui, H., Lee, J. and Yoon, Y. J. (2015), 'Characterization of negative regulatory genes for the biosynthesis of rapamycin in Streptomyces rapamycinicus and its application for improved production', *Journal of Industrial Microbiology and Biotechnology* **42**(1), 125–135.

Yuzawa, S., Deng, K., Wang, G., Baidoo, E. E., Northen, T. R., Adams, P. D., Katz, L. and Keasling, J. D. (2017), 'Comprehensive in vitro analysis of acyltransferase domain exchanges in modular polyketide synthases and its application for short-chain ketone production', *ACS Synthetic Biology* **6**(1), 139–147.

Zeng, B., Macdonald, J. R., Bann, J. G., Beck, K., Gambee, J. E., Boswell, B. A. and Ba, H. P. (1998), 'Chicken FK506-binding protein, FKBP65, a member of the FKBP family of peptidylprolyl cis–trans isomerases , is only partially inhibited by FK506', *Biochemical Journal* **330**, 109–114.

Zhang, L., Hashimoto, T., Qin, B., Hashimoto, J., Kozone, I., Kawahara, T., Okada, M., Awakawa, T., Ito, T., Asakawa, Y., Ueki, M., Takahashi, S., Osada, H., Wakimoto, T., Ikeda, H., Shin-ya, K. and Abe, I. (2017), 'Characterization of giant modular PKSs provides insight into genetic mechanism for structural diversification of aminopolyol polyketides', *Angewandte Chemie - International Edition* **56**(7), 1740–1745.

6 List of Tables

1 Devices used in this study. . . . 12
2 Equipment used in this study. . . . 14
3 Consumables used in this study. . . . 15
4 Chemicals used in this study. . . . 15
5 Primers used for the DACA. . . . 19
6 Primers used for overexpression studies. . . . 19
7 Primers used for simultaneous overexpression of regulators (AGOS system). . . . 21
8 Primers used for the module swap approach. . . . 22
9 Primers used for the AT domain swap approach. . . . 23
10 Primers used for the ACP domain swap approach. . . . 24
11 Enzymes used in this study. . . . 25
12 Kits used in this study. . . . 26
13 Size standards used in this study. . . . 26
14 Antibiotics and inductors used in this study. . . . 27
15 Strains used in this study. . . . 27
16 Plasmids used in this study. . . . 29
17 Cosmids used in this study. . . . 35
18 MGm-2.5 medium. . . . 37
19 Trace element solution for MGm-2.5 medium (100x, 10 mL). . . . 37
20 R2 medium. . . . 37
21 Trace element solution for R2 medium. . . . 38
22 TSB (Tryptone Soya Broth) medium. . . . 38
23 ISP4 (International Streptomyces Project) medium. . . . 38
24 LB (Lysogeny Broth) medium. . . . 39
25 YEME (Yeast Extract Malt Extract) medium. . . . 39
26 2xYT (Yeast Extract Tryptone) medium. . . . 39
27 MS (Mannitol Soya Flour) agar. . . . 39
28 SOB (Super Optimal Broth) medium. . . . 40
29 Solutions for the isolation of plasmids and cosmids. . . . 40
30 Solutions for protein isolation and processing. . . . 40
31 Bradford solution. . . . 41
32 Buffers used in this study. . . . 41

33 Software used in this study. 42
34 Pipetting scheme for standard PCR reactions. 44
35 Temperature program for standard PCR reactions. 45
36 Pipetting scheme for the Q5®High-Fidelity DNA polymerase. 49
37 Temperature program for the Q5®High-Fidelity DNA polymerase. 49
38 Pipetting scheme for the amplification of the extended resistance cassette. 51
39 Temperature program for the amplification of the extended resistance cassette. . 51
40 Temperature program for the amplification of Ptcs6a, Ptcs6b, PfkbO, PfkbG, PallA and P16S. 57
41 Pipetting scheme for the amplification of P16S. 57
42 Temperature program for the amplification of P16S from genomic DNA. 58
43 Proteins chosen for simultaneous overexpression. 61
44 Pipetting scheme for the overlap PCR. 65
45 Temperature program for the overlap PCR. 66
46 Gradient used for HPLC analytics. 71
47 Gradient used for LC-MS analytics. 72
48 Gradient used for HR-MS analytics. 72
49 Gradient used for VLC. 73

50 Amount of proteins detected on the different promoter fragments in the DACA. . 76
51 Intensities of proteins binding specifically to the different promoter fragments analyzed in the DACA. 80
52 Proteins of the tacrolimus biosynthetic gene cluster and their intensities on the different promoter fragments analyzed in the DACA. 83
53 Effect of an overexpression of selected regulators on tacrolimus production depending on cultivation scale. 89
54 Absolute tacrolimus production yields achieved by different mutant strains on various scales of cultivation. 90
55 Comparison of module 4 and module 10 of the FK506 cluster. 94
56 Comparison of the ACP domains of module 10 of the tacrolimus BGC and module 5 of the kirromycin BGC (KirACP5). 95
57 ^{1}H and ^{13}C NMR data of 9-deoxo-31-*O*-demethyl-FK506 in $CDCl_3$. 105

58 Mutant strains revealing significantly increased tacrolimus production in microfermentation. 109

59 Accession numbers of proteins analyzed in this study. 139

7 List of Figures

1 Mode of action of FK506. 2
2 Tacrolimus biosynthetic gene cluster. 3
3 Schematic representation of tacrolimus biosynthesis. 5
4 CRISPR-Cas9 editing in *S. tsukubaensis* NRRL18488 using the plasmid pCRISPR-TT. 55
5 Location of the selected promoter regions within the tacrolimus biosynthetic gene cluster. 56
6 Principle of AGOS used to simultaneously overexpress several regulators. 62
7 Overview of the three different PKS engineering approaches pursued in this study. 63
8 Working steps to prepare the module swap on pAC20N. 67
9 Amino acid sequence of the AT domain of module 4 including KAL and PAL linker sequences. 68
10 Working steps to prepare the ACP domain swap on pAC20N. 70
11 Cell dry weight and tacrolimus production of *S. tsukubaensis* NRRL18488 monitored during the 10 L fermentation. 74
12 Scatter plot of the intensities of all identified proteins in the DACA. 76
13 Tacrolimus production of the generated mutant strains overexpressing regulatory proteins. 86
14 Comparison of integrative versus non-integrative overexpression of seven regulators of tacrolimus biosynthesis. 88
15 Simultaneous overexpression of two and three positive regulators of tacrolimus biosynthesis. 92
16 Amino acid sequence alignment of the AT domains of module 4 and module 10. . 95
17 Representative extracted ion chromatograms of extracts resulting from module swap mutant strains and controls. 97
18 Extracted ion chromatogram of an extract resulting from an AT domain swap mutant strain compared to the controls. 99
19 Representative extracted ion chromatograms of extracts resulting from selected ACP domain swap mutant strains and controls. 100
20 Total ion chromatograms of extracts resulting from selected ACP domain swap mutant strains and controls. 101

21 ^{1}H NMR and ^{13}C NMR spectra of the new compound (9-deoxo-31-*O*-demethyl-FK506) and FK506. 103
22 Chemical structure of the compound isolated from *Streptomyces tsukubaensis* ACP E2-K7-6/pEM11CII. 104
23 HR-MS analysis of the purified compound isolated from *Streptomyces tsukubaensis* ACP E2-K7-6/pEM11CII. 104

24 Intermodular linker sequence located between module 9 and module 10. 121
25 Interpolypeptide linker sequence located downstream of module 10. 121
26 Post-AT linker sequences of module 4 and module 10. 122

27 Comparison of cultivations of *Streptomyces tsukubaensis* NRRL18488 on a 100 mL and a 10 L scale. 140
28 Aggregates observed during cultivations of *Streptomyces tsukubaensis* NRRL18488 mutant strains overexpressing regulatory proteins. 141
29 PCR reactions to confirm the predicted deletion on pTB67. 142
30 *Pci*I restriction analysis of pTB67-22. 143
31 HPLC chromatograms of the tacrolimus standard and the compound isolated from *S. tsukubaensis* ACP E2-K7-6/pEM11CII. 143
32 HR-MRM chromatograms of a culture extract resulting from *S. tsukubaensis* ACP E2-K7-6/pEM11CII. 144

8 Appendix

Table 59: **Accession number of proteins analyzed in this study.**
Assignment of the IFCAGPOI annotation numbers used for the proteome analysis of this study to the published annotation of the genome sequence of *Streptomyces tsukubaensis* NRRL18488 (NCBI accession number CP029159).

IFCAGPOI number	**STU number (locus_tag)**	**STU number (old_locus_tag)**
IFCAGPOI_05107	STSU_RS25525	STSU_025730
IFCAGPOI_04345	STSU_RS21790	STSU_021980
IFCAGPOI_03331	STSU_RS16760	STSU_016915
IFCAGPOI_00860	STSU_RS04560	STSU_004580
IFCAGPOI_01458	STSU_RS07515	STSU_007530
IFCAGPOI_02551	STSU_RS12910	STSU_012955
IFCAGPOI_03512	STSU_RS17650	STSU_017830
IFCAGPOI_04383	STSU_RS21965	STSU_022160
IFCAGPOI_04468	STSU_RS22385	STSU_022590
IFCAGPOI_05876	STSU_RS29260	STSU_029485
IFCAGPOI_05926	STSU_RS29510	STSU_029735
IFCAGPOI_05966	STSU_RS29700	STSU_029930
IFCAGPOI_05976	STSU_RS29750	STSU_029980
IFCAGPOI_06286	STSU_RS31235	STSU_031465
IFCAGPOI_00339	STSU_RS01990	STSU_002020
IFCAGPOI_01482	STSU_RS07635	STSU_007650
IFCAGPOI_03805	STSU_RS19110	STSU_019295
IFCAGPOI_06136	STSU_RS30545	STSU_030785
IFCAGPOI_05711	STSU_RS28495	STSU_028710
IFCAGPOI_01705	STSU_RS08750	STSU_008755
IFCAGPOI_02717	STSU_RS13735	STSU_013795
IFCAGPOI_03574	STSU_RS17955	STSU_018140
IFCAGPOI_04736	STSU_RS23690	STSU_023885
IFCAGPOI_05697	STSU_RS28425	STSU_028640
IFCAGPOI_06331	STSU_RS31450	STSU_031680
IFCAGPOI_00009	STSU_RS00355	STSU_000350
IFCAGPOI_00306	STSU_RS01830	STSU_001845
IFCAGPOI_05548	STSU_RS27680	STSU_027890
IFCAGPOI_06487	STSU_RS32100	STSU_032510
IFCAGPOI_06489	STSU_RS32110	STSU_032520

IFCAGPOI number	STU number (locus _tag)	STU number (old_locus_tag)
IFCAGPOI_04513	STSU_RS22620	STSU_022830
IFCAGPOI_05727	STSU_RS28570	STSU_028785
IFCAGPOI_00682	STSU_RS03675	STSU_003720
IFCAGPOI_01589	STSU_RS08165	STSU_008180
IFCAGPOI_02857	STSU_RS14435	STSU_014510
IFCAGPOI_03410	STSU_RS17140	STSU_017315
IFCAGPOI_03597	STSU_RS18065	STSU_018255
IFCAGPOI_04924	STSU_RS24625	STSU_024820
IFCAGPOI_05636	STSU_RS28120	STSU_028340
IFCAGPOI_06421	STSU_RS31825	STSU_032230
IFCAGPOI_01486	STSU_RS07655	STSU_007670
IFCAGPOI_06084	STSU_RS30290	STSU_030530
IFCAGPOI_06386	STSU_RS31710	STSU_031960

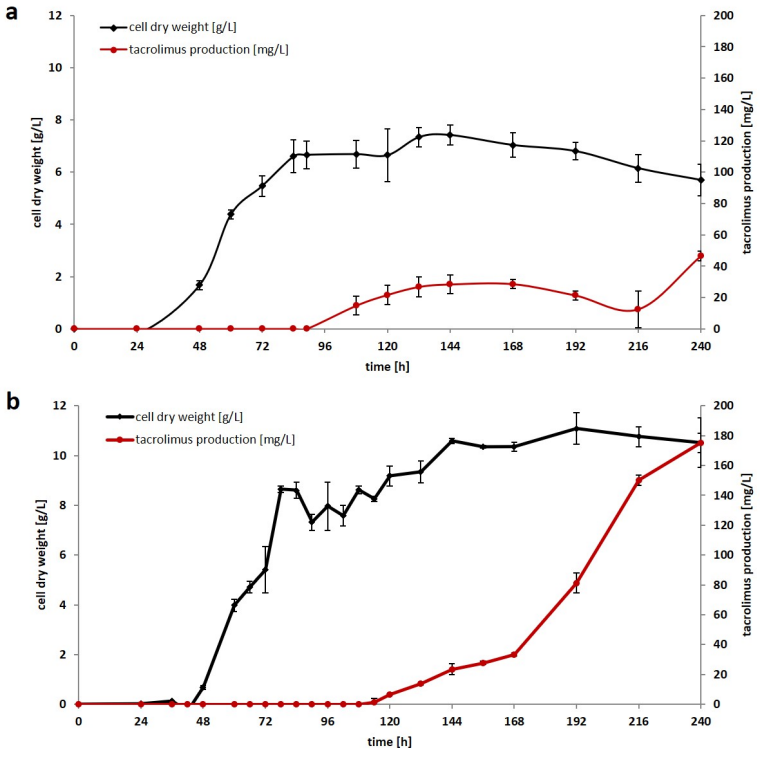

Figure 27: **Comparison of cultivations of *Streptomyces tsukubaensis* NRRL18488 on a 100 mL and a 10 L scale.**
a Cell dry weight [g/L] and tacrolimus production [mg/L] determined for 100 mL cultures of *Streptomyces tsukubaensis* NRRL18488. Values represent the average of five independent cultures. **b** Cell dry weight [g/L] and tacrolimus production [mg/L] determined for *Streptomyces tsukubaensis* NRRL18488 grown in a 10 L fermenter. Values represent the average of three technical replicates.

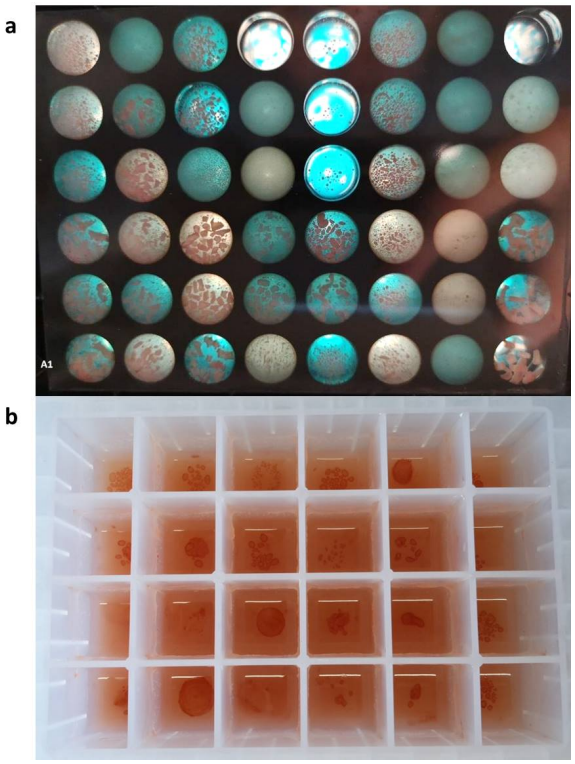

Figure 28: **Aggregates observed during cultivations of *Streptomyces tsukubaensis* NRRL18488 mutant strains overexpressing regulatory proteins.**
a 1 mL scale cultivation performed by SINTEF. **b** Cultivation in 24-square deepwell plates (3 mL volume).

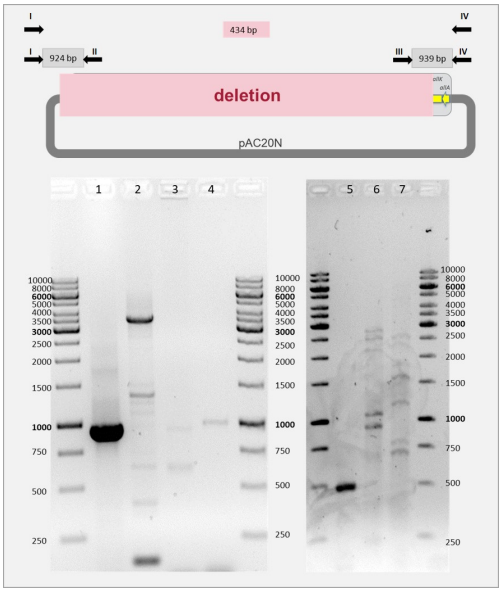

Figure 29: **PCR reactions to confirm the predicted deletion on pTB67.**
Above: binding sites of the testprimers designed to confirm the predicted deletion (for primer sequences see table 8; 20-21). Below: 1 % agarose gel stained with peqGREEN (7 V/cm; 1xTAE) with different PCR products. The following primers and DNA templates were used: 1: primer I and II, pAC20N; 2: primer I and II, pTB67-22; 3: primer III and IV, pAC20N; 4: primer III and IV, pTB67-22; 5: primer I and IV, pTB67; 6: primer I and IV, genomic DNA *S. albus* J1074/pTB67-21; 7: primer I and IV, genomic DNA *S. albus* J1074/pTB67-22.

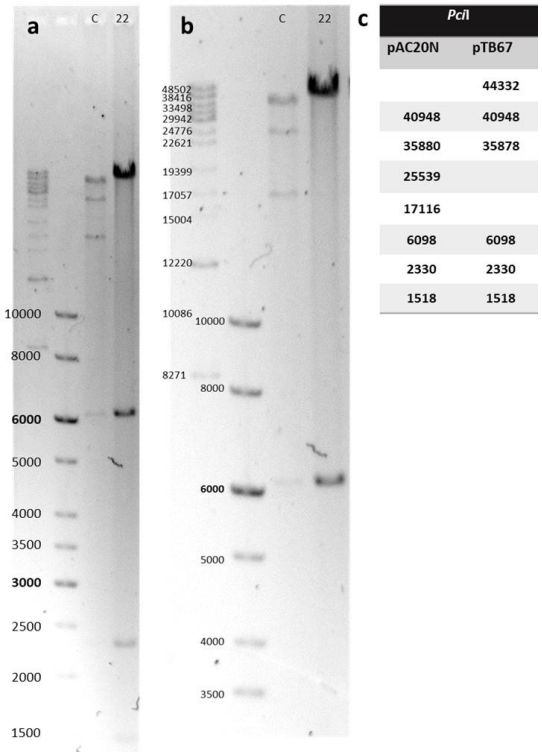

Figure 30: ***Pci*I restriction analysis of pTB67-22.**
a Total view of *Pci*I restriction digest performed to verify the DNA of pTB67-22 (DNA of pAC20N used as control (C)). **b** Magnification of the upper gel part to elucidate larger fragments. **c** Theoretically expected fragment sizes (bp) following *Pci*I restriction digest of pAC20N and pTB67.
0.5 % agarose gel stained with peqGREEN (2.7 V/cm; 1xTAE).

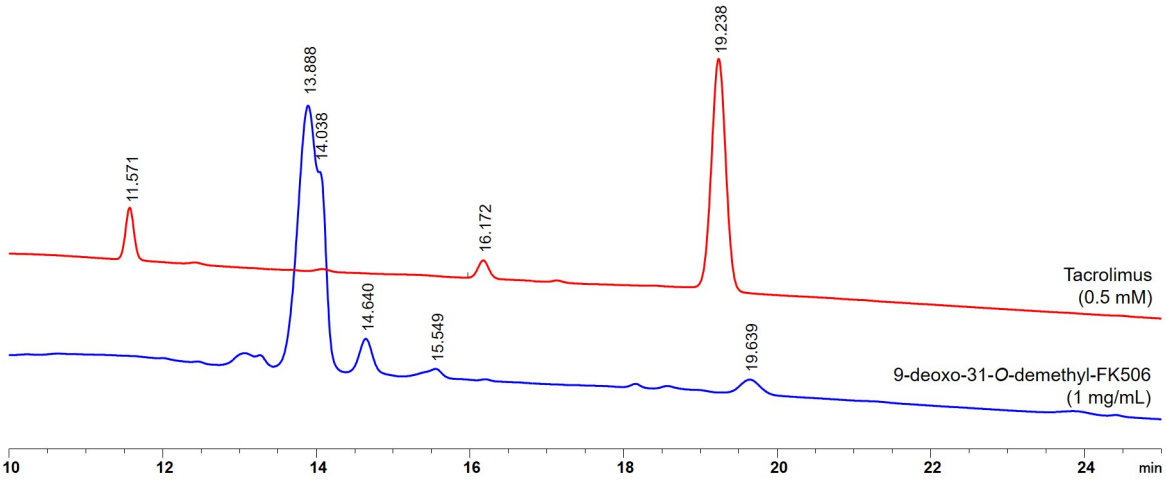

Figure 31: **HPLC chromatograms of a tacrolimus standard and the compound isolated from *S. tsukubaensis* ACP E2-K7-6/pEM11CII.**
The new compound already elutes after 13.888 minutes while tacrolimus depicts a retention time of 19.238 minutes under the given conditions (detection wavelength: 210 nm).

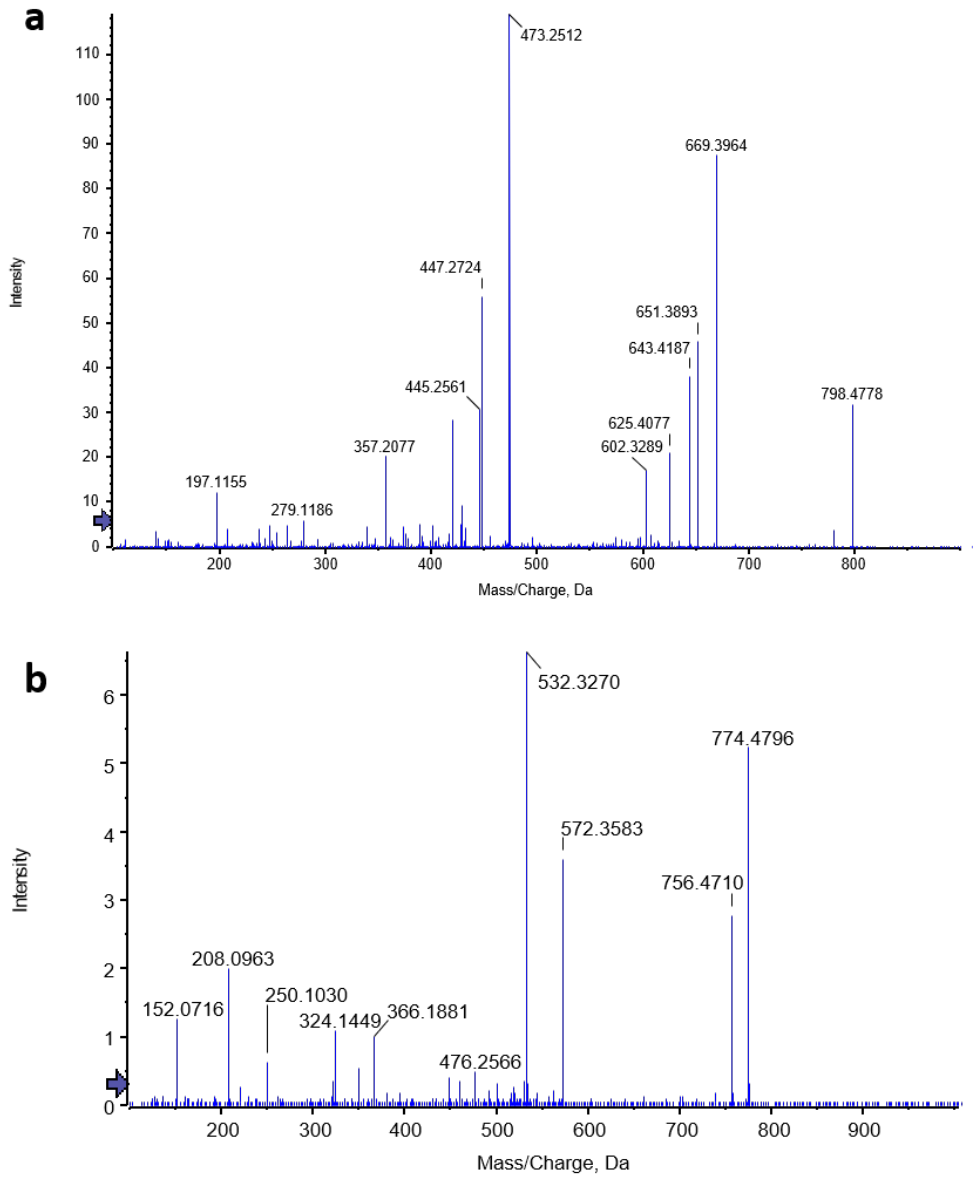

Figure 32: **HR-MRM chromatograms of a culture extract resulting from *S. tsukubaensis* ACP E2-K7-6/pEM11CII.**

a HR-MRM positive mode of *m/z* 798.5 (CE 80 V). Expected mass of the sodium adduct of 9-deoxo-31-*O*-demethyl-FK506: *m/z* 798.4768 (Δppm=1.25 for the observed mass of *m/z* 798.4778). **b** HR-MRM negative mode of *m/z* 774.5 (CE 80 V). Expected mass of 9-deoxo-31-*O*-demethyl-FK506 $[M\text{-}H]^-$: *m/z* 774.4792 (Δppm=0.52 for the observed mass of *m/z* 774.4796).

Acknowledgements

First of all, I would like to thank Prof. Dr. Harald Groß for entrusting me with this interesting and wide-ranging project. Thanks further for all advice and help regarding analytical questions and for the analysis of the NMR data set.

My special appreciation goes to PD Dr. Bertolt Gust for the excellent supervision. I would like to express my thanks for all the constructive and helpful discussions, for advice and for sharing his broad experience.

I thank Prof. Dr. Leonard Kaysser and Prof. Dr. Wolfgang Wohlleben for acting as examiner.

Furthermore, I would like to thank Andreas Kulik for supporting me with the 10 L fermentation and for his reliable and competent help with the LC-MS measurements.

I would also like to thank all members of the ERA-IB TacroDrugs consortium for fruitful meetings and discussions and for the good cooperation. Special thanks to the SINTEF project partners for the high-throughput-screening of my generated mutant strains and to Dr. Pedro Albuquerque for helping to establish the CRISPR-Cas9 technology.

I also owe gratitude to Prof. Dr. Nadine Ziemert and her doctoral student Shrikant Mantri for helping with the bioinformatic analysis of the Nanopore sequencing results. Prof. Dr. Kay Nieselt should also be thanked for providing the annotated protein database for the proteomics. Moreover, I thank Prof. Dr. Lämmerhofer and his doctoral student Ryan Karongo for performing the HR-MS measurements.

I would also like to thank PD Dr. Kristian Apel for the initial training at the beginning of my thesis and his advice regarding the DACA studies.

Thanks go also to Dr. Ewa Musiol-Kroll for her advice regarding the *trans*AT PKS engineering approach and for providing the plasmids pEM11CII and pEM221_matB.

I would also particularly like to thank Corinna Fischer, Emmanuel Wemakor and Lucy Westrich for the good organization of the institute and the lab and their helpfulness.

Further thanks go to my master students Alexander Hoffreiter and Panagiota-Channa Koutsandrea for their active and good cooperation on my projects.

I thank Irina Helmle for supporting me with the VLC and for implementing the NMR measurements.

Finally, big thanks go to all my colleagues for the enjoyable atmosphere in the lab and for the great time we had together at the countless events.

In the end, I also express my gratitude to my friends and family for always supporting me.